Carbon Dioxide Transport and Retention in Coal

Nikolai Siemons

Carbon Dioxide Transport and Retention in Coal

Proefschrift

ter verkrijging van de graad van doctor
aan de Technische Universiteit Delft,
op gezag van de Rector Magnificus Prof. dr. ir. J.T. Fokkema,
voorzitter van het College voor Promoties,
in het openbaar te verdedigen
op dinsdag 04 september 2007 om 17.30 uur

door

Nikolai SIEMONS

Diplom-Geologe (Rheinisch-Westfälische Technische Hochschule Aachen)

geboren te Essen (Duitsland)

Dit proefschrift is goedgekeurd door de promotoren:
Prof. ir. C.P.J.W. van Kruijsdijk
Prof.dr. J. Bruining

Samenstelling promotiecommissie:

Rector Magnificus,	voorzitter
Prof. ir. C.P.J.W. van Kruijsdijk,	Technische Universiteit Delft, promotor
Prof. dr. J. Bruining,	Technische Universiteit Delft, co-promotor
Prof. W.R. Rossen,	Technische Universiteit Delft
Prof. dr. C.J. Spiers,	Universiteit Utrecht
Dr. R. Schotting,	Universiteit Utrecht
Dr. B.M. Krooss,	Rheinisch-Westfälische Technische Hochschule Aachen
Dr. K-H.A.A. Wolf,	Technische Universiteit Delft, supervisor
Prof. dr.ir. P.L.J. Zitha,	Technische Universiteit Delft, reservelid

Dr. K-H.A.A. Wolf heeft als begleider in belangrijke mate aan de totstandkoming van het proefschrift bijgedragen.

Drukwerk : Gildeprint, Enschede

Printed in the Netherlands

To my family and friends

Table of Contents

List of abbreviations

ASTM	American Society for Testing and Materials
BET	Brunnauer Emmet Teller
CBM	Coalbed methane
CO_2	Carbon dioxide
CH_4	Methane
C_2H_6	Ethane
C_4H_{10}	Butane
d.a.f.	dry, ash free
D-R	Dubinin Raduskhjevich
ECBM	Enhanced Coalbed Methane
EOS	Equation of State
H_2O	Water
H/C	Hydrogen- carbon ratio
IEA	International Energy Agency
IPCC	Intergovernmental Panel on Climate Change
N_2	Nitrogen
O/C	Oxygen hydrogen ratio
PD	Pendant drop
ppm	Parts per million
Rmax	maxiumum vitrinite reflectance
RECOPOL	Reduction of CO_2 emission by means of CO_2 storage in coal seams in the Silesian Coal Basin of Poland
SANS	Small angle neutron scattering
TNO-NITG	Nederlands Instituut voor Toegepaste Geowetenschappen
UNFCCC	United Nations Framework Convention on Climate Change
Vt	total volume
Vm	matrix volume
Vol. %	Volume percentage
Vp	pore volume
Vmerc	Volume measured buy mercury porosimetry
Vmicro	Volume of micropores
Vn	Volume measured by nitrogen adsorption
wt.	weight
wf	water-free

Chapter One

Introduction

1.1 General introduction

1.1.1 The greenhouse gas carbon dioxide

Carbon dioxide (CO_2) is the main greenhouse gas produced from human activities, such as combustion of fossil fuels for energy generation, mobility and industrial activities. The amount of carbon dioxide in the earth's atmosphere has risen from pre-industrial levels of 280ppm to more than 365ppm. The major part of this increase has been created within the last 60 years (Whorf & Keeling, 1998). The concentration of CO_2 in the atmosphere in addition to other gases such as methane, nitrous oxides and halogenated compounds is expected to rise rapidly in the 21st century. According to studies reported by the International Energy Agency (and many others) it will contribute to global warming, and by that to rise in sea level and serious changes in meteorological conditions (IEA, 2002). This has a strong impact on ecosystems and infrastructures, especially in vulnerable parts of the world. The emission of CO_2 is of primary concern, because it is directly linked to our fossil fuel based society.

CO_2 emissions mainly depend on two factors, the technology to supply and use the energy and the level of energy consumption. The amount of energy used is a function of the world's rising population and the way energy is produced to supply the rising standard of living. It is generally accepted that human induced emissions

of greenhouse gases must be limited. The United Nations Framework Convention on Climate Change (UNCCC, 1992) was established to address this issue. Its goal is to stabilize greenhouse gas concentrations in the atmosphere. In the Kyoto protocol, the developed countries agreed to reduce their emissions by 5.2% below the levels of 1990, which is a step towards a stabilization of the climate (IPCC 2005). If CO_2 levels are stabilized now, it will take approximately 50 years before the concentration in the atmosphere will decrease (Socolow et al., 2004).

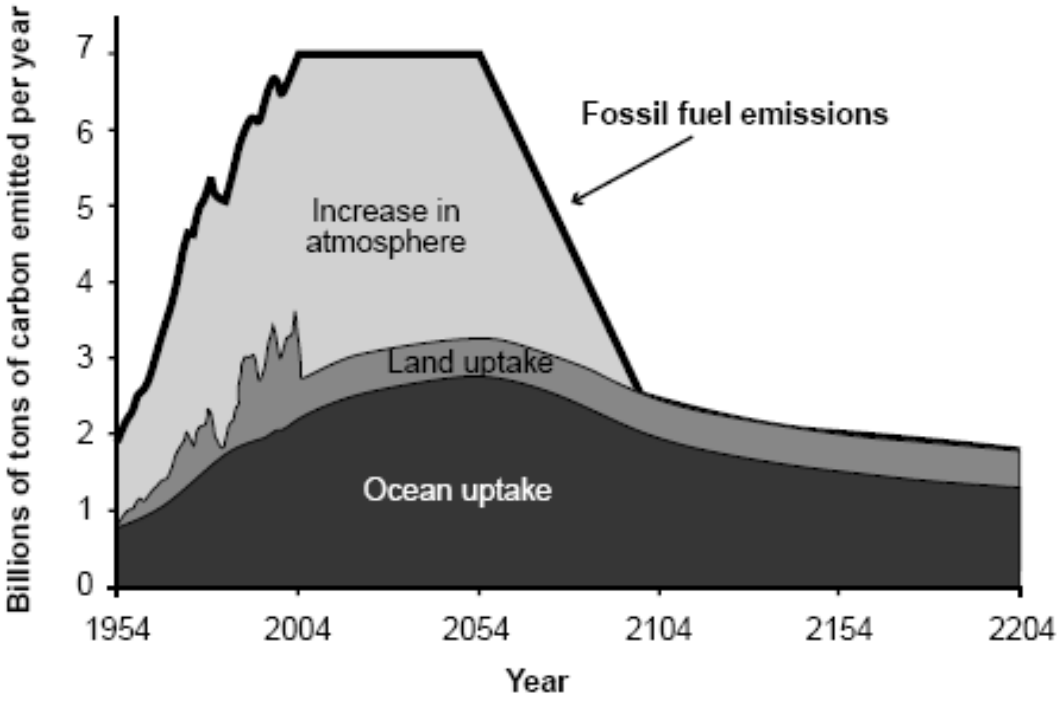

Figure 1.1: CO_2 emissions forecast, modified after Socolow et al, 2004.

However, for the reasons given above, greater reductions in emissions have to be considered to meet future UNCCC goals. If the concentration of CO_2 will be stabilized on a level that does not exceed 50% of the current level, a 60% reduction of emissions is needed in this century (IEA, 2002). To achieve such large reductions improved technologies are required to maintain today's living standards.

1.1.2 CO_2 sequestration strategies

To fulfill the Kyoto agreement on the reduction of emissions of greenhouse gases (UNFCCC, 1992), different methods are suggested to sequester CO_2. Concepts like

biofixation, which includes reducing deforestation, reforestation and afforestation as well as ocean disposal, can be seen as short-term storage strategies (IPCC, 2005; Gentzis, 2000). Sequestration strategies that cover geologic time scales are CO_2 injection in deep saline aquifers, depleted oil and gas reservoirs (Stevens & Gale, 2000), and unmineable coal seams (Reeves, 2001; Stevens et al., 1999). Those injection concepts require large point sources such as power plants, where the CO_2 can be captured and piped and/or shipped to the storage site.

The major drawback of all injection concepts is that they are energy and money consuming. A storage technique that has the potential to gain energy by producing natural gas is called Enhanced Coalbed Methane (ECBM) and its conceptual model is described in the following subsection.

1.1.3 CO_2 sequestration in coal

Coal seams can be considered as source rock and naturally fractured, low permeability, water saturated gas reservoir at the same time. One kg of bituminous coal can generate up to 300 liters of methane during coalification (Jüntgen & Karweil, 1966). The main part of this gas is released during the coalification process and may form conventional gas reservoirs. A small amount of the generated gas (~10-30 liters/kg) is adsorbed in on the internal coal surface depending on the prevailing coal rank. Under in-situ conditions, approximately less than 5% of the coal gas is present in the free state or is dissolved in pore water. Consequently, saturated coal reservoirs can easily contain up to five times the amount of gas contained in a conventional gas reservoir of comparable size, temperature and pressure. Excess gas is liberated to overburden rocks and may form conventional gas reservoirs, such as the Groningen gas field. Resources of coalbed methane, i.e. methane trapped within the porous structure of coal seams, may be as high as 250×10^{12} m³ worldwide (Gayer & Harris, 1996). That is many times more than the collective reserves of all the known conventional gas fields.

Coalbed methane is commonly recovered by reservoir pressure depletion. If the water pressure equals the desorption pressure, gas starts desorbing from the coal matrix to the adjacent cleats and can be produced together with the pore water via a production well (Seidle & Arri, 1990). This method is simple and effective,

but slow and in general not efficient. Reduction in reservoir pressure deprives the fluids of energy necessary to flow to the well bore (Gunter et al., 1997). Only a few countries in the world (USA, China, India and Australia) utilize this energy source commercially, benefiting from very favorable reservoir conditions. Due to initially enlightened tax concessions, the U.S. produces coalbed methane economically which covers a major part of its domestic gas supply.

In order to estimate the storage capacities of coal for gases, laboratory tests are performed on coal samples. Sorption isotherms are widely used to assess the amount of gas stored in coal as a function of pressure. Experimentally measured isotherms of CO_2, CH_4 and N_2 show that the gas sorption capacity of the same coal depends on the gas used. CO_2 is the most strongly adsorbing gas, followed by CH_4 and N_2. Chaback et al. (1996) found that the approximate ratios are 4:2:1, e.g. four molecules of CO_2 are adsorbed for two molecules of CH_4 and for every molecule of N_2 at same pressures and temperatures. Methane recovery can be enhanced either by N_2 stripping, i.e. lowering the methane partial pressure, or by injection of a higher adsorbing gas, such as CO_2 that displaces methane from its adsorption sites. The latter method is called CO_2-Enhanced Coalbed Methane (CO_2-ECBM).

The conceptual idea can be described as follows. CO_2 is injected into target coal seams, where it partly displaces water in the cleat system. CO_2 molecules diffuse into the coal matrix blocks, where they adsorb on the coal surface and displace methane molecules from the adsorption sites. It is expected that, depending on coal rank, substantially more CO_2 molecules can be sequestered for every released CH_4 molecule. Since CO_2 is sorbed on the internal surface, the target seams provide a safe storage medium over geologic time scales because CO_2 is mainly physically bound to the coal surface. In this way, coal layers serve as carbon dioxide sinks and energy producers at the same time.

Coal is an energy source commonly occurring on all continents but in a wide range of geologic settings. The ideal reservoir has to fulfill the following frame conditions in order to establish CO_2-ECBM as a successful, safe, and reliable method to sequester CO_2 and produce CH_4 (NITG-TNO, 2001):

- Simple geological structure: The reservoir should be minimally faulted and folded. Closely spaced faults can segment the reservoir into isolated blocks or act as pathways for CO_2 leakage.
- A homogenous reservoir: the reservoir is laterally continuous and vertically isolated to ensure efficient lateral sweep and containment of CO_2
- Coal geometry: Stratigraphically concentrated coal deposits. A few thick seams are preferred over dispersed multiple thin seams.
- Depth: Economic ECBM is limited to depths of 300 to 1500m.
- Gas saturation: Coal reservoirs that are saturated with methane are economically preferred.
- Adequate permeability: a permeability range of at least 1-5 mD is required. Most of the coal seams have even lower permeabilities. Finding adequate permeabilities will be a key exploration challenge.

There are currently only three known coalfield sites were CO_2 injection is being performed on a multi well scale. The "CO_2-Enhanced Coal Bed Methane Recovery Project" (Alberta ECBM) is a joint Industry-University project to investigate issues associated with CO_2 sequestration into deep coal beds. An isolated 5-spot pilot with four injection wells and one production well, sized between 20 and 40 acres, was used to inject CO_2 and later flue gas to enhance methane production (Alberta ECBM).

The Alliston Unit is situated in the San Juan basin in the U.S. and operated by Burlington Recourses. The Alliston site comprises of four CO_2 injection wells and nine methane producers. Formerly, these wells had been produced coalbed methane using conventional pressure depletion methods for over five years. Burlington drilled four injection wells and began CO_2 injection at an average rate of 20,000 m^3/day . In 5 years time, Burlington injected over 57 Billion m^3 of CO_2 with an increasing methane production (Stevens et al., 1999). Recently, one pilot CO_2 sequestration site in Poland (RECOPOL, 2001), operated by the Dutch geological survey TNO-NITG, has been established.

1.2 Research Problem

The process of CO_2 injection into coal for storage and enhanced coalbed methane production is not well understood and, therefore, requires information on the kinetics of transport and sorption in the micro porous coal structure. Fundamental research is crucial for reservoir models and CO_2 storage/methane production strategies. Whereas a vast amount of methane-coal interaction literature is available, work carried out on CO_2 interaction with coal is sparse and usually does not cover experimental work which is relevant for field applications. Therefore, CO_2 interaction with coal at high pressures and elevated temperatures has become a research topic in the last years. It has been shown that CO_2 does not follow common models or strategies of gas injection in coal.

This thesis covers experimental work on processes taking place during CO_2 injection into coal seams that have to be taken into account to assess the total storage capacity for CO_2. One key question is how different effects like surface wetting and gas diffusion processes into the heterogeneous, low permeable coal matrix control the total sorption capacity. Further the influence of water, occupying cleats and pore spaces in coal, is investigated. Water is considered to have a strong effect on the gas transport if the coal behaves as water-wet. The second key question is if the sorption capacity of coal determined by experiments is also the total capacity. Structural transitions of the coal properties may occur during measurements that have to be taken into consideration.

1.3 Outline of the Thesis

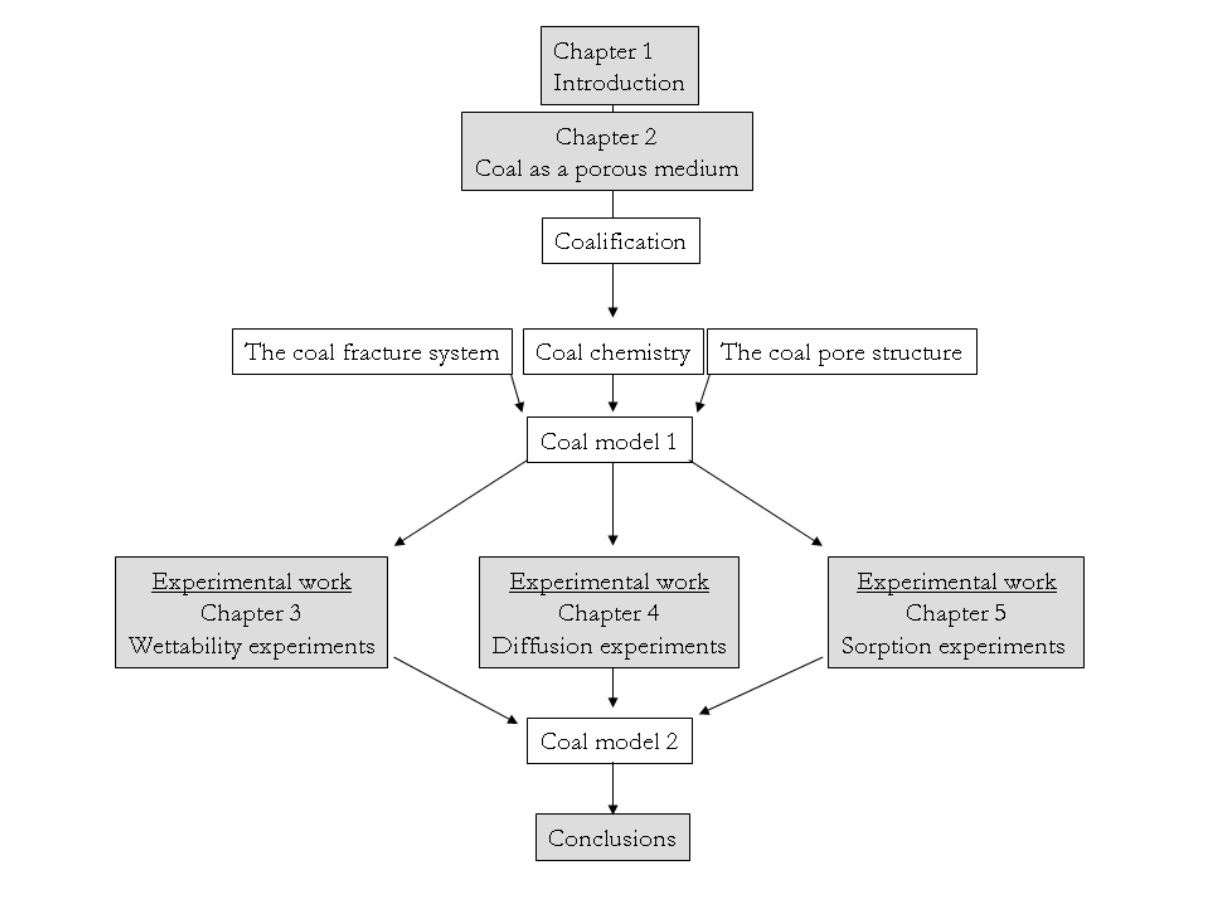

Figure 1.2: Outline of this thesis

This thesis is divided in three main parts, corresponding to studies on coal wettability in the water CO_2-coal-system (I), CO_2 diffusion in coal particles (II) and CO_2 sorption in coal (III). The leading thread of this thesis proceeds from the mechanism of CO_2 entering the coal matrix via the cleat system of the coal, the diffusive transport into the matrix blocks and finally the sorption processes at relevant reservoir pressures and temperatures. Within each part, specific problems, relevant both for the theory and for the practical implications, have been addressed and investigated. In *Figure 1.2* a schematic outline of this thesis is shown.

1.3.1 Part I: Wettability in a carbon dioxide-water-coal system

The effect of coal characteristics (coal composition, coal rank, mineral content) and temperature on wetting was the object of previous studies on the air- water-coal system only (Keller, 1987). Coal wettability is interpreted as a function of rank and composition. The CO_2-water-coal system in general and the influence of elevated pressures in particular have not been investigated. High pressure behavior, however, is crucial for CO_2 injection projects in coal seams at reservoir conditions. In this study, a modified pendant drop cell was used to measure the contact angles for two coal samples in a CO_2-H_2O-coal system. It was investigated whether a pressure increase (up to 14 MPa) has an effect by altering the coal wettability from H_2O-wet to CO_2-wet. Further, it was investigated to what extent a wetting change depends on coal surface chemistry which is related to rank differences. This Chapter is based on the following publications:

Nikolai Siemons, Hans Bruining, Hein Castelijns and Karl-Heinz Wolf, 2006. Pressure dependence of the contact angle in a CO_2–H_2O–coal system. Journal of Colloid and Interface Science, Volume 297, 755-761.

Nikolai Siemons, Hans Bruining, Karl-Heinz Wolf and Willem-Jan Plug, 2006. Pressure Dependence of the CO_2 Contact Angle on Bituminous Coal and Semi-Anthracite in Water. Paper 0605, Int. Coalbed Methane Symposium Tuscaloosa, USA, May 4-8.

1.3.2 Part II: Diffusive transport processes in coal

Coalbeds exhibit a multi-scale heterogeneity. Generally, coalbeds are characterized by a bimodal porosity system, the uniformly distributed network of fractures (cleats) and in between almost impermeable micro porous coal matrix blocks. Transport processes in cleats are commonly described by Darcy's law, whereas diffusion is the only transport mechanism in the coal matrix blocks. The generally accepted transport process into matrix blocks is diffusion, which may be the rate determining step for sorption during gas injection. Diffusion rates have been measured with a volumetric sorption set-up and interpreted in terms of coal

rank, water content and particle size. Experiments have been interpreted in terms of two independent characteristic diffusion times in the range of a surface diffusion process for both times. The work presented in this Chapter is based on the two publications. The first paper presents work on an upscaled diffusion model, accounting for diffusive gas transport in two structural coal matrix constituents (see Chapter 2) accounting for two different diffusion processes. Diffusion experiments on different coal samples, however, showed that the model is not able to reflect the prevailing coal structure from the experimental data. For this reason it was decided to build a set-up and experimentally measure diffusion behavior. The results are presented in the second paper.

Nikolai Siemons Johannes Bruining Bernhard M. Krooss 2004. Upscaled diffusion in coal particles. Geologica Belgica (Geol. Belg.) 7, 129-135.

Nikolai Siemons, Karl-Heinz A.A. Wolf and Johannes Bruining, 2007. Interpretation of carbon dioxide diffusion behavior in coals. International Journal of Coal Geology xx, xxx – xxx. in press,

1.3.3 Part III: Sorption characteristics

Sorption isotherms on ground coal samples are commonly used to assess the storage capacity of coals. The amount of sorption data increased in open literature in the last years, but supercritical CO_2 sorption isotherms on coal are sparse (Krooss et al., 2002; Fitzgerald et al., 2005). The fundamental problem that arises in interpreting the measurements is a volumetric change of the samples during sorption. This volume change cannot be measured directly due to experimental constraints. A model was developed and applied to correct excess sorption isotherms by a single volume factor to account for several effects occurring during the experiments. To investigate a wide range of coal ranks, parts of the measurements have been performed at TU Delft. Other raw data sets were provided by the Lehrstuhl für Geologie, Geochemie und Lagerstätten des Erdöls

und der Kohle, RWTH-Aachen. The outcome of this research is summarized in the following article:

Nikolai Siemons and Andreas Busch, 2007. Measurement and interpretation of supercritical CO_2 sorption on various coals. International Journal of Coal Geology 69, 229-242.

1.4 References

Alberta ECBM. Web resource: http://www.co2captureandstorage.info/

Chaback, J.J., Morgan, W.D., Yee, D., 1996. Sorption of Nitrogen, methane, carbon dioxide and their mixtures on bituminous coals at in-situ conditions. Fluid Phase Equilibria 117, 289-296.

Fitzgerald, J.E., Pan, Z., Sudibandriyo, M., Robinson, Jr., R.L., Gasem, K.A.M., Reeves, S., 2005. Adsorption of methane, nitrogen, carbon dioxide and their mixtures on wet Tiffany coal. Fuel 84, 2351-2363.

Gayer, R.A., Harris, I., 1996. Coalbed Methane and Coal Geology. Special Publication No 97, Geological Society London, London 340 pages.

Gentzis, T., 2000. Subsurface sequestration of carbon dioxide - an overview from an Alberta (Canada) perspective. International Journal of Coal Geology 43, 287-305.

Gunter, W.D., Gentzis, T., Rottenfusser, B.A., Richardson, R.J.H., 1997. Deep coalbed methane in Alberta, Canada: A Fuel resource with the potential of zero greenhouse gas emissions. Energy Convers. Mgmt. 38, 217-222.

IPCC special report, 2005. Carbon dioxide capture and storage. Intergovernmental Panel on Climate Change on the invitation of the United Nations Framework Convention on Climate Change.

IEA International Energy Agency, 2002. World Energy Outlook 2002. OECD/IEA, Paris Cedex.

Jüntgen, H., and Karweil, J., 1966. Gasbildung und Gasspeicherung in Steinkohlenflözen, Teilen 1 und 2. Erdöl Kohle-und Erdgas-Petrochemie 19, 339-344.

Keller, D.V., 1987. The Contact angle of water on coal. Colloids and Surfaces 22, 21-35.

Krooss, B.M., van Bergen, F., Gensterblum, Y. Siemons, N., Pagnier, H.J.M., David, P., 2002. High-pressure methane and carbon dioxide adsorption on dry and moisture-equilibrated Pennsylvanian coals. Int. J. Coal Geology 51, 69-92.

NITG-TNO, 2001. CO_2 sequestration in coal. NITG – Information May 2001. Web resource, http://www.nitg.tno.nl .

RECOPOL, 2001. http://recopol.nitg.tno.nl/index.shtml.

Reeves, S.R., 2001. Geological sequestration of carbon dioxide in deep unminable coalbeds: An integrated research and commercial-scale field demonstration project. Society of Petroleum Engineers, SPE 71794, 10 pages.

Stevens, S.H., Gale, J., 2000. Geologic carbon dioxide sequestration. Oil and Gas Journal 98, 40-44.

Stevens, H.S., Kuuskra, V.A., Spector, D., Riemer, P., 1999. carbon dioxide sequestration in deep coal seams: pilot results and worldwide potential. In: B.

Eliasson, P.W.F. Riemer and A. Wokaun (eds). Greenhouse Gas Control Technologies, Pergamon, Elsevier Science Ltd. 175-180.

Seidle, J.P., Arri, L.E., 1990. Use of Conventional Reservoir Models for Coalbed Methane Simulation. Paper CIM/SPE 90-118, CIM/SPE International Technical Meeting, Calgary, Canada, June 10-13.

Socolow, R., Hotinski, R., Greenblatt, J.B., Pacala, S., 2004. Solving the climate problem. Technologies available to curb CO_2 Emissions. Environment 46, 8–19.

UNFCCC, 1992. United Nations framework convention on climate change. United Nations, Bonn, Germany.

Whorf, T.P., Keeling, C.D., 1998. Rising Carbon. New Scientist 157, 54-64.

Chapter Two

Coal Structure

2.1 Introduction

The origin and formation of coal as well as the chemical composition and structure has been studied extensively in the past decades and a vast amount of literature is available. Standard textbooks summarize results of coal research of the last 100 years (van Krevelen, 1993; Stach et al., 1982; Francis, 1961). This chapter summarizes the most relevant aspects on coal composition and physical properties relevant for the research presented in this study. Up to today, the chemical structure has not been revealed completely.

The reason for this is that coal's precursor is complex plant material that underwent sedimentologic processes and a chemical and physical alteration (coalification). The atomic composition of coal can be determined with sufficient precision. The main components are carbon, hydrogen, oxygen, and small amounts of nitrogen and sulfur. The composition, however, changes successively with coalification. In general, increasing rank (degree of coalification) leads to a decrease in hydrogen and oxygen. Different coal models have been published, which don't represent a general "coal molecule" but an average macromolecule at a certain rank. Some examples are shown in *Figure 2.1* and *Figure 2.2*.

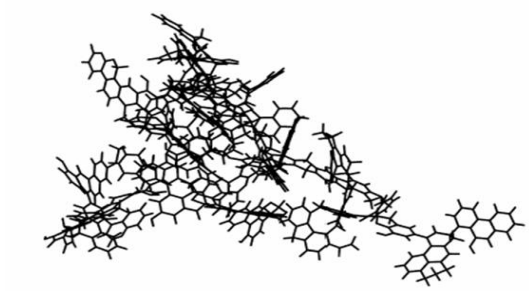

Figure 2.1: Coal macromolecule (Jones, 1999).

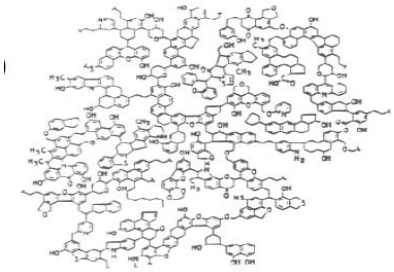

Figure 2.2: Coal macromolecule (Shinn, 1984).

2.2 Origin and formation of coal

Sedimentary organic matter like plant material is deposited and undergoes subsidence with a related burial history. The plant material progressively changes its chemical composition and macromolecular structure. The process is called organic metamorphism or, if referred to coal, coalification. Coalification stages are peat, lignite, coal and anthracite. The process can be subdivided in two main stages, biochemical degradation and physicochemical degradation.

2.2.1 Biochemical degradation

The biochemical degradation involves a chemical decomposition of organic matter by microorganisms such as bacteria and fungi. Humification affects the soft contents of the plants cells and not the cell walls, consisting of cellulose and lignin, which are the most resistant compounds. Hydrocarbons are extracted from the bulk and the material left behind is relatively enriched in oxygen and carbon.

Various humic substances such as phenols and humic acids are formed at this time. If the process continues the plant material will be completely degraded into carbon dioxide and water. When the plant material or degraded plant material is buried below the water table, aerobic organisms and oxidation can no longer attack. Anaerobic bacteria may still decompose the plant matter until it reaches a depth or ecological conditions which are unsuitable for these organisms. Anaerobic bacteria utilize the oxygen in the plant matter and even the more resistant compounds may

be attacked. Biochemical coalification ends at the rank of sub-bituminous coal, when humic substances have polymerized.

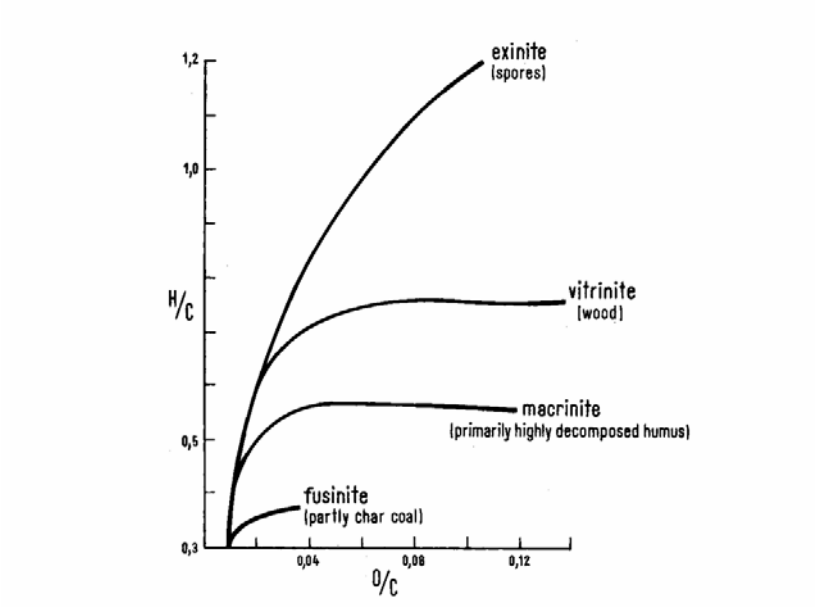

Figure 2.3: Coalification tracks of different macerals based on their H/C to O/C ratio (van Krevelen 1961).

2.2.2 Physicochemical degradation

Physicochemical degradation follows due to burial conditions. The overburden which is deposited, the increased heat flow due to subsidence and tectonic heat and pressure subsequently change the chemistry and structure of the remaining organic material. Water is pressed out and pore sizes decrease as pressure increases. Oxygen and hydrogen are released during thermal cracking. Water and carbon dioxide are first released. When coal rank is the range of a medium-volatile bituminous coal, a demethanation process starts (*Figure 2.4*). With these transformations, the carbon content increases and the oxygen content decreases (*Figure 2.3*).

Due to this relative increase in carbon, the calorific value of the coal increases with rank. Like other organic rocks, coal has the potential to generate hydrocarbons and other by-products (*Figure 2.4*). However, oil which is generated by coal is enclosed in the microporous structure and cannot be liberated. It will be further cracked down to natural gas, if coalification continues. During coalification,

huge amounts of gaseous compounds (mainly CH_4 and CO_2) are liberated. Jüntgen & Karweil (1966) reported a methane production of 0.3m³ gas/kg coal with coal increasing coalification from lignite to bituminous coal. If these gaseous products remain in the coal, they are called coal gas. Up to 90% of this coal gas is methane, which is adsorbed on the internal surface of the coal seam.

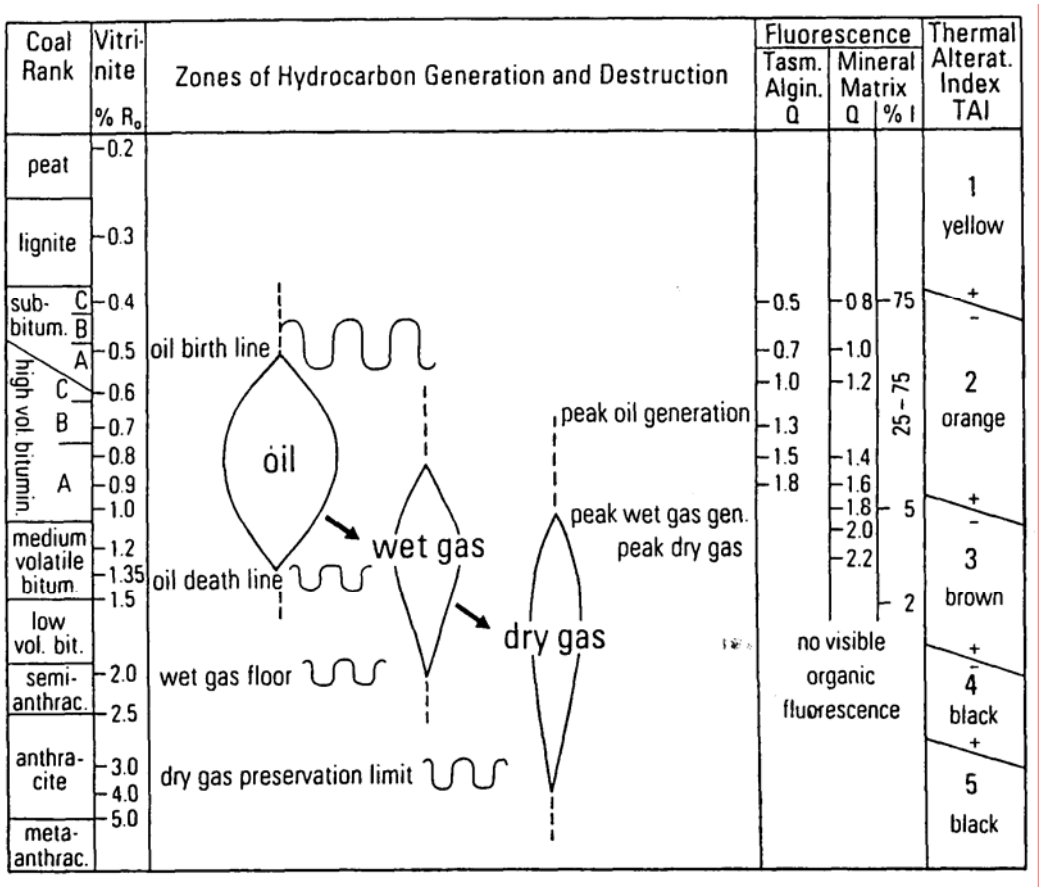

Figure 2.4: Hydrocarbon generation during coalification (Levine, 1993).

2.3 Developments in coal science

Due to the prevailing micro pore structure and the highly heterogeneous composition coal doesn't exhibit a unique molecular structure. Before 1960, coal was described as large three dimensional interconnected polycyclic structure with a slit shaped pore system (Given, 1960), comparable to the molecular structure of

graphite. New technologies and analytical methods helped to develop a new picture of the coal structure. These methods are:

(1) Oxidative degradation

(2) Solvent extraction techniques

(3) Spectroscopic measurements

(4) Sorption experiments

(5) Proximate and ultimate analysis

Francis (1961) reported, based on oxidation experiments, that coal is predominately aromatic and contains many condensed rings. Chakrabartty & Berkowitz (1974) came to the conclusion that coal contains large amounts of quaternary aliphatic carbon, its structure is diamond like with less than 50% aromatic carbon. Extraction experiments revealed that coal contains a varying amount of smaller molecules with a molar weight of less than 1000 which are mobile and extractable and a fraction of larger, fixed molecules (van Krevelen, 1961; Vahrman, 1970).

Ergun & Tiensuu (1959) and Friedel & Queiser (1959), using UV-techniques, also proposed the diamond-like structure. They concluded that coal could not be polyaromatic but also contains large amounts of aliphatic structures. X-ray diffraction was used by Hirsch (1954) to determine the distance between the aromatic rings in coals from 78-94% carbon content (*Figure 2.5*). In his classic work he concluded that the predominant coal structure changes its aromatic structure when containing 50-80% aromatic carbon. He introduced a rank depending coal structure model and distinguished between three cases.

(1) The open structure (C <85%) consists of cross linked and randomly distributed carbon lamellae exhibiting a high porosity.

(2) The liquid structure with carbon contents between 85% and 91% which is characterized by an ordered distribution of lamellae and a reduced amount of cross links that result in a low porosity.

(3) A carbon content that exceeds 91%. This structure is anthracitic with almost no cross links and graphite like carbon lamellae.

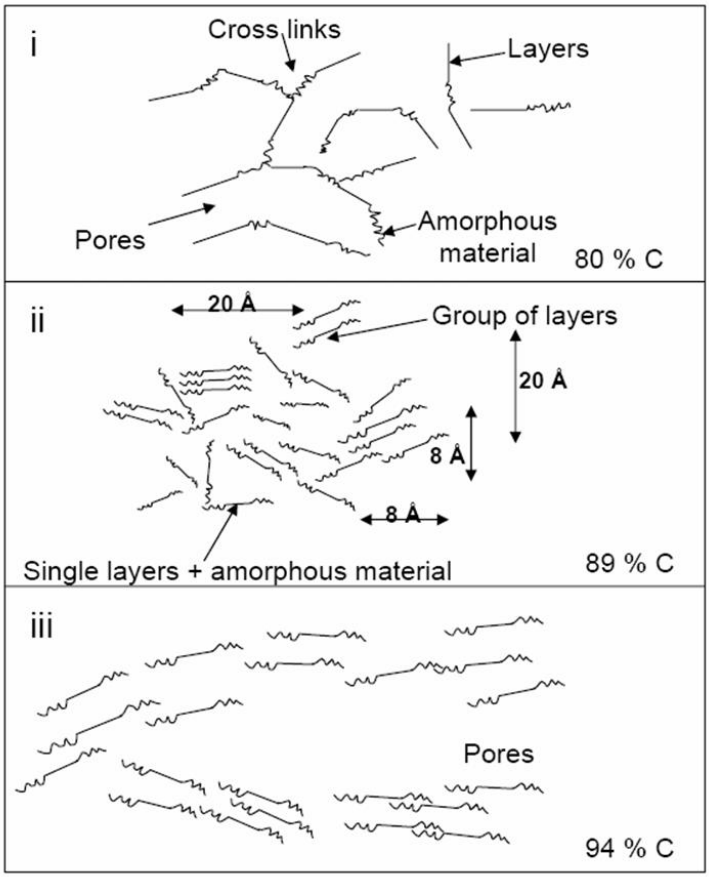

Figure 2.5: Structural coal model, modified after Hirsch (1954).

Low-pressure adsorption experiments are usually performed in the range of the vapor pressure of the adsorbate. Physical adsorption of gases and vapors at low pressures has shown to be a useful method for the characterization of micro

porous carbonaceous adsorbens (Ding & Bhatia, 2002), specific inner surfaces (Walker & Kini, 1965; Walker & Patel, 1970), pore volume, and pore size distributions (Mahajan, 1981).

The model today accepted that summarizes the several different findings in coal characterization mentioned above is called the "two-component model" (van Krevelen 1991). The basic approach of this model was already put forward by the turn of the century (Levine, 1993). In 1961 van Krevelen stated that "coal has a polymeric character" consisting of macromolecules. Brown & Waters (1966a; 1966b), and later Vahrman (1970) and Wiser (1973) described coal as a macro-polymeric network with small cross-linked aromatic parts exhibiting a host-guest structure.

The strength of this model is the combination of compositional parameters and the observable coal behavior. Levine (1993) states that "virtually every measurable property of coal can be interpreted (or reinterpreted) in the light of this model including gas sorption capacity, diffusion rates optical properties, liquefaction behavior, and cooking characteristics". As already mentioned in 2.2, coal can be described as a composition of a fixed polymeric component and a mobile, extractable bituminous component. The fixed polymeric component is also called the macromolecular network, exhibiting a three-dimensional interconnected structure (Larsen et al. 1995). The bituminous component is trapped in the pores of the first one.

The macromolecular component is build by crystallites which consist of basic structural units (BSU). BSU's are layers of aromatic rings bonded by covalent forces. The size of the BSU's lies between 6.0Å and 12Å for one (Lu et al., 2001), with up to five condensed rings (Bratek et al., 2002). The height or stacking of aromatic layers increases with rank but the dimensions are still not known well. Lu et al. (2001) reports a height of up to 13.75Å. Bratek et al (2002) concluded that the height of BSU's remains constant with a value of 16Å but increase in width. Agreement was achieved on the distances of the aromatic layers. Hirsch in 1954 and more recently Lu et al. 2001 and Bratek et al. (2002) reported values of about 3.4 and 3.9Å. The question is, however, if these sub-micropores contribute to the

sorption capacity of coal since they range in the same diameter as a CO_2 molecule. This issue is addressed in Chapter 4.

The molecular phase, occluded in the macromolecular structure, is more or less loosely bound to the macromolecular network. It consists of low-molecular-weight components like CO_2, H_2O, N_2, C_2H_6, C_4H_{10}, and furthermore condensates and oil. The composition of the molecular component is dominated by the prevailing coal rank. At low coal ranks, the dominant component is water, at medium rank oil, and at high rank methane and water (Levine, 1993).

The fact that coal swells by the use of solvents like pyridine or organic vapor but does not dissolve completely gave rise to the idea to characterize coal as a polymer and apply techniques from polymer sciences. Macromolecular networks can be described by their glass transition temperature T_g At that temperature, polymers change from glassy to a rubbery state. The glassy state is characterized by a restricted mobility of the macro molecules and only short movements are possible. A glassy solid is brittle and the intermolecular interaction energy is larger than the available thermal energy. If the thermal energy rises by warming the coal and exceeds T_g, the polymer becomes rubbery (Larsen 2004). In the rubbery state, the constituents are mobile (Tekely et al., 1987) and alter the structural properties like the porosity, diffusivity and elastic moduli (Haward, 1973).

The glass transition temperature T_g for coal depends on the coal rank and on solvent used. For coal, T_g varies between 580° and 623°K, but is lower when solvents act on the coal structure (Lucht et al., 1987). Khan & Jenkins (1985) found that helium had no effect on T_g whereas CO_2 lowered the softening temperature from 673 to 300K with pressures ranging from 0.3 to 5.5MPa. This finding, however, is the only publication that reports a coal softening at these low temperatures and has been criticized recently. Furthermore, attempts have been made to reproduce this experiment without any result, and therefore the outcome is questionable.

All findings discussed above provide useful information about the microstructure of adsorbents. These methods are useful for the classification purposes but they cannot be used to quantitatively predict adsorption capacities,

for instance. Experimental adsorption experiments for a specific applications e.g. under reservoir conditions, are therefore crucial from an applications point of view.

2.4 The concept of coal rank

The petrographically distinguishable constituents of coal are called macerals, following a concept introduced by Stopes (1935). Macerals evolve from different organs or tissues of the initial coal-forming plant materials during the course of coalification. Because of the variable but severe alteration it is not always possible to recognize the original materials. Macerals themselves are the microscopically recognizable individual constituents of coal and coal type depends on their quantitative participation. They control the chemical, physical and technological properties of a coal of a given rank (ICCP, 1963). Vitrinite is derived from woody plant material, mainly cellulose and lignin, and is the most common maceral. Coalification products of spores, algae, waxes and lipids are called liptinites (formerly known as exinite) and consist of hydrogen-rich aliphatic chains. Inertinite originates from a weakly oxidized plant material or natural chars, generated by forest fires. This maceral is rich in carbon fixed in condensed aromatic structures and low in oxygen and hydrogen (Wolf, 1988).

The maturity level of coal refers to the degree of coalification of the organic matter. It is estimated by measuring the moisture content, specific energy, and reflectance of vitrinite or volatile matter, also known as rank parameters. It should be mentioned that there is no single rank parameter that can be used for all coal ranks. Low-rank coal is usually characterized by the calorific heating value and water content, whereas higher rank coals are distinguished by means of vitrinite reflectance, fixed carbon content and volatile matter content. *Table 2.1* indicates the difference in rank parameter with increasing rank after Diesel (1992).

Table 2.1: coal rank parameters

rank	Carbon [wt % d.a.f.]	Volatile matter [wt % d.a.f.]	Specific energy [MJ/kg]	In situ moisture [wt %]	Vitrinite reflectance [wt %]
Wood	50	>65	-	-	-
Peat	60	>60	14.7	75	0.2
Brown coal	71	52	23.0	30	0.42
Sub-bituminous	80	40	33.5	5	0.63
High volatile bituminous	86	31	35.6	3	1.0
Medium volatile bituminous	90	22	36.0	<1	1.6
Low volatilebituminous	91	14	36.4	1	1.9
Semi-antracite	92	8	36.0	1	2.8
Anthracite	95	2	35.2	2	7

2.5 The porous system of coal

In general, transport and sequestration processes in coal depend on the following structural features:

Porosity: The ratio between the volume of the pore space in reservoir rock and the total bulk volume of the rock. The pore space determines the amount of space available for storage of fluids.

Permeability: A measure of the ability of a material (typically, a rock or unconsolidated material) to transmit fluids through it. It is of great importance in determining the flow characteristics of hydrocarbons in oil and gas reservoirs, and of groundwater in aquifers. The usual unit for permeability is the darcy, or more commonly the milli-darcy or md (1 darcy = 1 x 10^{-12}m²).

Specific (micro) pore volume: The volume occupied by one unit volume of substance. Molecules with different effective diameters lead to different micro pore volumes because pores smaller than the molecules are not occupied.

Specific inner surface: Represents the total surface area of the porous or powdered compound with respect to its volume or mass.

Wettability: The relative degree to which a fluid will spread into or coat a solid surface in the presence of other immiscible fluids.

The difference between clastic rocks and coal is articulated in these parameters. The today state of knowledge is described briefly in the following sections.

2.5.1 Coal density

The density is defined as mass per unit volume. The latter is difficult to define for coal and this has its implications on coal density measurements. Three methods can be considered to determine the coal volume that lead to three different densities, called the bulk or grain density excluding the pores, the apparent density, where the measuring fluid only penetrates parts of the pore space and the true or absolute density including the whole pore space.

The bulk density is measured by mercury by applying a very low fluid pressure, the grain is enclosed by mercury and it is assumed that the liquid does not intrude into the pores. Helium is considered to be the best measuring fluid to determine the matrix density because it is considered to penetrate the entire open pore space of coal. The helium atom is very small (≈0.2nm) and may access pores smaller than 0.3nm. Furthermore, helium is considered to be inert, remains gaseous and shows no interaction with the coal surface forces. This assumption is acceptable regarding the negligible heat of wetting values of helium on coal (Malbrunot 1997). All other gases or liquids used for density measurements result in apparent density values. The coal densities shown in *Table 2.3* are densities measured by helium displacement.

2.5.2 Macro- and microporosity in coal

Due to its macromolecular three-dimensional structure, coal exhibits an extensive and complex porosity. Coal and coal seams are generally represented by a dual-porosity model. A macro pore or cleat (fracture) porosity and a micropore or primary porosity can be distinguished. The intermediate mesopores are found in cleats and larger pores of the matrix blocks. In general, two main sets of cleats are distinguishable and are called face and butt cleats. Face and butt cleat systems are usually oriented orthogonal to each other and commonly perpendicular to the bedding plane. The face cleats are more extensive in length and terminate the short butt cleat system. This leads to permeability anisotropies in coal seams. The cleats origin from tectonic activity and the coalification process itself.

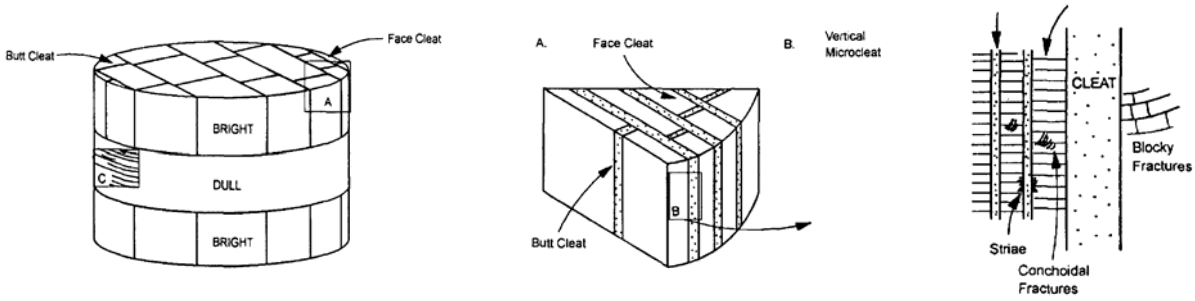

Figure 2.6: Butt and face cleats in coal. Dull and bright represent the different macroscopic coal bands, modified after Gamson et al. 1992.

The macro porosity serves as highways for gas and liquids and mass flow obeys Darcys Law. The micro porosity, that is responsible for more than 90% of the coal porosity, is situated in the coal matrix blocks bounded by the fracture system of coal.

The microporosity is one of the main factors that control the gas storage capacity of coal. Microporosity can be related to two phases within the matrix blocks, e.g., the crystallite phase formed by the BSU's and the amorphous phase between crystallites (Milewski-Duda et al, 2000). The pore space inside the crystallites is responsible for the sub-microporosity in coal. The ratio between the aromatic (crystallite) and aliphatic (amorphous) phase in coal is rank dependent, the aromatic part increases with increasing rank (Lu et al., 2001). This rank dependency alters the microporous structure inside the matrix blocks. Prinz (2004) found in his work that the linear growth of the crystalline phase with rank leads to a linear

increase in sub-microporosity. In low-rank coals the micropore spectrum is wide and crystallites are small and less abundant. Due to a loss in aliphatic groups and side chains and the formation of aromatic rings, the pore spectrum becomes smaller for higher-rank coals, and also pore sizes become smaller. In high-rank coals (anthracites) the sub-micropores are dominant.

In order to estimate pore characteristics several techniques have been developed and were also applied in coal research. The total volume V_t of coal consists of the matrix volume V_m and the pore volume V_p

$$V_t = V_m + V_p. \qquad \textit{Eq. 2.1}$$

The porosity φ is defined as the fraction of the pore volume of the total volume

$$\Phi = V_p / V_t = V_p / (V_p + V_m). \qquad \textit{Eq. 2.2}$$

If the porosity is determined by pycnometric techniques, the pore volume which is accessible for the medium used is measured. The widely used pore size classification was proposed by Dubinin (1960) and later accepted by the IUPAC (International Union of Pure and Applied Chemistry) and plotted in *Table 2.2*.

Table 2.2: Pore size classification [nm] IUPAC

<0.4	sub-micro pores
0.4 - 2.0	micro pores
2.0 - 50	meso pores
>50	macro pores

The microporous pore space in coal can be quantified by measuring the pore size distribution, the internal surface and the pore volume. Mercury porosimetry, low pressure adsorption experiments, and X-ray and neutron scattering are the most common techniques (Radinsky et al., 2004). Mercury porosimetry was used in the past to characterize the meso- and macroporous structure with the drawback of the unknown coal compressibility. The different techniques mentioned above

provide different insights in the porous system because they characterize different pore size classes. Gan et al. (1972) performed an extensive study on the nature of porosity in coal, using gas adsorption and mercury porosimetry to cover the whole spectrum of pore sizes. Accordingly, the total open pore volume is the volume penetrated by helium V_t. The pore volume V_{merc} of pores larger than 300 nm is measured by mercury intrusion, between 300 and 12nm by nitrogen adsorption V_n, and the volume of pores smaller than 12nm. V_{micro} is the total volume minus the mercury volume minus the nitrogen volume

$$V_{micro} = V_t - V_{merc} - V_n. \qquad \textit{Eq. 2.3}$$

It is assumed that coal exhibits a molecular sieve-structure and the surface area of coal is predominantly present in the micropores. Furthermore, they found the pore size distribution to be rank dependent. Macro pores are more abundant in low rank coals, whereas micro pores become dominant in high rank coals. Alexeev et al. (1999) reported that the contribution of closed pores to the total porosity in coals ranging from high volatile bituminous to anthracite coal in most cases exceeds 60%.

2.5.3 Permeability in coal

In general, permeability is the ability of a material to transmit fluids or gases through its connected pore system when subjected to a pressure difference without physically or chemically alterating the material. In coal the expression permeability covers two transport mechanisms. Firstly, the pressure-driven Darcy transport of gases and liquids via a network of natural fractures (cleats) through a coal seam. Secondly, permeability describes the concentration-driven, diffusive transport of gases and liquids through the macromolecular and microporous network of the coal matrix blocks.

Relative permeability curves in coal cleat systems for water and gas have been reported by several researchers and their results are summarized in the article of Meaney & Patterson (1996). They conclude that relative gas permeability strongly depends on water saturation. A small decrease in saturation results in a strong

increase in gas permeability. However, the amount of literature is limited and mainly relevant to specific field situations. As fast mass transport in coal mainly occurs in the cleat system, the permeability of a coal seam is strongly related to stress conditions in the seam, the moisture content, and mineral inclusions which reduce the effective cross section contributing to flow. As coal is known to be extremely heterogeneous and complex in structure and chemistry, and the fact that coal is not inert to the phases passing through, general conclusions are difficult to obtain.

Next to the stress pattern in coal seams, cleat spacing and height are also affected by the lithotype and its thickness. Fracturing is abundant in bright bands (Patterson et al., 1992) and decreases with increasing lithotype thickness (Close, 1993). Levine (1996) reported that initial absolute permeabilities in coal seams vary over several orders of magnitude, ranging from millidarcy (md) to darcy. Further, there exists no absolute lower limit for permeability in coal seams. As a rule of thumb, with respect to coalbed methane production, he considers values in the range of a few tens of md "excellent" and values below 1 millidarcy (md) to be "poor". Dabbous et al. (1997) measured relative permeabilities and drainage air-water capillary-pressure curves on US cylindrical coal samples at various overburden pressures. They obtained cleat permeabilities for the Pittsburgh coals used ranging between 1 to 13mD. They found that P_C-curves are strongly depending on the applied confining pressure, and computed fracture permeability were lower than the measured ones. Relative permeability, derived from P_C-curves using Purcell's capillary model were not in agreement with the measured ones.

Clarkson & Bustin (1997) found that permeability varies with lithotype composition ranging from bright coal (4.1 md) to dull coal (0.016 md) and concluded that bright coal provides the most permeable pathways for gas transmission. A dependence of gas permeability on coal rank could not be shown. Data published in the last decades are difficult to compare due to the variety in measurement techniques. A range of 10^{-4} to 10^{2} md is widely accepted but should be used more as an indication rather than quantitatively. Permeabilities in matrix blocks depend on its pore size distribution, on molecules occupying the pore space, and on pore sizes, which are a function of coal rank. In general, micropores are

abundant, with a broader micropore spectrum in low rank coals than in anthracites (Prinz, 2004). Therefore, the transport process inside the matrix blocks is mainly diffusive.

The connectivity of micropores in coals still remains unclear. Some researchers state that the pore system in coal is interconnected, with slit shaped pores and bottleneck pore openings in the size of molecules, which constrict the diffusional transport. Larsen et al. (1995), Radovic et al. (1997) and Cui et al. (2004) studied the pore system of selected U.S. American coals by adsorption experiments and concluded that coal pores are isolated and can only be reached by diffusion through the solid coal matrix. They reported diffusion rates of CO_2 in coal roughly in the order of 10^{-10} m^2/s. General observations of molecule diffusion in coal assuming a polymer structure have been summarized by Larsen et al. (2004). They found that the diffusion coefficient decreases as molecular size increases and linear molecules (like CO_2) diffuse faster than branched molecules of the same size. Further, diffusion increases with greater flexibility of the polymer chains, whereas the degree of crosslinking decreases the diffusion coefficient.

2.5.4 Specific inner surface/micropore volume

The surface of an adsorbent is defined as the area accessible for the binding of gas and liquid molecules. Since coal exhibits a porous structure, this area is defined as the inner surface of the entire pore space. The measured area of the inner coal surface depends strongly on the used technique. However, the inner surface is not an absolute value but serves as a relative characterization of a substance. The inner surface of coal is considered to be one of the key factors to determine the adsorption capacity and depends on rank, the petrographic composition, i.e., maceral content and moisture content.

The inner surface, like the porosity, decreases with rank. At ranks around 1.0 to 1.3% VR_m, the surface area values reach a minimum and increase again until coal reaches the anthracitic rank. This behavior is expressed by many adsorbtives (CO_2, CH_4, N_2, and H_2O). A vast amount of literature on inner surface measurements has been published (Moffat & Weale, 1955; Anderson et al., 1966; Walker & Kini, 1965; Walker & Patel, 1975; Gan et al., 1972). A review on surface area

measurement literature on coal by Mahajan (1991) discusses and summarizes the developments and findings of the last 50 years. The discrepancy in surface area values measured with different gases is explained by the effect of activated diffusion. BET- N_2 surfaces (Brunauer et al., 1938) have values of several tens of m^2 and are an order of magnitude smaller than surfaces measured with CO_2. N_2 is not able to penetrate the micropores of coal. Therefore N_2-isotherms are measured to characterize only the mesoporous structure of multiporous materials. Recently, Prinz (2004) showed that N_2-surfaces correlate very well with surface area measurements obtained by small angle neutron scattering (SANS).

CO_2 as a measuring gas was proposed in the middle of the last century because it has a much smaller effective diameter (~0.33 nm) and a far higher critical temperature (31.5°C) that allows performing experiments at higher pressures. However, there is an increasing amount of concern that CO_2 overestimates the inner surface by the effect of CO_2-induced swelling in coal. It is postulated by Reucroft and Sethuraman (1987) and Mahajan (1991) that CO_2 dissolves in coal, swells the pore structure and, therefore, penetrate closed pores by surface diffusion that is inaccessible for other gases. This process may account for up to 50% of the surfaces for lignite and sub-bituminous and up to 20% for bituminous coals (Mahajan, 1991). The quantification of coal swelling is still under discussion and lately back in the scope of interest with respect to CO_2 storage in coal seams. This issue is discussed separately in Chapter 2.5.6. It can be concluded that surface-area measurements can be used semi-quantitatively and more reliable interpretation of the adsorption data can be obtained by the determination of the micropore volume capacity following Dubinin's (1960) approach, based on the *T*heory of *V*olume *F*illing of *M*icropores (TVFM) developed by Polanyi. He assumes an adsorption field with short range attraction forces that drags molecules towards the surface. The adsorption potential is therefore a function of the distance of the molecule from the surface.

A quantitative description of microporosity in coals is based on this model and utilizes low-pressure CO_2 adsorption isotherms at ~273K. However, this approach has the drawback that it only interprets sub-critical adsorption behavior of gases and vapors. Up to now, no adsorption theory exists that accurately describes the

adsorption processes of gases beyond their critical temperature, except the model of Langmuir, developed in 1916. This model is described in Chapter 5.

2.5.5 Wetting of coal

The wettability of a solid with a liquid or gas is usually determined from their contact or wetting angle Θ. In general, contact-angle measurements are easily performed by establishing the tangent angle of a drop with a solid surface at the base. Furthermore, it is possible to estimate solid surface tensions from contact angles using the relation recognized by Young in 1805.

$$\gamma_{lv} \cos\Theta_Y = \gamma_{sv} - \gamma_{sl} \qquad \textit{Eq. 2.4}$$

with the liquid-vapor interfacial tension γ_{lv}, the solid-vapor interfacial tension γ_{sv} and the solid-liquid interfacial tension γ_{sl}. Θ_Y denotes the Young contact angle. Since γ_{lv}, γ_{sv}, and γ_{sl} are thermodynamic properties of the liquid, vapor and solid, Young's equation implies a single unique contact angle. However, the experimentally measured contact angle may or may not be equal to Θ_Y that is inserted in *Eq. 2.4*. This is due to heterogeneities in solids of natural matter. The difference in contact angle of an advancing liquid Θ_a and of a receding liquid Θ_r is called contact angle hysteresis H. On ideal smooth homogenous surfaces there is no hysteresis and the measured angle Θ_m equals Θ_Y.

$$H = \Theta_a - \Theta_r \qquad \textit{Eq. 2.5}$$

Contact angle hysteresis appears if the solid surface is rough and/or chemically heterogeneous. In general, contact angles measured on rough surfaces are larger than on smooth surfaces of the same composition, (Grundke et al., 1996) and were also recognized in experiments described in detail in Chapter 3. This surface roughness leads to errors because the measurements partly reflect the topography rather than surface energies. There are no general criteria how smooth a solid surface has to be in order to have no influence on the contact angle measured. The general point of view is to polish a surface as smooth as possible. Drehlich et al.

(1997) developed a method to prepare coal surfaces for contact-angle measurements that results in representative and repeatable results for the air-water-coal system. This procedure was followed to prepare coal surfaces for the experiments conducted in Chapter 3. Another effect that may influence contact-angle measurements is surface heterogeneity. Chemically patterned surfaces like coal introduce a variety of patches with different surface tensions. This leads to a multiplicity of equilibrium contact angles. A contact angle in equilibrium is associated with the global minimum in free energy of the system. Other contact angles reflect metastable equilibrium states. This transition towards equilibrium depends on the energy available to overcome energy barriers that exist between metastable states (Brandon & Mamur, 1996).

Wettability of coal is known to be one of the main factors controlling coal-utilization processes like flotation and oil agglomeration to remove significant amounts of mineral matter. Extensive work published on wettability of coal is thus mainly related to this topic and presented in Chapter 3. The surface composition depends on the rank of a coal. The chemical heterogeneity of coal surfaces is due to a mixture of constituents. Metoxy-, hydroxyl-, carboxyl- and carbonyl- groups are hydrophilic, whereas paraffin, graphite and naphtalene groups behave hydrophobic (Polat & Chandler, 1999). Due to coalification coal loses its hydrophilic functional groups and the coal structure enriches in aromatic carbon (Lu et al., 2001). This leads to an increasing hydrophobicity with increasing rank (Keller, 1987). Different methods have been developed to measure contact angles, e.g. the sessile drop technique, static and dynamic captive-bubble technique. The experiments, described in Chapter 3, were conducted using the captive-bubble technique.

2.5.6 Coal swelling

As already mentioned in 2.5.4, coal swelling is back in focus of interest due to CO_2 storage in coal seams. Coal is considered to exhibit a polymeric macromolecular cross-linked structure. These cross-links are formed by side reactions between the aliphatic chains.

Early work on this phenomenon (~1930s) is mainly related to extraction experiments with solvents like methanol, acetone, benzene and pyridine. Later, coal swelling and shrinkage was also recognized in adsorption and desorption experiments with gases like CO_2, CH_4 and N_2. Several hypothesizes have been brought forward to explain coal swelling. Van Krevelen (1961) summarized previous work on solvent swelling of coal. Since coal does not dissolve, even in solvents that swell it to more than twice the original volume, it must be three-dimensionally cross-linked and has to consist of such large macromolecules that entanglements cannot be separated. Brenner (1985) concluded from his experimental study that some solvents have the ability to remove polar hydrogen bonds, leading to a mobilization of the macromolecular chains. This increase in flexibility, while the coal is swollen, is interpreted as a loss of effective crosslink density. If the solvent is removed, secondary interactions lead to partly new arrangement of the chains and less cross-links than before. Bodiliy et al. (1989) found that polar cross-links were not entirely reformed upon removal of the solvent. Larsen and Kovacs's (1978) results on the evaluation of time/stress curves revealed that the coal structure recovers to 99% after removal of the stress and, therefore, they considered coal to be covalently cross-linked. Weak forces only make a small contribution to the macromolecular association. All the findings discussed until now are related to the use of strong solvents. It is questionable if gases, especially N_2 and CH_4, would follow the same mechanism. Lately, Kelemen et al. (2006) found that strain is correlated with the quantity of gas adsorbed, i.e., CO_2, CH_4 and N_2. The dependence of the coal matrix shrinkage/swelling coefficient on both the type and quantity of gas adsorbed was characterized by plotting swelling (the ratio between strain and adsorbate concentration) against the adsorbate concentration. A constant value for the swelling coefficient indicated a linear correlation of strain with the quantity of gas adsorbed, independent which gas was used (Figure 2.7).

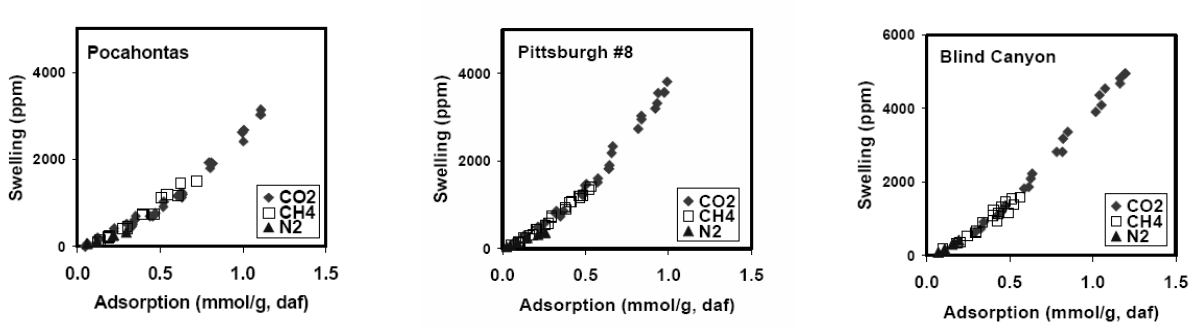

Figure 2.7: Relationship between strain versus sorbate concentration for CO_2, CH_4 and N_2. (Kelemen et al., 2006).

The phenomenon of gas-induced or differential swelling seems to be only related to the fact that the amount of CO_2 is reaching smaller pore spaces due to its smaller effective diameter and adsorbs in higher quantities than the other gases with larger diameter. Therefore, the term "adsorption-induced swelling" should be used instead. Pan & Connell (2006) developed a general model for adsorption-induced swelling of coal. Their model assumes that the surface energy change caused by adsorption is equal to the elastic energy change of the coal solid. This model was tested on sorption data available in literature and is in good agreement with the experiments (Pan & Connell, 2006). From this viewpoint, the idea of CO_2 as a strong solvent responsible for swelling is questionable. For field applications it means that if the moles of CH_4 produced equals the moles CO_2 injected no swelling of the coal matrix occurs (*Figure 2.7*).

2.6 Coal samples used

The coal samples, provided from mines in Europe, were delivered in blocks of several hundreds of kilos. All delivered samples where sealed in plastic to prevent the coal from moisture loss and oxidation. Prior to all experiments performed for this study, cylindrical coal samples of 75 mm diameter and 10-25 cm length were drilled from the lumps, parallel to the bedding plane and sealed in evacuated plastic sleeves. The samples were ground to a particle diameter smaller than 3 mm, and then transferred to sealed glass bottles for further use in the sorption and diffusion experiments. For the wetting experiments, small blocks of coal of several cm in

length were cut from the drilled cylinders and stored in degassed and distilled water. The coal properties are shown in table *Table 2.3*

Table 2.3: sample properties

Proximate analysis	Selar Cornish	Warndt Luisenthal	Tupton H
Moisture [%]	1.26 - 1.4	1.39	10.09 - 15.7
Volatile matter (w.f.) [%]	7.9- 10.35	40.51	29.2 - 36.15
Ash (w.f.) [%]	3.94 - 5.5	2.77	2.05 - 6.2
Fixed Carbon (d.a.f.) [%]	89.27	58.36	63.24
Calorific value [MJ/m³]	33.2		26.2
Ultimate analysis			
Carbon [%]	85.68	81.3	73.01
Hydrogen [%]	3.36	5.58	5.26
Nitrogen [%]	1.56	1.88	1.95
Sulphur [%]	0.68	0.69	0.57
Oxygen (diff.) [%]	5.58	5.47	5.53
H/C	0.47	0.82	0.86
O/C	0.05	0.05	0.06
Coal Petrology			
R_{max} [%]	2.41	0.71	0.53
St. dev.	0.06	0.05	0.01
N	100	100	100
Vitrinite	73.6	74.4	59.4
Liptinite	0	15.6	14
Inertinite	24.6	9	25.8
Minerals	1.8	1	0.8
rank	Semi-Anthracite	High. Vol. Bit. B	High vol. Bit A
Dubinin –Raduskevic method (CO_2)			
Inner surface m³/g	207	***	244
Micropore volume cm³/g	0.07	-	0.08

Sample Selar Cornish

This sample origins from Selar colliery, South Wales Coalfield.

Sample type: Coal seam: Cornish, open cast, 4 samples from stockpile. Coal excavated 5 to 10 days previously
Stratigraphy: Westphalian B strata

Sample Warndt Luisenthal

The lumps were mined in the intramountain Saar Basin in Western Germany and origin from seam nr. 1 (code 495).

Sample type: 6 samples taken in-situ from excavated seam.
Stratigraphy: Westphalian A.

Sample Tupton H

This sample origins from the South Wales Coalfield.
Sample type: 4 samples taken in-situ from excavated seam.
Stratigraphy: Westphalian A strata

2.7 Gases and gas properties

All measurements were performed with gases helium, carbon dioxide and methane.

Table 2.4: Gases used in this study

gas	purity	Purity [Vol %]	Mole weight
Helium	4.6	99.996	4.0026 g/mol
Carbon dioxide	3.5	99.95	44.0098 g/mol

In order to determine the amount of gas present in the system, the real-gas law for the individual gas was used:

$$n = PV/(z(P,T)\,RT), \qquad \text{Eq. 2.5}$$

where n is the molar mass [mol], P the pressure [MPa], V the volume [m^3], R the gas constant [8.3143 kJ mol^{-1} K^{-1}] and z the gas compressibility, depending on gas pressure and temperature.

For Helium, the z factor is calculated using compressibility data published by Michels and Wouters (1946) and is valid for temperatures from 0-150°C and pressures ranging from 1 to 17.4 MPa. Carbon dioxide densities are calculated using the equation of state developed by Span and Wagner (1996).

2.8 Conclusions

In this chapter a brief introduction in the state of the art knowledge of coal is given. Ongoing research in coal science and the application of different analytical methods for more than 70 years revealed much of the coal origin, formation, structure and chemistry such that a general coal model could be developed. However, this general model fails in predicting any of the processes related to gas transport, retention and reactions taking place in coal with respect to CO_2 sequestration and methane generation when it comes to simple laboratory experiments, not to mention field or reservoir simulation studies. This is mainly related to the complex chemistry and microporous structure coal exhibits, which is dependent on rank. Up to now the only way to assess transport and retention properties are laboratory experiments. A new promising approach might be the use of SANS measurements, because this method is able to characterize the sub-microporous pore space (<0.4nm in diameter) of coal where diffusion, sorption and reaction of the penetrants take place. The findings described in the following chapters, however, are based on sorption and wettability experiments conducted with experimental set-up designed and built at the Dietz laboratory.

2.9 References

Alexeev, A.D., Vsilenkoand, T.A., Ulyonova, E.V., 1999. Closed porosity in fossil coals. Fuel 78, 635-638.

Anderson, R.B., Bayer, J., Hofer, L.J.E., 1966. Equilibrium sorption studies of methane on Pittsburgh Seam and Pocahontas No. 3 seam coal. In R.F. Gould (ed.): Coal science Advances in Chemistry Series 55, American Chemical Society, New York, pp. 386-399.

Bodiliy, D.M., Wann, J.P. and Knopp, V., 1989. The effect of solvent swelling on coal structure. Proc. Int. Conf. Coal Sci. Volume 1. Tokyo, October 3-6, 201-204.

Brandon, S., Mamur, A. 1996. Simulation of contact angle hysteresis on chemically heterogeneous surfaces. Journal of Colloid and Interface Science 183, 351-355.

Bratek, K., Bratek, W., Gerus-Piasecka, I., Janseinko, S., Wilk, P., 2002. Properties and structure of different rank anthracites. Fuel 81, 97-108.

Brenner, D., 1985. The macromolecular nature of bituminous coals. Fuel 64, 167-173.

Brown, H.R., Waters, P.L., 1966a. The function of solvent extraction products in the cooking process. I. Yields, properties, and mode of release of chloroform extracts. Fuel 45, 17-40.

Brown, H.R., Waters, P.L., 1966b. The function of solvent extraction products in the cooking process. II. A theory of the mechanism of of thermal softening. Fuel 45, 41-49.

Brunauer, S., Emmet, P.H., Teller, E., 1938. Adsorption of gases in multimolecular layers. J. Am. Chem. 60, 309-319.

Chakrabartty, S.K., N. Berkowitz, N., 1974. Studies on the structure of coals. 3. Some inferences about skeletal structures. Fuel 53, 240-245.

Clarkson, C.R., Bustin, R.M., 1997. Variation in permeability with lithotype and maceral composition of cretaceous coals of the Canadian Cordillera. Int. J. Coal Geology 33. 135-151.

Close, J.C., 1993. Natural fractures in coal. In: B.E. Law and D.D. Rice. Hydrocarbons from coal. AAPG Studies in Geology 38. American Society of Petroleum Geologists, Tulsa, pp 39-77.

Cui X., Bustin, R.M., Dipple, G.M. 2004. Selective transport of carbon dioxide, methane and nitrogen in coal: insights from modeling of experimental gas adsorption data. Fuel 83, 293-303.

Dabbous, M.K., Reznik, A.A., Mody, B.G., Fulton, F.F., Taber, J.J., 1974. Gas-water permeability in coal at various overburden pressures. SPE Journal 16, 261-268.

Diesel, C.F.K., 1992. Coal- bearing depositional Systems. Springer Verlag, New York.

Ding, L.P., Bhatia, S.K., 2002. Vacancy solution theory for binary adsorption Equilibria in Heterogeneous Carbon . AIChE Journal 48, 1938-1956.

Drelich, J., Laskowski, J.S., Pawlik, M., Veeramasuneni, S., 1997. Preparation of coal surface for contact angle measurements. J. Adhesion Sci. Technol. 11, 1399-1431.

Dubinin, M.M., 1960. The potential theory of adsorption of gases and vapours for adsobents with energetically nonuniform surfaces. Chem. Rev. 60, 235-241.

Ergun, S., Tiensuu, V., 1959. Tetrahedral structures in amorphous carbons. Acta Cryst. 12, 1050-1061.

Francis, W., 1961. Coal, its formation and composition. Edward Arnold Publishing, London.

Friedel, R.A. Queiser, J.A., 1959. Ultraviolet-visible spectrum and the aromaticity of coal. Fuel 38, 369-380.

Gan, H., Nandi, S.P., Walker, P.L., 1972. Nature of the porosity in American coals. Fuel 51, 272-277.

Given, P.H., 1960. The distribution of hydrogen in coals and its relation to coal structure. Fuel 39, 147-153.

Grundke, K., Bogumil, T., Gietzelt, T., Jacobasch, H.J., Kwok, D.Y., Neumann, A.W., 1996. Wetting measurements on smooth, rough and porous solid surfaces. Prog. Colloid. Polym. Sci. 101, 58-68.

Haward, R.N., 1973. The Physics of Glassy Polymers. Wiley, New York.

Hirsch, P.B., 1954. X-ray scattering from coals. Proc Roy. Soc. London 226, London, 552-562.

ICCP International Committee for Coal Petrology, 1963. International Handbook of Coal Petrography, 2nd edition, Suppl. to 2nd edition, Centre Nat. de Rech. Sci., Paris.

Jones, J.M., Pourkashanian, M., Rena, C.D., Williams, A., 1999. Modeling the relationship of coal structure to char porosity. Fuel 78, 1737-1744.

Jüntgen, H. J., Karweil, J., 1966. Gasbildung und Gasspeicherung in Steinkohlenflözen. Erdöl, Kohle, Erdgas, Petrochemie 19, 251-258.

Kelemen, S.R., Kwiatek, L.M., Lee, A.G.K., 2006. Swelling and sorption response of selected Argonne Premium Bituminous Coals to CO_2, CH_4, and N_2. Paper 0604, Int. Coalbed Methane Symposium Tuscaloosa, USA, May 4-8.

Khan, M.R., Jenkins, R.G., 1985. Thermoplastic properties of coal at elevated pressures: effects of gas atmospheres. Proc. Int. Conf. on Coal Science, Sydney.

Keller, D.V., 1987. The Contact angle of water on coal. Colloids and Surfaces 22, 21-35.

Krevelen, D.W. van, 1993. Coal, Typology-physics-chemistry-constitution. Elsevier Scientific, Amsterdam.

Krevelen, D.W. van, 1961. Coal, Typology-physics-chemistry-constitution. Elsevier Scientific, Amsterdam.

Larsen, J.W., 2004. The effects of dissolved carbon dioxide on coal structure and properties. Int. J. Coal Geology 57, 63-70.

Larsen, J.W., Hall, P., Wernett, P.C., 1995. Pore Structure of the Argonne Premium Coals. Energy and Fuels 9, 324-330.

Larsen, L.W., Green, T.K., Choudhury, P., Kuemmerle, E.W., 1981. The effect of reagent access on the reactivity of coals. In M.L. Gobaty, K. Ouchi (eds.) Coal Structure, Advances in Chemistry Series 192, Washington.

Larsen, J.W., Kovac, J., 1978. Polymer structure of bituminous coal. ACS Symposium Series 71, 36-39.

Levine, J.R., 1996. Model study of the influence of matrix shrinkage on absolute permeability of coal bed reservoirs. In: R. Gayer and I. Harris (eds.), Coalbed

Methane and Coal Geology. The Geological Society Special Publication, London, 197-212.

Levine, J.R., 1993. Coalification: The evolution of coal as source rock and reservoir rock for oil and gas. In: B.E. Law and D.D. Rice (eds.), Hydrocarbons from coal. AAPG Studies in Geology 38, American Society of Petroleum Geologists, Tulsa, 39-77.

Lu, L., Sahajwalla, V., Kong, C., Harris, D., 2001. Quantitative X-ray diffraction analysis and its application to various coals. Carbon 39, 1821-1833.

Lucht, L.M., Lamon, J.M., Peppas, N.A., 1987. Macromolecular structure of coals. 9. Molecular structure and glass transition temperature. Energy and Fuels 1, 56-58.

Mahajan, O.P., 1981. Physical characterization of Coal. Fuel 60, 744-746.

Mahajan, O.P., 1991. Carbon dioxide surface area of coal: The 25 year paradox. Carbon 29, 735-742.

Malbrunot, P., Vidal, D., Vermesse, J., 1997. Adsorbent helium density measurement and its effect on adsorption isotherms at high pressure. Langmuir 13, 539-544.

Meaney, K., Patterson, L., 1996. Relative permeability in coal. SPE Journal 29, 735-742.

Michels, G., Wouters, H., 1941. In Landolt-Börnstein (1971): Zahlenwerte und Funktionen aus Physik, Chemie, Astromomie Geophysik und Technik. 6th. edition Vol. 2 part 1, p14 Springer Verlag.(in German).

Milewsky-Duda, J., Duda, J., Nodzensky, A., Lakatos, J., 2000. Absorption and adsorption of methane and carbon dioxide in hard coal and activated carbon. Langmuir 16, 54-58.

Moffat, D.H., Weale, K.E., 1955. Sorption by coal of methane at high pressure. Fuel 34, 449-662.

Pan, Z., Connell, L.D., 2006. A theoretical model for gas adsorption-induced coal swelling. Int. J. Coal Geology, in Press.

Pan, Z., Connell, L.D., 2006. Measurement and modeling of gas adsorption induced coal swelling. Paper 0636, Int. Coalbed Methane Symposium Tuscaloosa, USA, May 4-8.

Patterson, L., Meaney, K., Smyth, M., 1992. Measurements of relative permeability, absolute permeability and fracture geometry in coal. In: B.B. Beamish and P.D. Gamson (eds.), Coalbed methane research and development in Australia 4, James Cook University, N. Queensland, Australia, 79-86.

Polat, J., Chandler, S., 1999. Adsorption of PEO/PPO triblock co-polymers and wetting of coal. Colloids and Surfaces A: Physicochemical and Engineering Aspects 146, 199-212.

Prinz, D., 2004. Die Porenstruktur von Kohlen. PhD thesis (in German), University of Technology Aachen (RWTH). Aachen, Germany.

Reucroft P.J., Sethuraman A.R., 1987. Effect of pressure on carbon dioxide induced coal swelling. Energy & Fuels 1, 72-75.

Radinsky, A.P., Mastalerz, M., Hindea, A. L., Hainbuchner, M., Rauch, H., Baron, M., Lin, J.S., Fan, L., Thiyagarajan, P., 2004. Application of SAXS and SANS in

evaluation of porosity, pore size distribution and surface area of coal. Int. J. Coal Geology 59, 245-271.

Radovic, L.R., Menon, V.C., Leon Y Leon, C.A., Kyotani, T., Danner, R.P., Anderson, S., and Hatcher, P. G., 1997. On the porous structure of coals: Evidence for an interconnected but constricted micropore system and implications for coalbed methane recovery. Adsorption 3, 221-232.

Shinn, J. H., 1984. From coal to single-stage and two-stage products: A reactive model of coal structure. Fuel 63, 1187-1196.

Stach E., M.T., Mackowsky, M.T., Teichmuller, M., Taylor, G.H., Chandra, D., Teichmuller, R., 1982. Stach's Textbook of Coal Petrology. 3t^{h} edition. Gebruder Bortraeger, Berlin, Stuttgart.

Stopes, M., 1935. On the petrology of banded bitumonous coals. Fuel 14, 4-13.

Tekely, P., Nicole, D., Delpuech, J.J., Julien, L., Bertho, C., 1987. Carbon-13 CP-MAS NMR study of changes in molecular mobility of coal after pyrolysis at 590°C. Energy and Fuels 1, 121-122.

Tissot, B.P., Welte, D.H. 1984. Petroleum formation and occurrence. Second edition. Springer, Berlin.

Vahrman, M., 1970. The smaller molecules derived from coal and their significance. Fuel 49, 5-16.

Walker, P.L., Kini, K.A., 1965. Measurement of the ultrafine surface area of coal. Fuel 44, 453-459.

Walker, P.L., Patel, R.L., 1970. Surface areas of coals from carbon dioxide adsorption at 298 K. Fuel 49, 91-94.

Wiser, W.H., 1973. In: Proceeding of the EPRI Conference on Coal Catalysis, Conference Proceedings, Paolo Alto, CA, (1973), pp. 3.

Wolf, M., 1988. Torf und Kohle. In: H. Füchtbauer (ed), Sedimentpetrologie, Sedimente und Sedimentgesteine Vol. II. Schweitzerbart, Stuttgart.

Young, T., 1805. An essay on the cohesion of fluids. Trans. R. Soc. London 95, 65-87.

Chapter Three

Pressure Dependence of the Contact Angle in a CO_2-H_2O-Coal System

3.1 Abstract

Carbon dioxide (CO_2) injection into coal layers serves the dual purpose to enhance coal bed methane production (ECBM) and to store CO_2. The efficiency of this process is expected to be much higher if water is the non-wetting phase in the coal-water-gas system. Therefore, carbon dioxide contact angles in two coal-water-CO_2 systems have been measured. The captive bubble technique was used within a pressure range from atmospheric pressure to 140 bar at a constant temperature of 45° C.

Two sets of measurements have been performed, one on a polished semi-anthracite, the second set on a polished high volatile bituminous B (hvbB) coal sample. For the anthracite the following observations have been made. At atmospheric pressure, the contact angle of a CO_2 droplet increases with time, but stays below 90°. At higher pressures (>3 bar) the contact angle increases beyond 90°. This shows that the semi-anthracite coal sample behaves CO_2-wet at system pressures above 3 bar.

CO_2 contact angles on the bituminous coal sample show a different behavior. In the pressure range from atmospheric to 85 bar, CO_2 contact angles are independent of pressure and exhibit values of around 85°. At pressures beyond 100

bar, the coal surface becomes CO_2 wet. The bituminous coal sample is water wet up to much higher pressures than the anthracite. This behaviour is related to the difference in stability of the water film between the coal surface and the CO_2. The hydrophobicity of coal increases with rank due to a loss of functional groups which are responsible for hydrogen bonds between coal molecules and water. For the relevant pressures during CO_2 storage, the anthracitic coal behaves as CO_2-wet, whereas in bituminous coal the injection pressure has to exceed a pressure of 100 bar in order to wet the coal surface.

It can be concluded that the efficiency of carbon dioxide injection and retention in coal strongly depends on surface properties of the prevailing coal.

3.2 Introduction

Coal exhibits an extensive fracturing system called the cleat system, in which it is possible to discern a number of cleat systems at different scales. The matrix blocks between the smallest cleat system have diameters of a few tens of microns (Gamson et al. 1993). If the cleat system is filled with water, the CO_2 molecular diffusion rate is small ($D \approx 2 \times 10^{-9}$ m²/s) and independent of pressure. If the cleat system is filled with gas the diffusion rate is much larger i.e. $D \approx 1.7 \times 10^{-7}$ m²/s at 100 bar (Bird et al, 1960). It is expected that the smaller cleat network is filled with water if the coal-water-gas system is water-wet and filled with gas if water is the non-wetting phase. Therefore it is asserted that wetting behavior plays an important role in CO_2-ECBM production. Moreover, the presence of water impedes the process of gas sorption (Mavor et al., 1990; Nishino, 2001; Krooss et al, 2002). For this reason an experimental study of the wetting behavior of a coal-water-CO_2 system as a function of pressure was undertaken. It can be asserted that the exposed coal surface originally formed the bounds of a cleat.

Contact angle measurements provide a simple method to characterize the interfacial energies of a solid in contact with fluids and thus the wetting behavior (Adamson & Gast, 1990). In general, these measurements are performed by direct observations of drops deposited on the solid, and viewed from one side. Overview

articles describe in detail various technical aspects of a set-up that measures droplet shapes (Spelt & Vargha-Butler, 1996).

Chapter 3.5 describes the experimental set-up that was developed to measure contact angles from atmospheric pressure to 144 bar. Furthermore the sample preparation and experimental procedure are described. This section also explains the image-processing procedure to remove artifacts and to enhance the droplet contour line. Chapter 3.7 discusses the contact angle measurements in terms of the wetting behavior of the coal. The findings are summarized in the conclusions.

3.3 Wetting properties of coal

Investigations of the wettability behavior of coal reported in the literature are largely based on contact angle measurements for the coal-water-air system at atmospheric pressure. Gutierrez-Rodriguez et al. (1985) found that the contact angle depends on coal rank. They quantified the effect of surface oxidation using the captive bubble technique. In general, three types of surface components can be distinguished i.e. strongly hydrophobic, weakly hydrophobic and hydrophilic. Low rank coals appear to be hydrophilic and coals become increasingly hydrophobic with increasing rank. Murata (1981) performed measurements on pressed pellets of pulverized coal. He found that the contact angle depends on the hydrogen and oxygen content of the coal. Keller (1987) has summarized literature data (Gutierrez-Rodriguez et al., 1984; Murata, 1981; Gutierrez-Rodriguez & Aplan, 1984; Fuerstenau, 1981) on the coal-water-air system. The contact angles appear to be largely in the range between 60°-90°. Keller (1987) is able to represent observed trends in measurements of the contact angle θ by assuming that $\cos\theta$ is an area-weighted average of the cosine of the contact angles on the heterogeneous surface. To our knowledge there are no contact angle measurements of coal at elevated pressures.

The usual problems with contact angle measurements are all encountered with contact angle measurements on coal. First, surface oxidation alters the properties of the coal surface. Gutierrez-Rodriguez et al. (1984) and Gutierrez & Aplan (1984) observed a contact angle decrease (increased hydrophilic behavior) in a water-air

coal system after exposing its surface for several hours to oxygen-sparged water. Secondly, the wettability of the coal surface is highly variable due to its heterogeneous composition. Keller (1987) found strongly hydrophobic behavior for the paraffinic hydrocarbon fraction, intermediate behavior for the aromatic fraction and strongly water wet behavior for the minerals and water filled pores. However, as in crude-oil-rock-water systems, it is expected that the wetting properties depend on the complex chemistry as a whole.

The wettability heterogeneity leads to a varying contact angle. Consequently the droplet will have a non-spherical shape and a non-circular three-phase contact line. As a result the left and right contact angles observed in a vertical cross-section will be slightly different. However, large variations of contact angles along the three phase contact line lead to a large water-gas interface, which is energetically unfavorable. Therefore the equilibrium droplet shape favors smooth variations along the three phase contact line. This also explains the empirical equation proposed by Keller (1987) i.e. the cosine of the contact angle equals a weighted average of the cosines of the contact angles of the components constituting the coal surface.

3.4 Effects of surface heterogeneity

Determination of the contact angle puts severe demands on the smoothness of the surface (Spelt & Vargha-Butler, 1996; de Gennes, 1985; Fox & Zisman, 1950). The contact angle hysteresis i.e. the difference between the advancing and receding angle may be 10° or more for non-smooth surfaces. Joanny & de Gennes (1984) point out that the main reasons for contact angle hysteresis are the surface energy fluctuations related to rough surfaces and chemical heterogeneity. Rough parts of the surface are partially smoothed because the wetting fluid fills the crevices leading to composite surfaces consisting of substrate and the wetting fluid.

The same phenomenon is also expected to remove roughness on a very small scale. De Gennes (1983) relates the force exerted by the surface heterogeneity on the contact line to the force originating from the distortion of the interface on the contact line. The latter is described as an elastic force proportional to the deviation

of the position of the contact line with respect to its unperturbed position. When the surface energy heterogeneity is small there is only one solution and there is no contact angle hysteresis. When the surface energy heterogeneity is sufficiently large there is more than one stable solution and hysteresis is expected. From the analysis it is clear that the solid surface must be smooth and homogeneous. Drelich et al. (1997) state that in practice reproducible contact angles on coal can be obtained if the micro-roughness of the coal surface i.e. the height distance between tops and valleys is less than 40-55 nm. Equilibrium contact angles are established after all three phases get in contact with each other.

A number of electrochemical processes are relevant. A water film formed on the coal surface must be ruptured before contact between the carbon dioxide and the coal surface is established (Hirasaki, 1991a; Hirasaki, 1991b; Hirasaki, 1991c). As a result an equilibrium contact angle will only be established after some time. In addition, two aspects that are specific for the coal-carbon dioxide-water system are important. Contact angles between coal and carbon dioxide are expected to be influenced by the adsorption of CO_2 on the surface.

According to Gibbs' adsorption equation, the surface tension between water and coal decreases due to adsorption on the surface. This would lead to a contact-angle increase. Furthermore, to avoid random formation of CO_2 droplets the water was not saturated with carbon dioxide at the prevailing pressure. As a consequence, however, diffusion of CO_2 into the water phase will occur and the droplet will decrease in size. From the view point of the CO_2 droplet two receding contact angles at the left and right side of the droplet are observed.

3.5 Experimental

3.5.1 Sample preparation

Two coal samples have bee used for this study. The Warndt Luisenthal (hvBb) and Selar Cornish (semi-anthracite) sample were mined in the Saar basin in Germany and South Wales respectively. The coal properties are given in *Table 3.1*.

Several coal samples were drilled from lumps of coal and cut into small blocks of a few centimeters length using a diamond saw. One side was polished according to a method given elsewhere (Drehlich et al., 1997). The coal samples were wet polished with a series of abrasive papers with a grit from 60 to 1200, followed by polishing with 0.5 μm abrasive alumina powder and a fibrous cloth. Water washing and ultrasonic cleaning finalized each polishing step. The samples were submersed in doubly distilled water and evacuated for 48 h. This procedure allowed the removal of air from the coal pores and water to penetrate the pore system. The coal sample was taken out of the water, built in the sample holder and transferred to the experimental set-up.

Table 3.1: Results of the coal petrology, proximate and ultimate analysis

sample	Warndt Luisenthal	Selar Cornish
rank	hvbB	Semi anthracite
Vmax [%]	0.71	2.41
Vitrinite [%]	74.4	73.6
Liptinite [%]	15.6	0
Inertinite [%]	9	24.6
Minerals [%]	1.0	1.8
Volatile Matter (w.f.) [%]	40.5	10.4
Calorific value [MJ/m^3]	-	33.2
Carbon [wt %]	81.3	85.7
Hydrogen [%]	5.58	3.36
Nitrogen [%]	1.88	1.56
Sulfur [%]	0.69	0.68
Oxygen [%]	5.47	5.58

3.5.2 Experimental set-up

The experiments were carried out in a pendant drop (PD) cell (Huygens, 1990) adapted to perform captive-bubble contact-angle measurements. The cell itself is a stainless steel tube with a void volume of approximately 16 cm³. Thermally pre-

stressed glasses serve as windows at both ends of the cell. Viton O-rings seal between the glasses and the cell. Through the back window, light is provided.

An endoscope is placed near the front window. A digital camera with a pixel resolution of 640×400 is mounted on the endoscope and records the images. The cell can withstand pressures up to 600 bar at temperatures up to 200 °C. This is well beyond the limit of the conditions of interest to us, i.e. pressures ranging from 1 bar to 144 bar and a temperature of 45°C.

The cell is placed in an insulated air cabinet that provides stable temperatures (±0.2°C). The set-up is connected to a single high-pressure displacement pump. This pump enables water injection into the cell and is used to generate the desired experimental pressure within the system.

A capillary tube is connected to the bottom of the cell and serves as a gas injection device. At the end of the capillary, an exchangeable tip with an outer diameter of 1.59 mm is mounted. The capillary is connected to a micro-needle valve and a high-pressure gas reservoir. The needle valve restricts the amount of gas transferred from the reservoir to the injection tip to control the bubble volume at the end of the tip.

3.5.3 Conduct of experiments

First the PD-cell (Figure 3.1) with the coal sample is evacuated while valves 1, 2, and 3 are closed. Then, with the vacuum pump still running, valve 2 is opened and degassed water is slowly injected into the cell. When the cell is completely filled with water, the vacuum pump is switched off. At this point the cell contains water at atmospheric pressure. Valve 1 is opened and degassed water is circulated at atmospheric pressure for eight hours to clean the cell and tubing. A Du-Nouy ring tensiometer was used to measure the surface tension of the injected and produced water, both were found to be 0.054 N/m. Carbon dioxide was flushed via valves 4, 5, 7, and 6 to avoid air contamination in the experiment. If a higher pressure than atmospheric is required, the piston pump is used to increase the water pressure in the cell. Subsequently, the gas reservoir is filled with carbon dioxide via the gas booster and valves 4 and 5 until the pressure exceeds the water pressure in the cell by 10 bar. Finally all valves are closed and the system is allowed to reach thermal

equilibrium for 48 hours before it is ready to use. In order to simulate in-situ conditions the set-up was kept at a constant temperature of 45°, i.e. above the critical temperature of CO_2 (31.2°C).

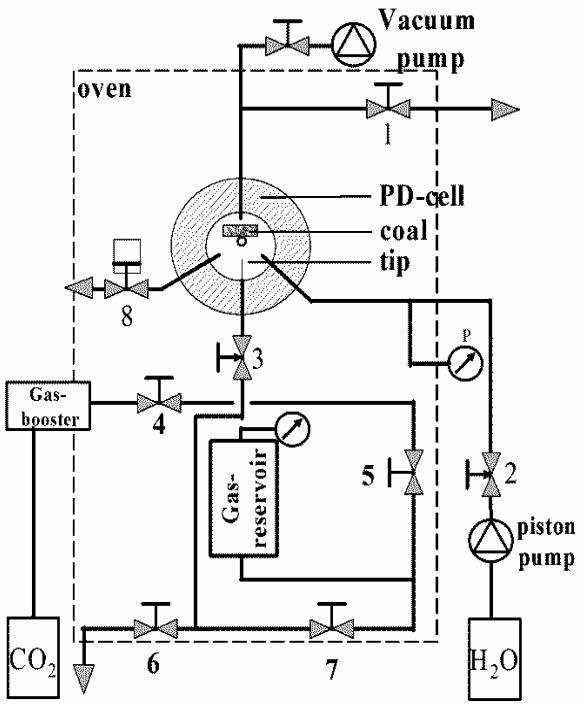

Figure 3.1: schematic view of the set-up.

For experiments at atmospheric pressure valve 1 remains open. For high-pressure experiments this valve is closed. In order to inject small portions of gas, valve 7 is opened and subsequently closed to fill the small volume between valves 3, 6, and 7 with carbon dioxide. Needle valve 3 is then repeatedly opened to allow small amounts of gas to enter the PD-cell. After some time the carbon dioxide becomes visible as a bubble at the end of the tip. The bubble grows until it hits the coal surface. Gas injection is stopped by closing valve 3. The bubble gradually decreases in size. During this process a camera, connected to an endoscope, captures images of the bubble until the bubble has disappeared completely.

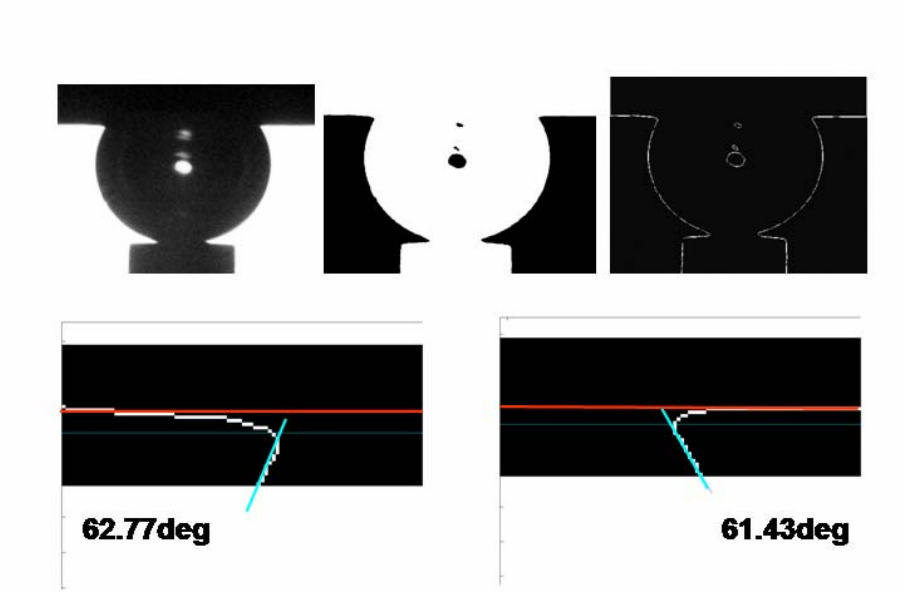

Figure 3.2: Image processing of a droplet and determination of left and right contact angles. Top left: the raw image. Top middle: the same droplet converted to a black and white image. Top right: droplet after edge enhancement. Below: the magnified image near the three phase contact line and determination of the contact angles. The slope near the surface is attributed to a spurious shadow. Such an abrupt change in curvature would be incompatible with gravity/ capillary pressure equilibrium.

A Matlab routine was programmed to convert the images (see Figure 2) into black and white (top-middle), followed by an edge enhancement procedure (top-right). Finally, the images were cropped by a selected set of coordinates (bottom) to magnify the three phase contact line of the top right image. The cropped images were subjected to the following procedure to determine the contact angles. The procedure uses only a few parameters that need to be adjusted. The parameters are chosen such that (1) the white ring due to refraction in the middle part of the bubble is removed, (2) distorted points (due to the shadow of the bubble on the coal surface) are ignored, (3) five adjacent points at the coal water interface at the leftmost part of the image are connected with five adjacent points at the rightmost part to find the base line. For the bottom left image the X- and Y-coordinates of

the white pixels are used to calculate the mean coordinates of the left-side curve representing the water-CO_2 interface and also the slope and direction. The same is done for the bottom right image. With these mean coordinates and the slopes with respect to the base line the angles can be calculated (Figure 3.2).

3.6 Experimental Results

Experiments have been performed at various pressures from atmospheric to ~144 bar. In all experiments the following behavior is observed. When the bubble is released from the tip, it settles at some position at the coal surface that represents an optimum in terms of interfacial and gravitational energy, depending on its size. It is therefore always slightly shifted from a position vertically above the tip.

The difference between the right and left contact angle is always less than 10° and usually less than 5°. Contact angles can be measured until the diameter of the bubble drops below 0.3 mm. In a control experiment the coal surface was covered by a coated microscope glass plate and the measured contact angles were about 85° ± 2° in a pressure range from atmospheric pressure to ~140 bar. In all experiments, the bubble disappearance rate is about the same whether the coal surface is covered with a glass plate or not. In particular a disappearance time exceeding 450 minutes was observed in the atmospheric pressure experiments with and without glass plate. In all other experiments the disappearance time is less than 60 minutes.

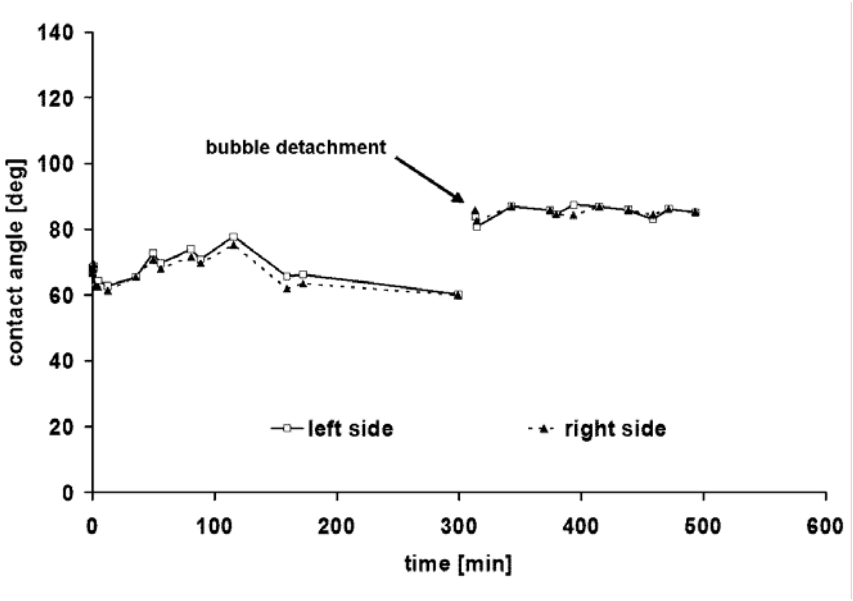

Figure 3.3: Contact angle history for the atmospheric pressure experiment. Left and right contact angles are indicated. At the discontinuity the droplet is detached from the tip.

At atmospheric pressure the following typical sequence of events is observed (Figure 3.3). The gas pressure is slightly increased until CO_2 forms a bubble at the top of the tip. The bubble grows to a size of about 2mm diameter and is captured between the tip and the coal surface. The contact angle is about 66°. The bubble size decreases and the contact angle increases up to 77°. The pressure remains constant, but still small amounts of CO_2 are released by the tip. This CO_2 merges with the bubble, which consequently increases in size, while the contact angle decreases. During the first 190 minutes occasional releases of CO_2 occur and the bubble size fluctuates accordingly. As the CO_2 supply stops, the bubble size decreases and the contact angle reduces to 62°. The bubble size steadily decreases with time until a critical volume is reached at 300 minutes. The bubble is subsequently detached from the tip and is captured by the coal surface above. During a further 220 minutes its size decreases until it disappears. In that period the contact angle slightly increases fluctuating around 84°. The bubble shape is almost spherical throughout the experiment.

At higher pressures the same procedure is used as for the atmospheric experiments. The same sequence of events occurs when the bubble size fluctuates due to occasional releases of CO_2 from the tip. In this period, however, the bubble shows an overall trend of decreasing in size much faster than in the atmospheric experiment. After detachment from the tip, the bubble shrinks much faster than in the atmospheric experiment, e.g. for the 2.6-bar experiment with Selar Cornish and Warndt Luisenthal the bubble completely disappears in 60 minutes and 75 minutes respectively. After detachment the bubble is no longer spherical and starts to spread on the coal surface.

For the high pressure (> 2.6 bar) experiments the bubble, after its release from the tip, disappears in around 20-30 minutes. A plot of the disappearance time versus the pressure shows, in spite of large scatter, a trend inversely proportional to the square root of the pressure.

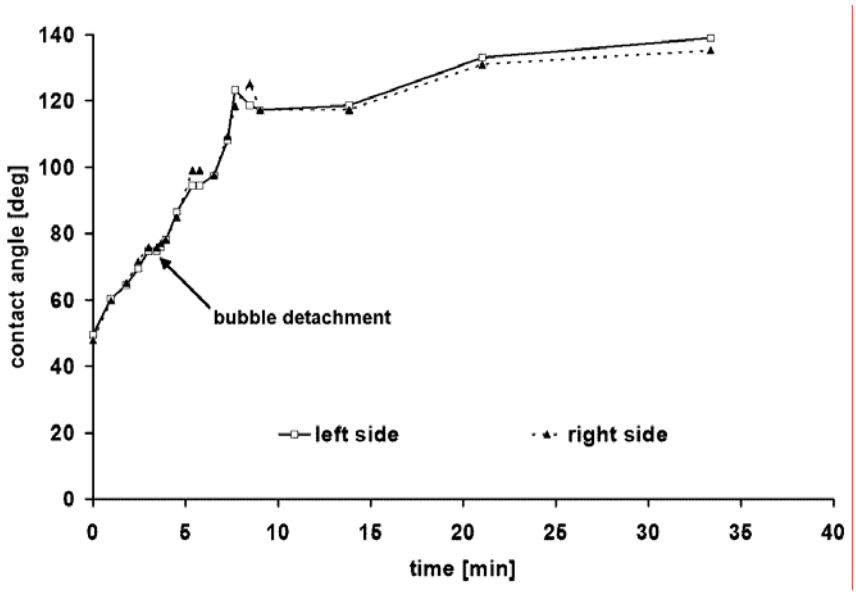

Figure 3.4: Contact angle history at 96 bar.

A typical example of the sequence of events in a high pressure (96 bar) experiment is shown in Figure 3.4. At t = 0 the bubble just touches the coal surface, but is still attached to the tip. A contact angle of about 50° is observed. As time progresses, the contact angle steadily increases as the bubble size decreases.

After three minutes the bubble is detached from the tip. The initial contact angle is about 75° and increases in a time span of 6 minutes to 120°. The bubble shrinks during the next 25 minutes until it completely disappears.

Figure 5 shows the contact angles for all 15 experiments with Selar Cornish at the start and the end of the experiment. At the start of the experiments the bubble is still attached to the tip and contact angles below 90° are observed. In all experiments with P>2.6 bar, contact angles larger than 90° are observed some ten minutes after the bubble is released. Figure 5 shows these average (between left and right) contact angles just before the bubble becomes too small to be measured. Only for the atmospheric experiment the contact angle remains below 90°.

A linear regression analysis using fourteen data points for contact angles, observed at the end of each experiment, was carried out. The square of the correlation coefficient r (Pearson's correlation) is equal to 0.34. The slope for the large contact angles for 95% confidence limits (two times the standard deviation) is 0.17±0.14 degree/bar i.e. a significant increase of the contact angle with pressure.

We excluded the atmospheric pressure point in the linear regression analysis because the atmospheric pressure experiment behaves different from all the other experiments. The intercept for the contact angle for P=0 is 111° ± 10.5°, also for 95% confidence limits. The standard deviation for the contact angles with respect to the line obtained by the linear regression method is less than 15°. If the atmospheric pressure point is included a stronger positive correlation between pressure and contact angle is found. Contact angles at the start of the experiment observed in Figure 5 do not show a trend with pressure.

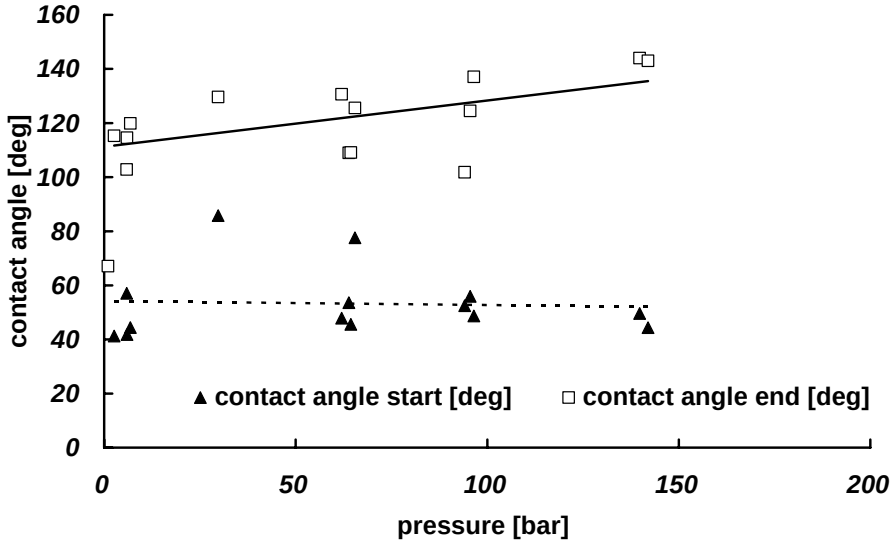

Figure 3.5: Contact angles at start and end of the experiments for sample Selar Cornish as a function of pressure. Contact angles at the start are all below 90°. Contact angles at the end of the experiment exceed 90°, except for the experiment performed at atmospheric pressure.

Contact angles at the start and the end for sample Warndt Luisenthal are plotted in Figure 3.6. Both, the start and the end contact angles below 87 bar (*Figure 3.6*) don't exhibit a significant trend with pressure. At the start the experiments show contact angles between 35 and 46°. Furthermore, they are more scattered than their corresponding end values exhibiting an average value of 85°. The standard deviation for the start contact angles with respect to the line obtained by the linear regression method is less than 5° and for the end values less than 1.5°.

For experiments exceeding 100 bar, all measured contact angles exceed 90 degrees. The end contact angles increase with pressure from 124° to 144°. The intercept for the contact angle for P=0 is 87° ± 10.7°. The square of the correlation coefficient r (Pearson's correlation) is equal to 0.42. The slope for the large contact angles for 95% confidence limits (two times the standard deviation) is 0.34 ± 0.11 degree/bar.

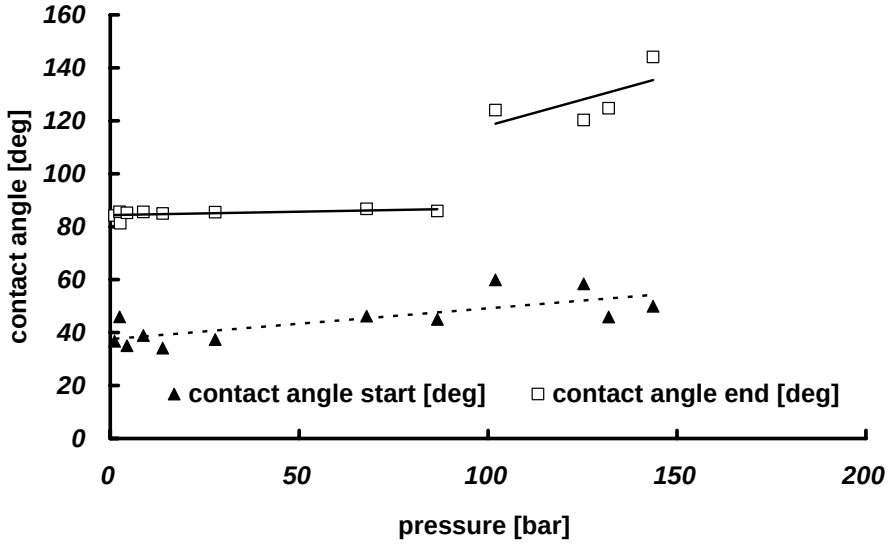

Figure 3.6: Contact angles at start and end of the experiments for Warndt Luisenthal as a function of pressure. Contact angles at the start are all below 60°. Contact angles at the end of the experiment exceed 90°at pressures higher than 100 bar.

3.7 Discussion

The reason for the slow disappearance rate of the bubble at atmospheric pressure is not clear. Given the fact that the CO_2 concentration in the gas phase (0.04 mol/l) and the concentration in the liquid phase (0.034 mol/l at P=1 bar) are similar it is expected that the characteristic disappearance time τ for a bubble with a radius R of 1mm can be estimated as $\tau = R^2/D = 10^{-6}/2\times10^{-9}=500$ seconds, independent of pressure. Here D is the diffusion coefficient for CO_2 in water in m^2/s. This characteristic time is indeed observed for the high-pressure experiments, but at atmospheric pressure the bubble survives much longer (see *Figure* 3.3).

As the same slow dissolution of the bubble is observed when the coal surface is covered with a glass plate, it is concluded that the bubble mainly disappears due to dissolution in the water phase and not due to adsorption on the coal. The same observation is valid for experiments performed at elevated pressures. Therefore, the effect of CO_2 penetrating the coal and lowering the interfacial tension is considered to be negligible.

The contact angle behavior can be qualitatively understood as follows. Initially the bubble is trapped between the tip and the coal surface. The tip causes a bubble deformation such that the apparent contact angle at the coal surface is smaller than the equilibrium value (Figure *3.3, Figure 3.4, Figure 3.5 and Figure 3.6*). As the bubble is released from the tip, the system finds a new equilibrium configuration. Upon its release, the contact spot with the coal surface increases and an advancing contact angle is observed in *Figure 3.4*. In most of our experiments the equilibrium configuration is established almost instantaneously. Subsequently the bubble decreases in size due to dissolution in water and a receding contact angle is observed. However, the difference between the advancing and receding contact angle is small and therefore it is concluded that the observed contact angles are a good representation of the equilibrium contact angle.

The CO_2 bubble rests against a surface that consists of coal and patches of water films on the surface. The difference between receding and advancing contact angle on the coal surface is mainly attributed to the existence of these water patches. As the bubble advances it encounters a surface with more water than when the bubble recedes.

The three phase contact line cannot follow the local contact angle behavior on a heterogeneous surface as this would imply a highly irregular water-CO_2 surface with a high surface energy. Therefore, it can be expected that the contact angle varies more smoothly. Indeed, the left and right contact angle usually differ less than 5°. It can also be expected that the bubble finds an energetically optimal position that changes with time as the bubble gradually dissolves. As the coal surface consists of hydrophilic mineral parts, initially water filled pores, hydrophobic aliphatic parts and intermediately wet aromatic parts, it is expected that the coal surface is on average neither totally water wet nor totally carbon dioxide wet.

For all experiments with Selar Cornish and Warndt Luisenthal the contact angle increases to $111° \pm 10.5° + (0.17 \pm 0.14)$ P [bar] and $78.7 \pm 10.7° + (0.34 \pm 0.11)$ P [bar], respectively.

It is unlikely that the interaction of CO_2 with the Selar Cornish coal surface at atmospheric pressure and a pressure of 2.6 bar is completely different. For

instance, the interfacial tension between carbon dioxide and water drops from 68mN/m at atmospheric pressure to 60 mN/m at 20.7 bar (Chun & Wilkinson, 1995). One explanation is that contact angle hysteresis effects are more pronounced for the experiments where the bubble size decreases more rapidly. Another explanation is that water films at the coal surface remain more stable for the same reason that the dissolution rate for the atmospheric pressure bubble is low. For the semi-anthracite used in these experiments the surface is carbon-dioxide-wet at pressures relevant for carbon dioxide storage in coal layers. Possibly this coal surface is also carbon-dioxide-wet at atmospheric pressure, but for the duration of the experiment water films prevent the exposure of the coal surface to carbon dioxide. Indeed, the lower rank Warndt Luisenthal coal behaves water-wet up to pressures of ~ 90 bar. This behavior can be related to the different surface chemistry of the two coal samples used. Nishino (2001) found that the affinity for water depends on functional groups (mainly carboxylic and hydroxyl) groups which are more abundant in a coal of the hvbB rank (Gutierrez-Rodriguez et al., 1984; Crawford et al., 1994; Arnold & Aplan, 1989). Further Plug et al (2006) observed the same wettability trends as a function of pressure for the same coal samples, using a high pressure capillary pressure device.

3.8 Conclusions

- Reproducible contact angles were measured in two water-CO_2-coal systems for pressures ranging between atmospheric and 144 bar.
- When the bubble is released from the tip of the injection capillary, the apparent contact angles are below 90°, indicating the influence of the tip on the bubble shape.
- From the behavior of the contact angle of the bubble after its detachment from the tip it is concluded that the observed contact angle is a good representation of the equilibrium contact angle.
- At atmospheric pressure the semi-anthracite remains water-wet with contact angles θ of 85°. Above 2.6 bar the contact angle increases with pressure i.e.

θ= (111° +10.5°) + (0.17 ± 0.14) P [bar] with 95% confidence limits. This shows that Selar Cornish behaves CO_2-wet at pressures above 2.6 bar.

- Sample Warndt Luisenthal changes its wetting behavior towards CO_2 wetting at much higher pressures. The contact angle θ increases with pressure i.e. θ= (87.7° ± 10.7°) + (0.34 ± 0.11) P [bar].
- For Selar Cornish It is unlikely that the different behavior of the atmospheric experiment with the higher pressure experiments starting at 2.6 bar is due to a difference in interaction energy between the coal surface and the gas molecules. It is more plausible that this behavior is related to the difference in stability of the water film between the coal and the CO_2.
- At atmospheric pressure the captured CO_2 bubble dissolves in the water in a time span of several hours. At higher pressures (>2.6 bar) dissolution takes place in several tens of minutes. This may suggest that the same mechanism accounts for the stability of the water film (low contact angles) and the slow dissolution rate of the bubble at atmospheric pressure.
- Water film stability may also be the reason for the water-wet behavior of sample Warndt Luisenthal for pressures below 87 bar.
- We conclude that for the Selar Cornish sample the water-CO_2 -coal system is CO_2-wet at all pressures, becoming slightly more CO_2 -wet at higher pressures.
- For the relevant pressures during CO_2 storage semi-anthracitic coal behaves CO_2-wet.
- For CO_2 storage in hvBb coal the injection pressure of carbon dioxide has to overcome a pressure threshold of 87 bar to wet the surface.

3.9 References

Adamson A.W., Gast, A.P., 1990. Physical chemistry of surfaces, John-Wiley, New York 770 p.

Arnold B.J., Aplan, F.F., 1989. The hydrophobicity of coal. Fuel 68, 651-658.

Bird R.B., Stewart W.E., Lightfoot, E.N., 1960. Transport phenomena. John-Wiley New York.

Chun B.S., Wilkinson, G.T. 1995. Interfacial tension in high-pressure carbon dioxide mixtures. Ind. Eng. Chem. Res. 34, 4371-4377.

Crawford, R.J. Guy, D.W. and D.E. Mainwaring, D.E. 1994. The influence of coal rank and mineral matter content on contact angle hysteresis. Fuel 73, 742-746.

Drelich J., Laskowski J.S., Pawlik M., Veeramasuneni, S., 1997. Preparation of coal surface for contact angle measurements. J. Adhesion Sci. Technol. 11, 1399-1431.

Fox H.W., Zisman, W.A., 1950. The spreading of liquids on low energy surfaces. Polytetrafluoroethylene. J. Coll. Sci. 51, 514-531.

Fuerstenau D.W., 1981. Flotation and selective agglomeration of Western Coals. Office of Surface Mining and Reclamation Enforcement, U.S. Dept. Interior, final report 9/1979-12/1981.

Gamson P.D., Beamish B.B., Johnson, D.P., 1993. Coal microstructure and micropermeability and their effects on natural gas recovery. Fuel 72, 87-99.

Gennes, de, P.G., 1985. Wetting; statics and dynamics. Rev. Mod. Phys. 57, 827-863.

Gutierrez-Rodriguez J.A., Aplan, F.F., 1984. The effect of oxygen on the hydrophobicity and floatability of coal. Colloids and Surfaces 12, 27-51.

Gutierrez-Rodriguez J.A., Purcell R.J., Aplan, F.F., 1984. Estimating the hydrophobicity of coal. Colloids and Surfaces 12, 1-25.

Hirasaki G.J. in: N.R.Morrow, (ed.), 1991a. Interfacial phenomena in petroleum recovery. Dekker, New York, p. 23.

Hirasaki G.J. in: N.R.Morrow, (ed.) 1991b. Interfacial phenomena in petroleum recovery. Dekker, New York, p. 77.

Hirasaki G.J., (1991c). Wettability: Fundamental and surface forces. SPE 17367, Society of Petroleum Engineers, SPE Journal of Formation Evaluation, 217-226.

Huijgens R. J. M., 1990. The Influence of interfacial tension on nitrogen flooding. PhD dissertation, Delft University of Technology, TU Delft University Press,160p.

Joanny J.F., Gennes de, P.G., 1984. A model for contact angle hysteresis, J. Chem. Phys. 81, 552-562.

Keller D.V., 1987. The Contact angle of water on coal. Colloids and Surfaces 22, 21-30.

Krevelen van, D.W., 1993. Coal, typology-physics-chemistry-constitution. Elsevier, Amsterdam, 493p.

Krooss B.M., Bergen F. van, Gensterblum Y., Siemons N., Pagnier H.J.M., David, P., 2002. High-pressure methane and carbon dioxide adsorption on dry and moisture-equilibrated Pennsylvanian coals. Int. J. Coal Geology 51, 69-92.

Mavor M.J., Owen L.B., Pratt, T.J., 1990. Measurement and evaluation of coal sorption isotherm data. SPE 20728, Society of Petroleum Engineers 65th Annual Technical Conference and Exhibition, September 23-26, New Orleans, 1-14.

Murata T., 1981. Wettability of coal estimated from the contact angle. Fuel 60, 744-746.

Nishino, J., 2001. Adsorption of water vapor and carbon dioxide at carboxylic functional groups on the surface of coal. Fuel 80, 757–764.

Plug W-J., Mazumder S. Bruining J., Wolf, K.H.A.A., 2006. Capillary Pressure and wettability behavior of the coal-water-carbon dioxide system at high pressures", Paper 0606, 2006 International Coalbed Methane Symposium Alabama, May 22-26.

Spelt J., Vargha-Butler, E.L., 1996. in: A.W. Neumann, (eds.). Applied surface thermodynamics. Surfactant Science Series 63, 394p.

ACKNOWLEDGMENTS
This research was carried out as part of the project ENK6-CT-00095-ICBM under the ENERGY and SUSTAINABLE DEVELOPMENT PROGRAM founded by the European Commission. The financial support is gratefully acknowledged. L. Vogt is thanked for the technical support.

Chapter Four

Interpretation of Carbon Dioxide Diffusion Behavior in Coals

4.1 Abstract

Storage of carbon dioxide in geological formations is for many countries one of the options to reduce greenhouse gas emissions and thus to satisfy the Kyoto agreements. The CO_2 storage in unminable coal seams has the advantage that it stores CO_2 emissions from industrial processes and can be used to enhance coalbed methane recovery (CO_2-ECBM). For this purpose, the storage capacity of coal is an important reservoir parameter. While the amount of CO_2 sorption data on various natural coals has increased in recent years, only few measurements have been performed to estimate the rate of CO_2 sorption under reservoir conditions. An understanding of gas transport is crucial for processes associated with CO_2 injection, storage and enhanced coalbed methane (ECBM) production.

A volumetric experimental set-up has been used to determine the rate of sorption of carbon dioxide in coal particles at various pressures and various grain-size fractions. The pressure history during each pressure step was measured. The measurements are interpreted in terms of temperature relaxation and transport/sorption processes within the coal. The characteristic times of sorption increase with increasing pressure. No clear dependence of the characteristic time with respect to the particle size was found. At low pressures (below 1 MPa) fast gas

diffusion is the prevailing mechanism for sorption, whereas at higher pressures, the slow diffusion process controls the gas uptake by the coal.

4.2 Introduction

The storage of anthropogenic carbon dioxide (CO_2) in abandoned coal mines or unminable coal seams, in combination with enhanced coal bed methane (ECBM) production, has become a topic of increasing interest in recent years. A typical procedure is the injection of carbon dioxide via wells drilled into coal seams. Ideally, the injected CO_2 maintains the overall reservoir pressure and therefore keeps the water production at a low level (Akkutlu & Deutsch, 2006). The injected carbon dioxide fills the cleat system of the coal seam and diffuses into the matrix blocks. In fact, it is possible to discern a number of cleat systems at different scales. The matrix blocks between the smallest cleat system have diameters typically of a few tens of microns (Gamson et al., 1993). Carbon dioxide displaces methane sorbed on the internal coal surface inside the matrix blocks. A production well gathers the methane as free gas. This process, known as carbon dioxide enhanced coalbed methane production (CO_2-ECBM), is a producer of natural gas with the potential to reduce greenhouse gas concentrations, while more carbon dioxide molecules exchange for one molecule of methane. The target coal seams for CO_2 injection in Europe are usually at great depth, with correspondingly high reservoir pressures and temperatures (35-50°C, 6-15 MPa). In order to estimate CO_2-diffusion rates and storage capacities under the P/T conditions prevailing in the target seams, accurate laboratory experiments are crucial.

The aim of this paper is to determine the rate of sorption and its dependence on pressure, grain size and moisture. Gas sorption rates in coal are controlled by two processes, the sorption itself and gas diffusion. Supercritical CO_2 sorption experiments found in the literature primarily focus on sorption capacities of coal (Siemons & Busch, 2007; Fitzgerald et al., 2005; Krooss et al., 2002) and not on sorption rates.

A few papers can be found about CO_2 sorption rates in coal, i.e., Ciembroniewicz & Marecka (1993); Marecka & Mianowiski, (1998); Clarkson &

Bustin, (1999); Cui et al. (2003); Shi, & Durucan (2003); Busch et al. (2004); Akkutlu & Deutsch (2006). One of the well-known models commonly applied is Ruckenstein's bidisperse model (Ruckenstein et al., 1971). It describes relatively fast diffusion in a matrix, which forms the embedding of particulates with a much smaller diffusion coefficient. Other models are summarized in the paper of Bathia (1987), King & Ertekin (1995), and recently Wei (2005). Siemons et al. (2003) and Siemons et al. (2004) describe the sorption rate as a sequence of two independent diffusion processes.

This analysis is based on the observation of Lu et al. (2001). They concluded from their interpretation of X-ray scattering experiments that coal particles consist of two structural units, crystallite and amorphous carbon, which supports the assumption used by Ruckenstein (1971). Siemons et al. (2004) used an upscaling technique (homogenization) to show that Ruckenstein's bidisperse model assumes that the characteristic times of diffusion in particulates and the embedding is of the same order of magnitude. This means that the underlying assumption contradicts the existence of two separate characteristic times. Therefore, an alternative model was derived, assuming two characteristic times of different order of magnitude, e.g., two independent diffusion processes in coal particles. An excellent fit was obtained by assuming diffusion in spherical particles for both processes (Siemons et al., 2003).

It has also been suggested by Ritger and Peppas (1987a, b), that diffusional transport is enhanced by stress gradients which are caused by the accommodation of large molecules in the small cavities, providing the adsorption sites. At a critical concentration of the penetrants, the glassy polymer is transformed to a rubber state. In this state, the diffusion coefficient is about 1000 times larger than in the glassy state. Following Ritger and Peppas (1987a) an inclusion of stress induced diffusion (Case II diffusion) can also be represented as two processes occurring at different characteristic times.

In spite of the complexity of diffusional processes in coal, the common denominator appears to be that it consists at least of two processes occurring at two different time scales. The simplest way to represent these processes is by the

assumption of two exponential decay functions. Such exponential decay functions would approximately represent the diffusion in a spherical particle.

4.3 Experimental

4.3.1 Experimental set-up

The volumetric apparatus (*Figure 4.1*) was chosen to assess the characteristic sorption times. The set-up, experimental procedure and isotherm evaluation are described in detail in Chapter 5 and by Siemons & Busch (2006). This method includes a correction factor for volumetric effects (coal swelling), occurring during CO_2 sorption processes on coal. *Figure 4.1* shows schematically the experimental set-up, consisting of a stainless-steel sample cell, a set of actuator-driven valves and a high-precision pressure transducer (max. pressure 18 MPa) with a precision of 0.05% of the full-scale value. The volume between valve 1 and valve 2, including the void volume of the pressure transducer, is used as reference volume and determined by helium (He) pycnometry in a calibration run. The volumes of the reference cell (V_{ref}) and sample cell ($V_{sample\ cell}$) are 1.48 cm^3 and 17.92cm^3, respectively.

The volume of the sample cell consists of the volume of the sample V_{sample} and the void volume V_{void}. The experimental device is placed in a temperature-controlled oven to ensure constant temperature throughout the experiments. Single-gas sorption experiments were performed at 45°C (318.2 K). At this temperature CO_2 is either in the gaseous or, at pressures above the critical pressure Pc, in the supercritical state. (T_C = 304.1 K; P_C = 7.38 MPa). Due to experimental constraints, maximum CO_2 equilibration pressures of ~12 MPa were achieved.

4.3.2 Samples and preparation

All sorption experiments were performed on two coal samples of different rank. The coal samples were delivered in lumps from two coal fields in Great Britain. The semi-anthracite Selar Cornish (Westphalian B) was mined in South Wales, the high volatile bituminous A sample Tupton originates from the Nottinghamshire

coal field and is Westphalian A strata. Coal properties are listed in Table 4.1, the individual water and ash contents of the different particle sizes are summarized in Table 2.

Table 4.1: Coal properties

sample	Tupton H	Selar Cornish
rank	hvbC	Semi-anthracite
Vmax [%]	0.53	2.41
Vitrinite [%]	67.2	73.6
Liptinite [%]	9.2	0
Inertinite [%]	23.6	24.6
Minerals [%]	3.0	1.8
Volatile Matter (w.f.) [%]	34.9	10.4
Fixed carbon (d.a.f.) [%]	64.7	89.3
Calorific value [MJ/m3]	26.2	33.2
Carbon [%]	70.6	85.7
Hydrogen [%]	5.2	3.4
Nitrogen [%]	2.0	1.6
Sulfur [%]	0.5	0.7
Oxygen [%]	5.6	5.6
Micropore volume [cm^3/g]	0.083	0.071

For sorption measurements on dry coal, the crushed samples were dried under vacuum for at least 1.5 hours at a temperature of 105°C. The wet Selar Cornish samples and sample Tupton 0.04-0.06 mm moist were prepared by immersing the coal particles in demineralized and degassed water. Subsequently, the excess water was vacuum-filtered and the sample was transferred to the sample cell. All other Tupton moist samples exhibit an "as received" water content. The ash and water

contents of all samples and particles sizes were determined for each particle size fraction separately.

Table 4.2: Moisture and ash content of sample Tupton and Selar Cornish dependent on particle size fraction

sample	Tupton H		Selar Cornish	
Particle size [mm]	Water content a.r. [wt %]	Ash content [wt %]	Water content [wt %]	Ash content [wt %]
0.04 - 0.06	41.3	3.4	31.8	3.7
0.06 - 0.18	12.7	3.1	20.2	3.2
0.35 - 0.71	13.6	4.4	14.2	7.1
0.71- 2.0	13.5	2.2	9.7	14.2

4.3.3 Experimental procedure

Gas uptake curves of specific coal samples of varying grain size fractions and moisture content (0.04-0.06 mm, 0.06-0.18 mm 0.35-0.71 mm and 0.71-2.0 mm) were measured as a function of pressure. A defined amount of a dry or moist coal sample of one grain size fraction was placed in the sample cell. After evacuation of the whole system for 20 minutes, gas was transferred into the reference cell by switching valve 1 in *Figure 4.1*. After pressure and temperature equilibration in the reference cell (45 minutes), valve 2 is opened to expand gas into the sample cell (see *Figure 4.1*, step 4). This leads to adiabatic cooling and heating of the reference cell and the sample cell, respectively. For that reason the first measurement points of each sorption step have to be discarded, because it takes some time before thermal equilibrium is established. After expansion of gas into the sample cell, gas molecules are removed from the free gas phase by sorption. As a result the free gas pressure drops within the experimental system. This pressure drop is monitored every 10 seconds throughout the whole experiment until complete pressure equilibrium is achieved (*Figure 4.2*). This procedure is repeated such that measurements at increasingly higher pressures are obtained. The experimental pressure data sets have been used to assess the amount of gas sorbed and to study

the kinetic effects of the sorption process in coal. The pressure values divided by the compressibility factor Z is a measure of the sorbed amount. The gas compressibility factor Z was calculated by the single-gas equation of state (EOS) for CO_2 published by Span & Wagner (1996).

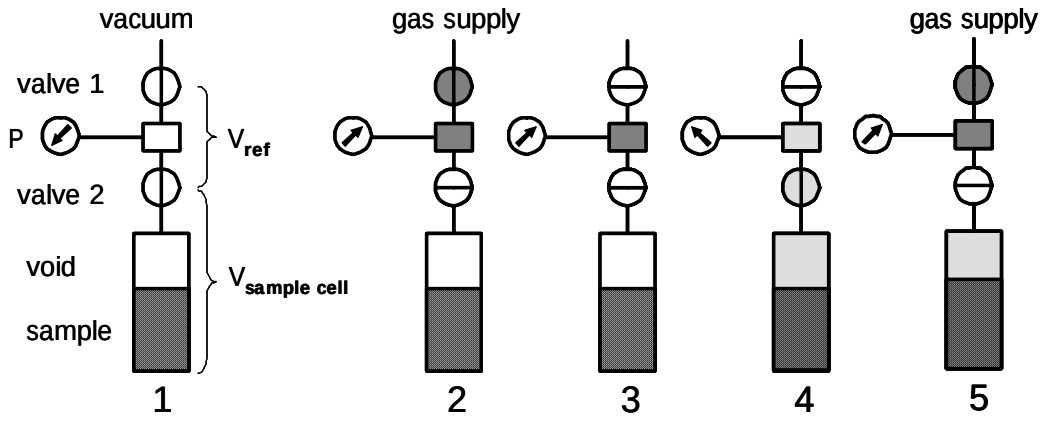

Figure 4.1: Schematic flow diagram for the volumetric method for gas sorption measurements: (1) evacuation of the entire system (2) filling of the reference cell and closure of valve 1 (3) thermal equilibration, (4) valve 2 is opened, gas transfer into the sample cell, start of the sorption process (5) after pressure equilibration, valve 2 is closed and the whole procedure is started again. Steps 3 to 5 are repeated until the maximum system pressure is reached.

4.4 Experimental results and discussion

4.4.1 Splitting procedure of the sorption contributions into a fast and a slow process

Figure 4.2 shows the procedure to obtain the characteristic times of sorption from the pressure history of each pressure step. The experimental data are indicated by unfilled diamonds. The black drawn line represents the sum of two exponential curves, which are characterized by the intensity *A* and *B* and the characteristic times *tauA* and *tauB*,

$$\left(\frac{P}{Z}\right)_{LMA}(t) = A\exp^{-\left(\frac{t}{tauA}\right)} + B\exp^{-\left(\frac{t}{tauB}\right)} + P_{off}\,, \qquad Eq.\ 4.1$$

where P_{off} is the pressure offset of the individual pressure step and t represents the experimental time in hours.

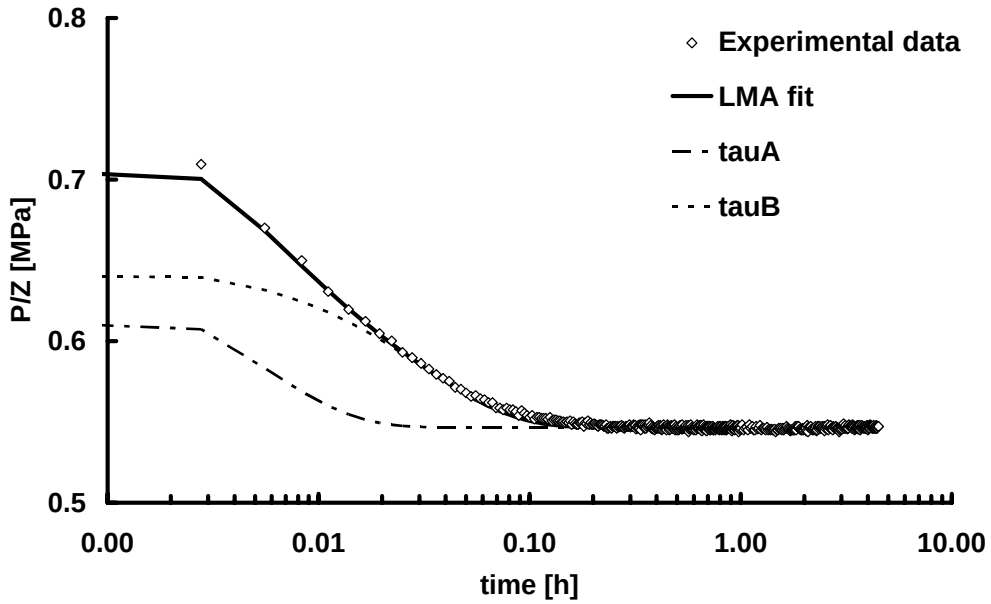

Figure 4.2: Pressure decay curve for dry sample Tupton dry 0.04-0.06 mm and the corresponding Levenberg-Marquardt (LMA) optimal fit. TauA and tauB are the characteristic times for Δn_{fast} and Δn_{slow}, respectively.

The Levenberg-Marquardt algorithm (LMA) (Marquardt, 1963) was used to find the optimal fit. The two characteristic times are obtained from the rate of exponential decay, i.e., tauA for the fast process and tauB for the slow process. The fast time behavior is indicated by the dashed-dotted line, whereas the long time behavior is indicated by the dotted line. It is observed that the fast line contains information of both the fast sorption and the adiabatic temperature effects. For the dimensions of the sample cell, (17 cm length and diameter of 1.4 cm) we expect that the thermal relaxation has a characteristic time of minutes. Therefore, the slow curve is not affected by these thermal effects. Consequently, the slow curve is extrapolated to t=0. The difference between the extrapolated pressure value

(P/Z)slow at t=0 and the equilibrium pressure (P/Z)eq is used in the EOS to obtain the amount of sorbed moles during the slow process, i.e.,

$$\Delta n_{slow} = \left((P/Z)_{slow} - (P/Z)_{eq} \right) / RT \quad , \qquad Eq.\ 4.2$$

where R is the gas constant, M_{CO2} the mole weight and T the experimental temperature. The mass balance (Siemons and Busch, 2006) was applied to calculate the theoretical equilibrium pressure $(P/Z)_{eq}$ for each step if no gas sorption on coal would occur. The pressure value obtained was used to obtain the total amount sorbed during the individual pressure step.

$$\Delta n_{tot} = \left((P/Z)_{calc} - (P/Z)_{eq} \right) / RT \, . \qquad Eq.4.3$$

The difference between Δn_{tot} and Δn_{slow} determines the amount sorbed during the fast process Δn_{fast}.

4.4.2 Characteristic times derived from the procedure

Figure 4.3 plots the characteristic times for fast and slow sorption. It is noted that *tauA* contains the combined behavior of the fast sorption process and the thermal relaxation process. *TauB* is the characteristic time for the slow process. The plot shows that the difference between *tauA* and *tauB* in the first pressure step is rather small. However, in all subsequent pressure steps the fast relaxation time is about 0.03 hours, whereas the slow time is about an hour. The same trend is observed in many of the experiments.

Figure 4.4 shows the characteristic times of all experiments on the Tupton dry sample as a function of pressure. The fast times are indicated by the open symbols. The lowest time values are found for a coal particle range between 0.06 to 0.18 mm. The highest time values are found for coal particles in the range between 0.71 to 2.0 mm in diameter. With respect to the particle size no general trend of the sorption times is observed. The values for the same particle size are strongly correlated. *Figure 4.4* to *Figure 4.7* show all measured values of the fast and slow relaxation times for different particle sizes of the two coal samples in moist and dry state.

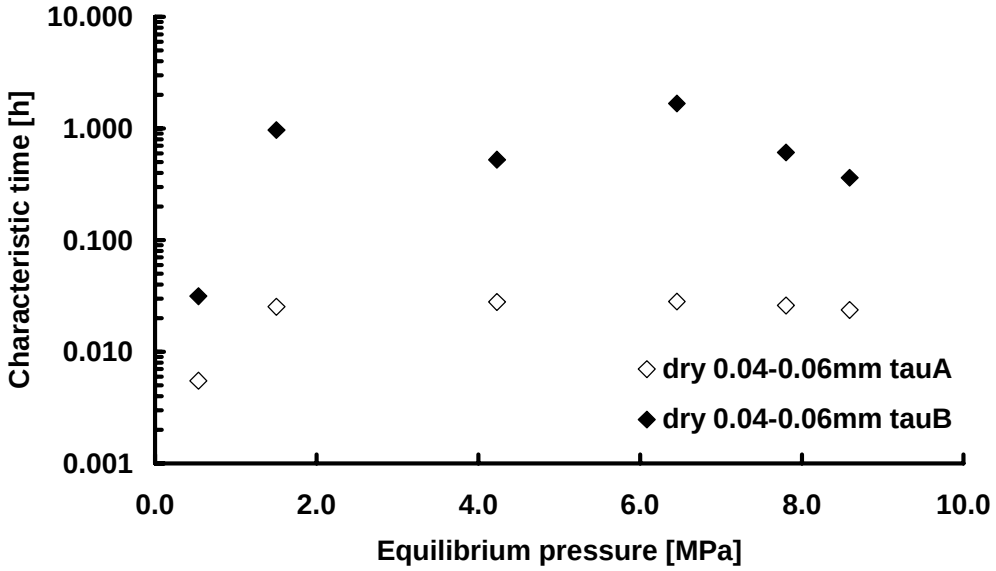

Figure 4.3: Extracted LMA times for dry sample Tupton 0.04-0.06 mm. TauA represents the short time behavior, tauB the long characteristic time.

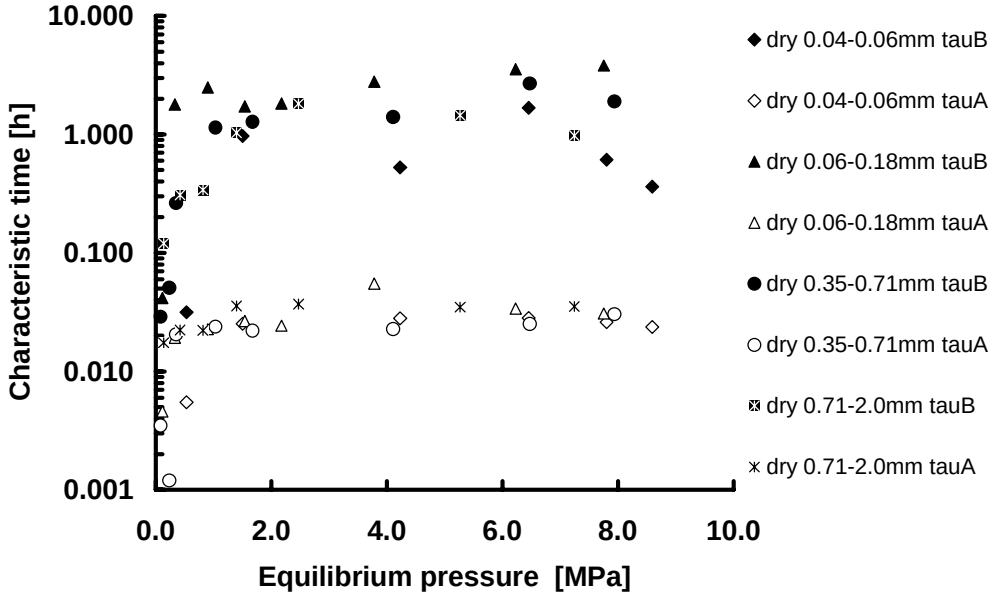

Figure 4.4: All measured values of the fast and slow relaxation times for different particle sizes of Tupton dry.

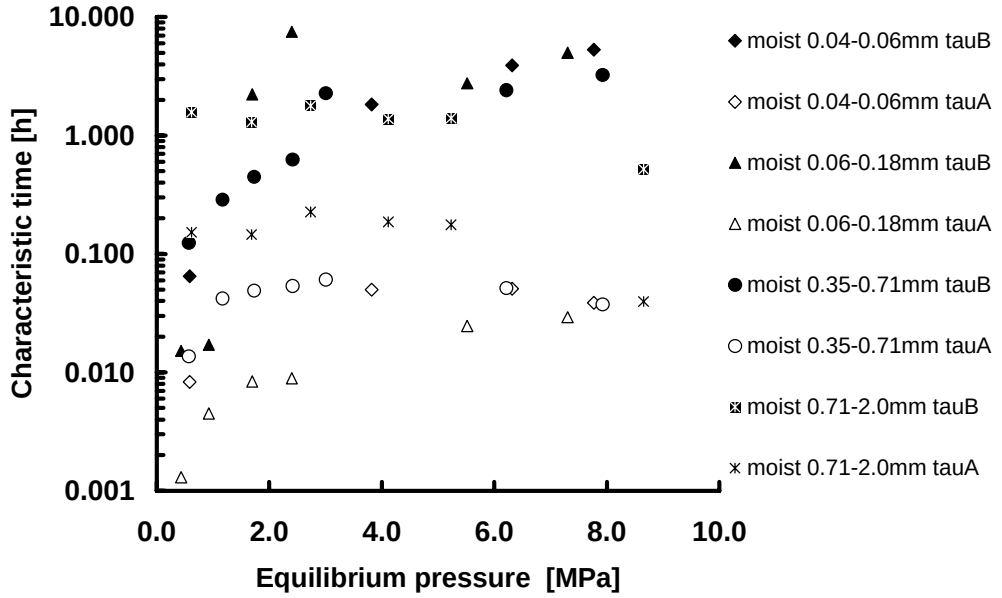

Figure 4.5: All measured values of the fast and slow relaxation times for different particle sizes of Tupton moist.

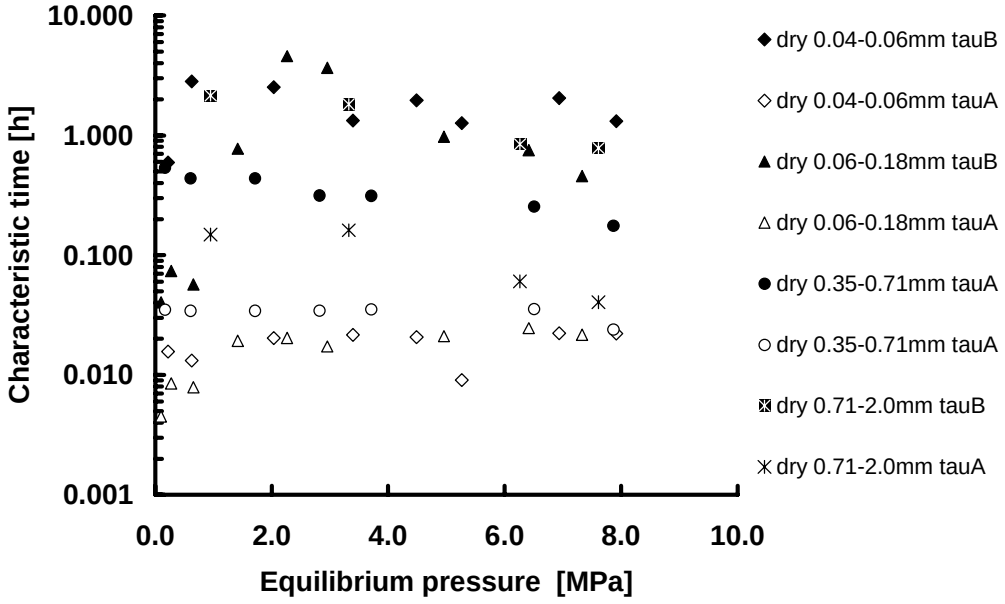

Figure 4.6: All measured values of the fast and slow relaxation times for different particle sizes of Selar dry.

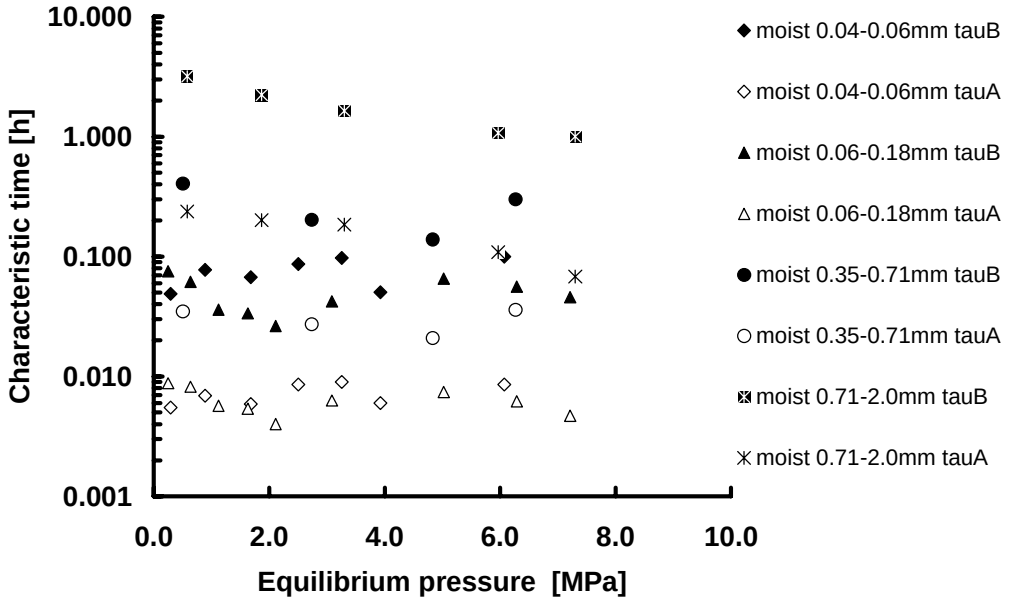

Figure 4.7: All measured values of the fast and slow relaxation times for different particle sizes of Selar moist.

It is observed in all figures that all relaxation times (*tauA* and *tauB*) are small at low pressures. At higher pressures the fast times are in the range of 0.01 to 0.2 hrs, whereas the slow times are in between 0.3 and 10 hrs. In every single experiment there is at least a factor five difference between slow and fast times. In general, larger particles lead to longer times; however, notable exceptions to this trend are observed.

The difference in behavior between the dry (*Figure 4.4* and *Figure 4.6*) and moist samples (*Figure 4.5* and *Figure 4.7*) is that the results of the dry samples show much less scatter than those of the moist samples. With respect to the fast times it is observed that for Tupton dry and Tupton moist there is no distinct dependence on particle size. However, for Tupton moist it is observed that the relaxation time of the largest particles (0.71-2.0 mm) is much longer than for the other particles. A similar behavior is also observed for the Selar Cornish except that for the moist sample the second largest particle size range (0.35-0.71 mm) shows the longest relaxation times.

The results of the slow relaxation times show that for Tupton, no clear difference between moist and dry samples is observed within the large scatter of the data. Also no particle size dependency is observed. Selar Cornish dry follows a similar behavior as found for the Tupton dry, albeit that the former shows a larger scatter of data. For the Selar Cornish moist samples the two largest size classes clearly exhibit a size dependency.

4.4.3 Amount sorbed for the fast and slow process

Figure 4.8 shows the total cumulative sorption isotherms for Tupton dry for all particle size fractions. The total sorption isotherm has been derived using the procedure that is extensively described by Siemons & Busch (2006). In this procedure a single void volume correction is applied over the whole pressure range to correct volumetric effects like coal swelling. The total sorption isotherm is different for different particle size fractions, but no clear dependency on the particle size was observed. As described above the sorption isotherms are split in a

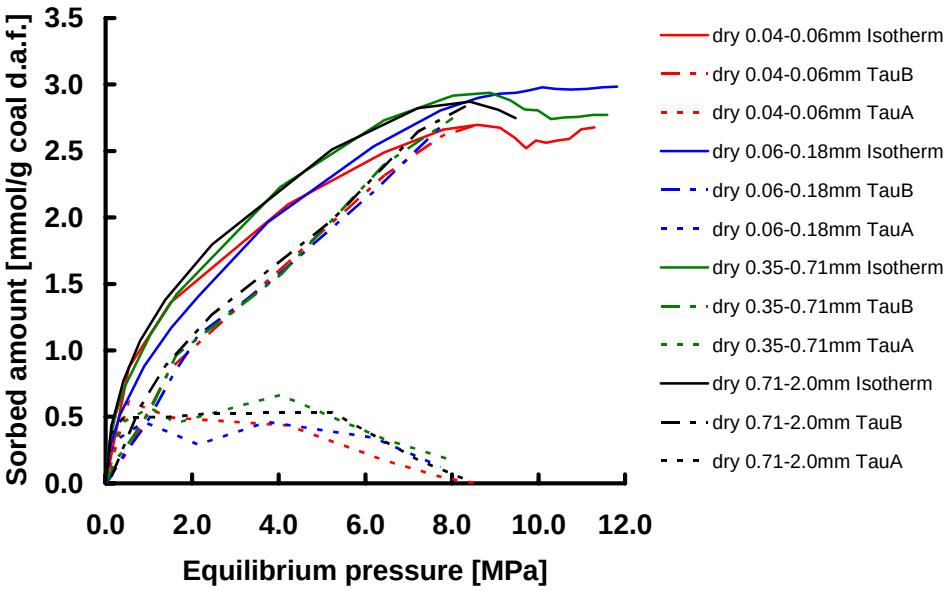

Figure 4.8: The total sorption isotherm split in a contribution due to fast (tauA) and a contribution due to slow (tauB) sorption for Tupton dry for all particle sizes.

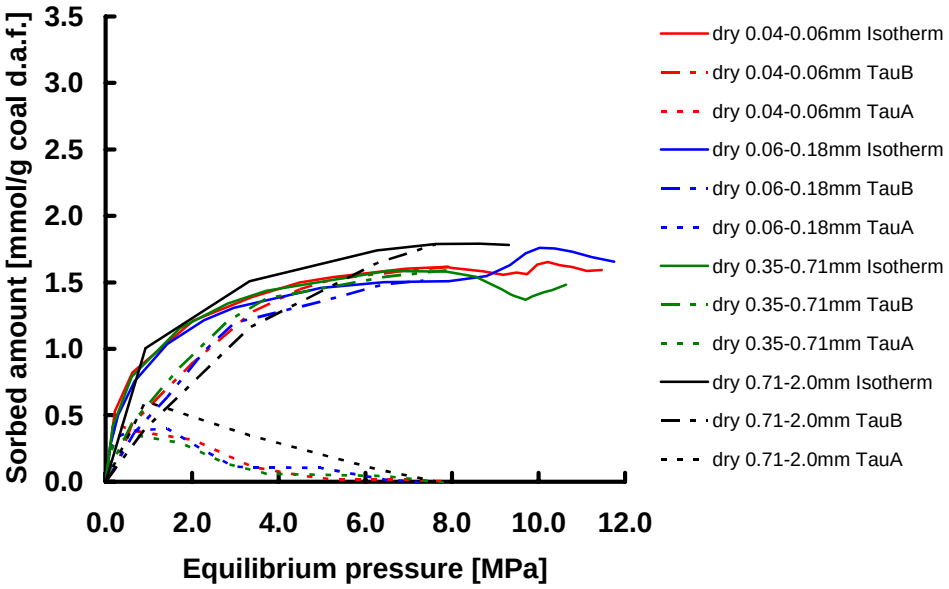

Figure 4.9: The total sorption isotherm split in a contribution due to fast (tauA) and a contribution due to slow (tauB) sorption for Selar Cornish dry for all particle sizes.

fast (*tauA*) and a slow (*tauB*) contribution. The slow curves (*tauB*) are increasing functions of equilibrium pressure. All curves show very similar behavior over the entire pressure range. Again there is no dependence on the particle size. For the high pressures the slow curve (*tauB*) starts to merge with the total sorption isotherm. The fast curves show initially a steep increase with pressure and reach a plateau value. Beyond 4 MPa the curves start to decrease. For low pressures it appears that the fast sorption (*tauA*) dominates over the slow sorption. However, at about 0.5 MPa the slow sorption starts to dominate. Beyond 8 MPa, the fast sorption cannot be detected anymore. Again there is no trend with particle size.

Figure 4.9 shows the behavior of Selar Cornish dry. The procedure as described above for Tupton dry is followed. Qualitatively, the behavior is similar to the Tupton dry experiments. However, no plateau beyond 0.5 MPa is observed. The sorption decreases to zero at a slightly lower pressure (6 MPa instead of 8 MPa). However, the most striking difference is that the amount sorbed is about half of the amount sorbed by Tupton dry.

The experiments on moist samples are as follows. *Figure 4.10* shows the results for Tupton moist. Qualitatively the behavior is again similar to Tupton dry. As for Tupton dry a plateau region is observed for the medium pressure range.

The zero value for *A* is obtained at 8 MPa. However, it appears that the fast sorption isotherm is nowhere above the slow isotherm. The major difference with Tupton dry is that sorption capacity for both slow and fast sorption is around 1/3 of the sorption of the dry sample. *Figure 4.11* shows the behavior of Selar Cornish moist. The behavior is very similar to the behavior of Selar Cornish dry. Again no plateau region is visible. The fast sorption dominates the slow sorption at pressures below 0.5 MPa. Zero sorption for tauA is obtained at about the same pressures as for Selar dry at about 7MPa. The amount sorbed for the moist sample is only 20% less than for the dry sample.

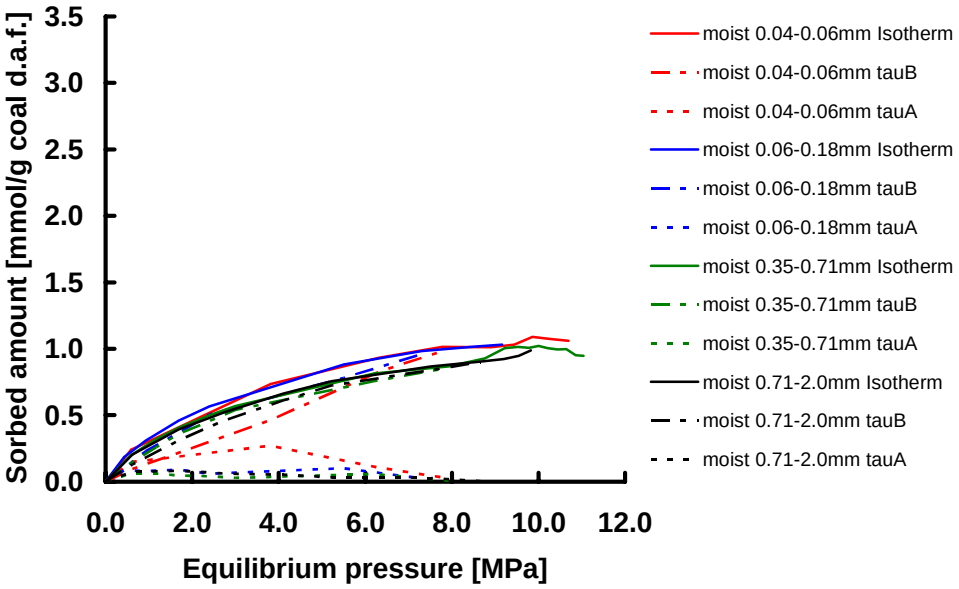

Figure 4.10: The total sorption isotherm split in a contribution due to fast (tauA) and a contribution due to slow (tauB) sorption for Tupton moist for all particle sizes.

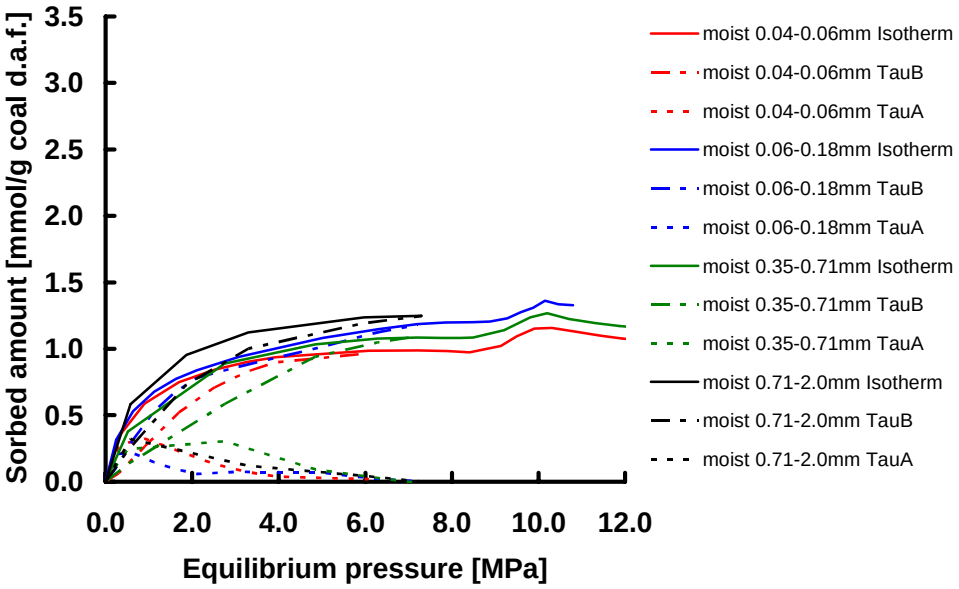

Figure 4.11: The total sorption isotherm split in a contribution due to fast (tauA) and a contribution due to slow (tauB) sorption for Selar Cornish moist for all particle sizes.

4.4.4 Tentative interpretation of the sorption behavior

Van Krevelen (1993) considers coal as consisting of a highly cross-linked macromolecular structure with aliphatic and aromatic constituents exhibiting a complicated porous structure. An estimate of the diffusion coefficient, which determines the rate of transport, can be obtained from the square of the radius of the coal particle divided by the characteristic times. The fast diffusion rate is between 10^{-8} and 10^{-10} m^2/s. The slow diffusion rate is about one to two orders of magnitude lower, i.e., between 10^{-9} and 10^{-12} m^2/s. These values are much smaller than a typical diffusion coefficient in the gas phase, i.e., ~10^{-7} m^2/s and also much smaller than a Knudsen diffusion coefficient D_K,

$$D_K = \frac{2r}{3}\sqrt{\frac{8RT}{\pi M}} \approx 92r\,, \qquad \textit{Eq. 4.4}$$

where *r* is the radius of the pore in meters. Hence, the transport mechanism is surface diffusion, even for the fast process. From all minerals present in coal in general, only clay minerals are able to transport and sorb gas. From the ash content measured, it is not possible to assess the mineral composition and, therefore, it is assumed that clay minerals are inert. Further, Hildenbrand et al. (2004) measured gas diffusion rates in clay plugs and found effective permeabilities of 10^{-18} to 10^{-23} m^2. From the comparison of Fick's law with Darcy's law one can derive

$$\frac{k}{\mu} = \frac{D\varphi}{RT}, \qquad \textit{Eq. 4.5}$$

where k is the permeability, μ the gas viscosity, φ the porosity and D the diffusion coefficient. Hence, the diffusion coefficient is about 5 x 10^8 times the permeability. Therefore, diffusion into clay is a candidate for slow diffusion.

One reason for the small diffusion coefficients in coal could originate from reversible sorption behavior. However, this would lead, even for fast diffusion, to retardation factors of the order of 10 - 10^3, meaning that the ratio of sorbed molecules to molecules in the free-state is about 10-1000. The retardation factor usually decreases with increasing surface coverage. In the experiments shown here, such a retardation factor remains more or less constant with higher pressures.

A more likely explanation is that even fast diffusion is surface diffusion. Indeed, the estimated diffusion coefficients fall in the range observed for surface diffusion. What is said above for fast diffusion is even more valid for slow diffusion. The different characteristic times indicate that there are at least two types of structures in the coal.

The experiments indicate that the "fast" sorption sites are occupied at lower pressures (<4 MPa) and dominate the sorption process. However, as the pressure increases, the "slow" sorption sites become increasingly dominant until slow sorption is the only sorption mechanism as sorption as a stand alone process cannot decrease with pressure (Landau & Lifshitz, 1980). The results indicate that a conversion process in the coal takes place as the gas pressure increases, and by that increasing CO_2 surface coverage. By conversion process it is meant that a physical or chemical change occurs in the coal that annihilates the original sorption

sites.The experiments seem to indicate that the fast sorption sites are occupied at lower pressures (<4 MPa) and dominate the sorption process. However, as the pressure increases, the slow sorption sites become increasingly dominant until slow sorption is the only sorption mechanism. As sorption as a stand alone process cannot decrease with pressure Landau & Lifshitz (1980), the results indicate that a conversion process in the coal takes place as the gas pressure increases, and by that the surface coverage. By conversion process it is meant that a physical or chemical change occurs in the coal that annihilates the original sorption sites.

4.5 Conclusions

- The pressure history of each individual step in a sorption experiment can be measured with a volumetric set-up.
- The pressure history can be split in a fast and a slow diffusion process which can be expressed by two exponentially declining functions using the Levenberg-Marquardt algorithm (LMA).
- The fast process shows characteristic times of 0.01 – 0.2 hrs, however, the first data points are influenced by adiabatic temperature effects.
- The slow process has characteristic times of 0.8 - 2 hours, i.e., ten times longer than the fast process.
- The amount sorbed by the fast process is generally much smaller than the amount sorbed by the slow process, except at pressures below 0.5 MPa. Between 6-8 MPa, the amount sorbed in the fast process advances towards zero.
- The amount sorbed by the slow process increases with pressure and becomes the only identifiable sorption mechanism at high pressures.
- The dry and moist samples show the same qualitative behavior, except that the moist samples sorb less than the dry samples. Moreover, the pressure at which the contribution of the fast process becomes zero is ~ 7MPa for the moist samples and ~ 8MPa for the dry samples.
- For pressures relevant in field applications (P > 8MPa) only the slow process contributes to the sorption capacity of coal.

Acknowledgements

The research reported in this paper was carried out as a part of the ICBM (ENK6-CT-00095) project of the European Commission. Furthermore, parts of this study have been conducted within the framework of the Dutch CATO (CO_2 capture, transport, storage) program. The financial support is gratefully acknowledged.

4.6 References

Akkutlu, I.Y., Deutsch, C.V., 2006. Gas adsorption/diffusion in bidisperse coal particles: Investigation for an effective diffusion coefficient in coalbeds. Paper 2006-111, 7th Canadian International Petroleum Conference, Calgary, Canada, June 13-15.

Bathia, S.K., 1987. Modeling the pore structure of coal. American Institute of Chemical Engineers Journal 33, 1707-1718.

Busch, A., Gensterblum, Y., Krooss, B.M., Littke, R., 2004. Methane and carbon dioxide adsorption/diffusion experiments on coal: An upscaling and modeling approach. International Journal of Coal Geology 60, 151-168.

Ciembroniewicz, A., Marecka, A., 1993. Kinetics of CO_2 sorption for two polish hard coals. Fuel 72, 405-408.

Clarkson, C.R., Bustin, R.M., 1999. The Effect of Pore Structure and Gas Pressure upon the Transport Properties of Coal: a Laboratory and Modeling Study. 2. Adsorption Rate Modeling. Fuel 78, 1345-1362.

Cui, X., Bustin, M.R., Dipple, G., 2003. Selective transport of CO_2, CH_4, and N_2 in coals: insights from modeling of experimental gas adsorption data. Fuel 83, 293–303.

Fitzgerald, J.E., Pan, Z., Sudibandriyo, M., Robinson, Jr., R.L., Gasem, K.A.M., Reeves, S., 2005. Adsorption of methane, nitrogen, carbon dioxide and their mixtures on wet Tiffany coal. Fuel 84, 2351-2363.

Gamson, P.D., Beamish, B.B., Johnson, D.P., 1993. Coal microstructure and their effects on natural gas recovery. Fuel 72, 87-99.

Hildenbrand, S., Schlömer, S., Krooss, B.M. R. Littke, R., 2004. Gas breakthrough experiments on pelitic rocks: comparative study with N_2, CO_2 and CH_4. Geofluids 4, 61–80.

King G.R., Ertekin T., 1995. State-of-the-art modeling for unconventional gas recovery, part II: Recent developments (1989-1994). SPE 29575 Society of Petroleum Engineers, Low Permeable Reservoirs Symposium, Denver, USA 20-22 March, 289-297.

Krevelen, D.W. van, 1993. Coal, typology-physics-chemistry-constitution. 3rd Edition, Elsevier Science, Amsterdam.

Krooss, B.M., Van Bergen, F., Gensterblum, Y., Siemons, N., Pagnier, H.J.M., David, P., 2002. High pressure methane and carbon dioxide adsorption isotherms on dry and moisture-equilibrated Pennsylvanian Coals. International Journal of Coal Geology 51, 69-92.

Landau, E.M., Lifshitz, L.D., 1980. Statistical physics. 3rd edition, Pergamon, Oxford.

Lu, L., Sahajwalla, V., Kong, C., Harris, D., 2001. Quantitative X-ray diffraction analysis and its application to various coals. Carbon 39, 1821-1833.

Marecka, A., Mianowiski, A., 1998. Kinetics of CO_2 and CH_4 Sorption on High Rank Coal at Ambient Temperatures. Fuel 77, 1691-1696.

Marquardt, D.W., 1963. An algorithm for the least-squares estimation of nonlinear parameters. SIAM Journal of Applied Mathematics 11 431-441.

Ritger, L.P., Peppas N.A., 1987a. Transport of penetrants in the macromolecular structure of coals. 4. Models for analysis of dynamic penetrant transport. Fuel 66, 815-826.

Ritger, L.P., Peppas N.A., 1987a. Transport of penetrants in the macromolecular structure of coals. 7. Transport in thin coal sections. Fuel 66, 1379-1388.

Ruckenstein, E., Vaidyanathan, A.S., Youngquist, G.R., 1971. Sorption by solids with bidisperse pore structures. Chemical Engineering Sciences 26, 1305-1318.

Shi, J.Q., Durucan, S., 2003. A bidisperse pore diffusion model for methane displacement desorption in coal by CO_2 injections. Fuel 82, 1219-1229.

Siemons, N., Busch, A., 2007. Measurement and interpretation of supercritical CO_2 sorption on various coals. International Journal of Coal Geology 69, 229-242.

Siemons, N., Bruining, J., Krooss, B.M., 2004. Upscaled diffusion in coal particles. Geologica Belgica (Geol. Belg.) Vol. 7, 129-135.

Siemons, N., Busch, A., Bruining, J., Krooss, B.M., 2003. Assessing the kinetics and capacity of gas adsorption in coals by a combined adsorption/diffusion method. SPE 84340, Annual Conference and Exhibition Denver, USA, 5-8 October 2003.

Span, R. and Wagner, W., 1996. A new equation of state for carbon dioxide covering the fluid region from the triple-point temperature to 1100 K at pressures up to 800 MPa. Journal of Physical and Chemical Reference Data 25, 1509-1596.

Chapter Five

Measurement and Interpretation of Supercritical CO_2 Sorption on Various Coals

5.1 Abstract

While the amount of CO_2 sorption data on various natural coals has increased in recent years, only few measurements have been reported under the experimental condition of supercritical CO_2 ($scCO_2$) at very high pressure (>5 MPa). The estimation of realistic CO_2 sorption capacities for different coals is crucial for the understanding of the processes associated with CO_2 storage and enhanced coalbed methane (ECBM) production.

In this study CO_2 sorption experiments up to 20 MPa at 45°C have been performed on dry and water-containing coals from various coal basins. The coal samples cover a broad spectrum in rank, ranging from 0.52 to 2.41% vitrinite reflectance (V_{Rr}). As shown in various studies on activated carbon, $scCO_2$ surface excess sorption isotherms do not increase continuously with pressure up to complete surface coverage of the sample. This is mainly caused by the static interpretation of excess sorption isotherms, not taking into consideration changes in the sample volume such as the volume of the sorbed phase, coal swelling, etc. This leads to difficulties in the interpretation of the experimental data in terms of adsorption isotherms, as they require models for all volumetric effects. In this context, this study provides an approach to account for the volumetric effects and,

hence for the estimation of total sorption capacities. For the fitting procedure, one generalized correction factor for the volume increase was calculated for each coal sample and applied to the whole experimental pressure range. Generally, it was observed that coals containing water show a smaller volume increase than their corresponding dry samples and no specific trend with coal rank was observed. In contrast, a trend for the dry samples was observed: The sample volume increase follows a U-shaped trend, i.e., decreasing from 0.5 to 1.1% V_{Rr} and increasing again from 1.1 to 1.7% V_{Rr}.

5.2 Introduction

The storage of anthropogenic carbon dioxide (CO_2) in abandoned coal mines or unminable coal seams in combination with enhanced coal bed methane (ECBM) has become a topic of increasing interest in recent years. Under European conditions several national and international projects (e.g. ICBM, RECOPOL, GESTCO, GEO-TECHNOLOGIEN) are presently studying this topic or have already been completed (Wolf et al. 2002; Pagnier et al. 2003; Piessens and Dusar, 2002; Kühn et al. 2005; Busch et al. 2004, 2006; Siemons et al. 2006; Mazumder et al. 2006). The target coal seams for CO_2 injection in Europe are usually at great depth, with correspondingly high reservoir pressures and temperatures (35-50°C, 6-15 MPa). In order to estimate CO_2-storage capacities under the P/T conditions prevailing in the target seams, accurate laboratory experiments are crucial. However, sorption isotherms measured at these high pressures and temperatures are rare in the literature. This study provides a comparison between CO_2 sorption isotherms measured on various coals that were used in the above-mentioned national and international projects.

The aim of this study is to assess the total CO_2 equilibrium sorption capacity of natural coal samples as a function of pressure with a special focus on scCO_2 conditions.

Much work has been carried out on the sorption capacity of coal with respect to CO_2 below the critical pressure (Yee et al. 1993; Stevenson et al. 1991; Arri et al. 1992; Hall et al. 1994; Nodzenski 1998; Clarkson and Bustin 1999, 2000; Busch et

al. 2003; Ozdemir et al. 2004; Goodman et al. 2004). However, only few data has been published for higher pressures. Krooss et al. (2002) and Fitzgerald et al. (2005) performed CO_2 sorption experiments on coals between 40 and 80°C and pressures up to 20 MPa. The result of these papers show that at high pressures (>7 MPa) the CO_2 excess (Gibbs) sorption capacity decreases with increasing pressure. A similar behavior has been observed for CO_2-sorption experiments on activated carbon at different temperatures (e.g. Humayun and Tomasko, 2000; Herbst et al. 2002).

The two commonly used methods to measure gas sorption isotherms are (1) the volumetric method and (2) the gravimetric method. The gravimetric method (e.g. Humayun and Tomasko, 2000) determines the sorption by monitoring the weight of the sample in a gas phase under well-defined P/T conditions, corrected for buoyancy effects. For the present study, the volumetric method (e.g. Mavor et al., 1990), in which sorption is determined from the pressure-change during gas transfer between a calibrated reference volume and a measuring cell (*Figure 5.1*), was used.

At low pressures, the gas phase has a substantially lower specific density than the adsorbed phase and the volume of the latter can be neglected. In this case, the evaluation scheme results in the so called "excess sorption" or Gibbs sorption.

In high-pressure sorption experiments this is no longer the case. The measurements are affected by the non-ideality of the gas phase and volumetric effects of the condensed phases (coal swelling, increase of sorbed phase volume etc.). The corresponding evaluation requires information on estimation of the density of the sorbed phase and the evaluation results in the "absolute sorption" values. The theoretical framework of Gibbs Surface Excess Sorption and the problems associated with the assessment of absolute sorption values have been discussed by Sircar (1999) and Sudibandriyo et al. (2003).

In the present study it has been attempted to account explicitly for these volumetric effects and to estimate total sorption isotherms from excess sorption measurements.

5.3 Samples

Various coal samples from different basins have been used for this study (*Table 5.1*). Fresh lumps of coal were obtained from mines in Great Britain, Germany and Poland to conduct the experiments. From these lumps representative parts have been drilled parallel to the bedding, exhibiting bright and dull coal layers to represent the variety of the coal seam. Samples from Australia and the U.S. were supplied as cores and ground coal.

The reflectance of the coals studied ranges from 0.53 to 2.41% random virtinite reflectance (VRr) with vitrinite contents varying mostly between 67 and 89%. Only one coal (Brzeszcze) exhibits a much lower vitrinite content of only 15%. Ash contents also show a broad variety in percentages, from 3.0 to 20.1 %.

Table 5.1: Coal properties

Sample name	Lab.	Origin	grain size [mm]	VRr [%]	Rank	Vitrinite [%]	Intertinite [%]	Liptinite [%]	Ash [wt%]	moisture (a.r.)[wt%]	moisture (moist)[wt%]
Tupton	TUD	GB	0.06-0.18	0.53	hvb C	67.2	22.8	9.2	3.0	13.5	n.a.
Silesia	RWTH	POL	<0.2	0.68	Hvb B	70.0	24.0	7.0	20.1	n.a.	n.a.
Warndt1	RWTH	GER	<0.2	0.78	Hvb A	79.4	10.3	10.3	3.2	0.78	1.72
Warndt2	TUD	GER	0.06-0.18	0.71	Hvb A	74.4	15.6	9	4.0	n.a.	n.a.
Brzeszcze	RWTH	POL	<0.2	0.88	Hvb A	15.0	71.0	14.0	19.4	n.a.	n.a.
German Creek	RWTH	AUS	<0.2	1.41	mvb	78.6	21.4	<0.1	22.1	n.a.	n.a.
Pocahontas	RWTH	USA	<0.15	1.68	lvb	89	10	1	4.74	n.a.	n.a.
Selar Cornish	TUD	GB	0.06-0.18	2.41	semi anth.	73.6	24.6	0	7.1	0.7	23.3

5.4 Experimental

5.4.1 Sample preparation

Sorption experiments in this study were performed on different grain sizes. For some samples one specific grain size fraction was used while for others the bulk sample was crushed down to <0.2 mm (Table 1). For sorption measurements on dry coal, the powdered samples were dried under vacuum for at least 1.5 hours at a temperature of 105°C.

Moisture equilibration was carried out according to the standard ASTM D 1412–93 procedure. These samples will be denoted as "moist". After moisturizing, the sample material was immediately transferred to the sorption cell. An aliquot of the same coal was used for the determination of the moisture content (for further details, see Krooss et al., 2002). The wet Selar Cornish sample was prepared by immersing the coal particles in distilled water under vacuum for 3 hours. Subsequently, the excess water was vacuum-filtered and the sample was transferred to the sample cell.

5.4.2 Experimental set-up and procedure

In this study the volumetric method was used to determine the sorption capacities of different coals as a function of pressure. The various measurements were performed in two laboratories (Aachen University of Technology, RWTH, and Delft University of Technology, TUD) with similar volumetric set-ups which differed mainly in the volumes of the reference cell (1.16 cm^3 and 1.48 cm^3, respectively) and sample cell (9.22 cm^3 and 17.92 cm^3, respectively).

Figure 5.1 shows schematically the experimental set-up, consisting of a stainless-steel sample cell, a set of actuator-driven valves, and a high-precision pressure transducer (max. pressure 18 and 25 MPa for TUD and RWTH, respectively), with a precision of 0.05% of the full-scale value. The volume between valve 1 and valve 2, including the void volume of the pressure transducer, is used as reference

volume and determined by helium (He) pycnometry in a calibration run. The volumes are denoted as follows:

Reference volume: V_{ref}

Sample cell volume: $V_{sample\ cell} = V_{sample} + V_{void}$ *Eq. 5.1*

V_{void} represents the volume occupied by the free gas phase.

Taking explicitly into account the volume of the sorbed phase, one can write:

$$V_{sample\ cell} = V_{sample} + V_{void} + V_{sorbed\ phase} \qquad \textit{Eq. 5.2}$$

The coal samples are kept in a stainless-steel sample cell. A 2-μm in-line filter is used to prevent coal or mineral particles from entering the valves.

Each of the experimental devices is placed in a temperature-controlled oven to ensure constant temperature (±0.2°C) throughout the experiments. Single-gas sorption experiments were performed at 45°C (318.15 K). At this temperature CO_2 is either in the gaseous or, at pressures above P_C, in the supercritical state. (T_C = 304.1K; P_C = 7.38 MPa). For CO_2 measurements, maximum equilibration pressures of ~16 MPa and ~20 MPa at TUD and RWTH, respectively, were achieved.

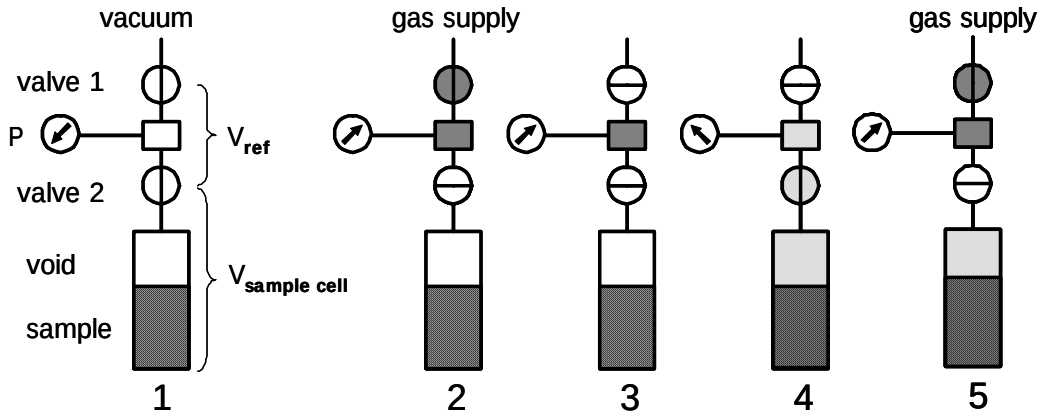

Figure 5.1: Schematic flow diagram for the volumetric method for gas sorption measurements: (1) evacuation of the whole system (2) filling of the reference cell and closure of valve 1 (3) thermal equilibration, (4) valve 2 is opened, gas transfer into the sample cell, start of the sorption process (5) after pressure equilibration, valve 2 is closed and the whole procedure is started again. Steps 3 to 5 are repeated until the maximum system pressure is reached.

5.4.3 Conduct of sorption experiments

Before the start of a sorption experiment, the void volume of the sample cell (V_{void}), i.e. the volume not occupied by the sorbent, is determined volumetrically using He as a non-adsorbing gas. With the known volume V_{ref} of the measuring cell, the measurement yields the void volume of the sample cell and the volume of the sample at the beginning of an experiment.

Volumetric gas sorption experiments are conducted in the sequence shown in *Figure 5.1*. At the beginning of the experiment both the sample cell and the reference cell are evacuated to establish a defined starting condition (step 1). Subsequently, the two cells are separated by closing the shut-off valve 2.

In the next step, a certain amount of gas is admitted to the reference volume by opening the gas access valve 1 (step 2). After closing this valve, 45-60 minutes are allowed for pressure and thermal equilibration (step 3). During this period, the pressure in the reference cell is monitored. The shut-off valve 2 between the cells is then opened and the sorbate gas is admitted to the sample cell (step 4). Sorption starts and gas molecules are removed from the free gas phase, resulting in a pressure drop in the free gas phase. This pressure drop is accurately monitored at time intervals between 1 second and 30 minutes until pressure equilibrium is achieved. Depending on coal type, particle size and pressure, between 1 hour and up to 20 hours are required to establish sorption equilibrium. After recording the equilibrium system pressure, the cells are separated again (step 5). These steps are repeated until the maximum pressure level of the individual set-up is reached.

The equation of state (EOS) for CO_2 developed by Span and Wagner (1996) was used throughout this work. The equation is considered to be the most reliable EOS and is based on the latest and most comprehensive sets of experimental data. The EOS was used to compute the amount of substance (moles of gas) in reference and sample cell from the gas pressure, temperature, and the volumes of the cells.

Helium densities were calculated by a van der Waals equation of state with "a" and "b" parameter values reported by Michels and Wouters (1941).

5.4.4 Isotherm models

The Langmuir model is a simple sorption model and widely used for the assessment of high-pressure gas sorption on coal in particular and on micro-porous media in general. It is also used to describe the dissolution (absorption) of gases in, e.g., clathrates (Van der Waals and Platteeuw, 1959; Zhu et al, 2005). This model is commonly used to represent supercritical CO_2 sorption data on coal (e.g. Fitzgerald et al. 2005; Sudibandriyo et al. 2003; Ozdemir et al. 2003). The applicability of different adsorption models for gas adsorption on coal are described by Clarkson and Bustin (1997). The Langmuir sorption isotherm is given as:

$$n_L^{sorb} = \frac{n_L P}{P + P_L}, \qquad \textit{Eq. 5.3}$$

with n_L^{sorb} denoting the sorbed mass, P the gas pressure, P_L and n_L the Langmuir parameters for Langmuir pressure and molar mass, respectively.
For comparison, the Dubinin-Astakhov (*D-A*) model (Dubinin & Astakhov, 1971) was chosen to represent the sorption isotherm for Silesia coal. The D-A model is given as follows:

$$w = w_0 \exp\left(-\left[\frac{RT}{\beta E} \ln \frac{P_s}{P} \right]^n \right), \qquad \text{Eq. 5.4}$$

where w represents the volume of the adsorbate, w_0 the micropore volume, R the universal gas constant, T the temperature, β the sorbate affinity coefficient, E the characteristic energy, P_S the pseudo saturation vapor pressure, P the experimental pressure and n the heterogeneity factor. Parameters in this model are βE, P_S, and n. Here, P_S is estimated using an empirical formula proposed by Dubinin (1975) for any temperature beyond T_C. The adsorbed amount is determined by:

$$n^{sorb} = w_0 \exp\left(-\left(A/E \right)^n \right), \qquad \textit{Eq. 5.5}$$

where A is defined as the differential molar work of adsorption (Dubinin & Astakhov, 1971).

5.5 Experimental results

Excess (Gibbs) sorption isotherms have been determined for CO_2 on moist, "as received," and dry coal samples at 45°C. *Figure 5.2* shows the result of these experiments for the different coal samples on a dry, ash-free basis. As expected, sorption capacities for dry samples are higher than for coals containing water, with maximum values of ~2.2 mmol/g for the Silesia and Tupton coals (*Figure 5.2* and *Figure 5.3*). For the samples investigated here, no trend is observed for sorption capacity with respect to rank for the dry samples. However, coals containing water (*Table 5.1*) show this trend and the sorption capacity increases (from 0.7 to 1 mmol/g) with increasing rank and decreasing moisture content.

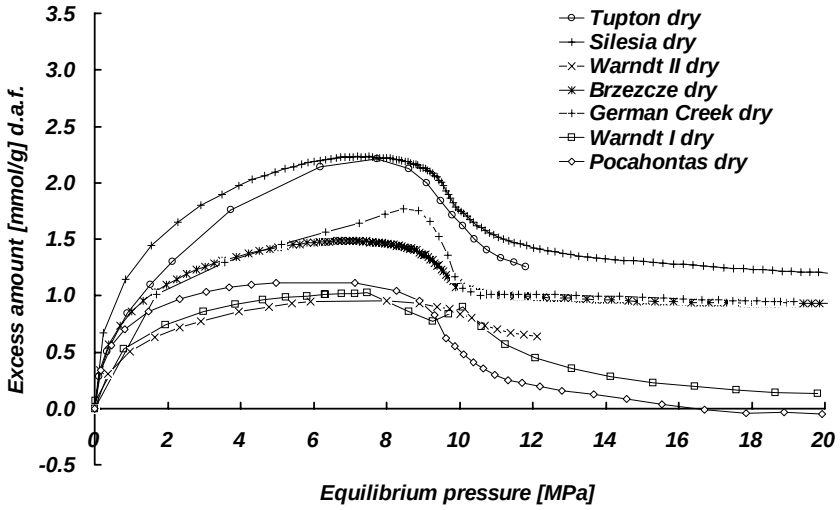

Figure 5.2: Excess sorption for different dry coals samples, measured at 45°C.

Furthermore, *Figure 5.2* and *Figure 5.3* show different shapes of the isotherms for dry samples and samples with certain moisture content. The dry samples exhibit a maximum in the excess sorption isotherm between 8-10 MPa, followed by a sharp decrease. However, for the "moist" and "as received" samples a different behavior is observed. Sorption isotherms show a smooth decrease in excess sorption values above 8-10 MPa. It is interesting to note that the Brzeszcze dry, German Creek dry, and Warndt "as received" samples tend to achieve saturation in

sorption capacity. Other samples do not show this behavior and rather a continuous decrease in excess sorption isotherms above 8-10 MPa can be recognized.

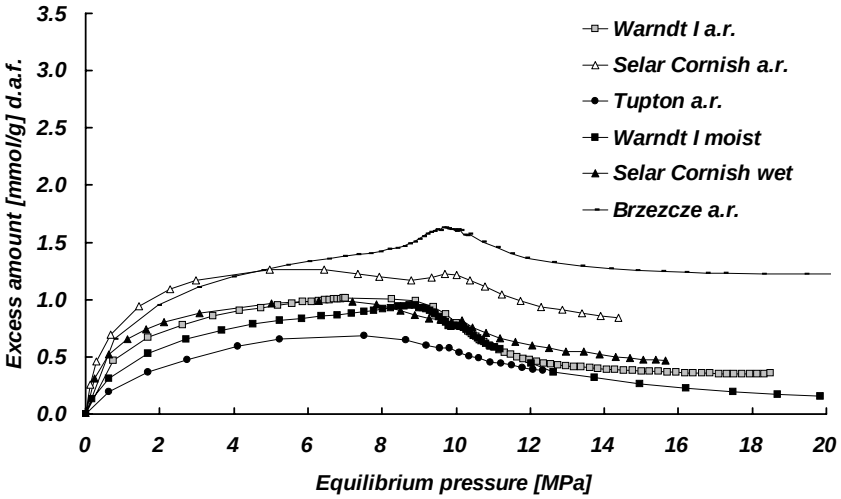

Figure 5.3: Excess sorption for different coal samples containing water, measured at 45°C.

5.6 Void volume correction

5.6.1 Uncertainties in estimating volumetric effects during CO_2 sorption

Several volumetric effects are reported in the literature and have to be taken into account. Four aspects are briefly discussed here.

One initial uncertainty is the calculation of the absolute sorption capacity, assuming a certain density of the sorbed phase. This approach can be used for CO_2 isotherms, considering a constant density of the sorbed CO_2 phase, independent of pressure and temperature. However, sorbed phase CO_2 density values given in literature vary greatly (*Table 5.2*).

Table 5.2: Adsorbed phase densities of CO_2 based on literature values

CO_2 density (g/cm^3)	Source
1.080	Hall et al. (1994)
1.178	Saturated liquid density at triple point (Span and Wagner, 1996)
1.227	Liquid density at boiling point (IUPAC, 1976)
1.40	Fitzgerald et al. (2005)
2.75	Humanyun and Tomasko (1998)

Based on the excess sorption isotherm for Silesia coal in the "as received" moisture state, the absolute sorption capacity has been computed (*Figure 5.4*) using the sorbed gas densities in *Table 5.2*. The calculation is based on the following equation (e.g. Mavor et al., 2004):

$$n_{abs} = \frac{n_{ex}}{1 - \frac{\rho_{gas}}{\rho_{ads}}} \qquad \textit{Eq. 5.6}$$

where n_{abs} and n_{ex} denote the absolute and excess sorption capacities (e.g. in mmol/g), respectively, and ρ_{gas} and ρ_{ads} are the density of the free gas and the adsorbed gas phase, respectively. The resulting absolute sorption isotherms in *Figure 5.4* demonstrate the dependence of the absolute sorption capacity on the value assumed for the sorbed gas density. This introduces a significant uncertainty in the determination of absolute sorption values.

A second volumetric factor that needs to be considered is the ability of coals to swell when interacting with CO_2, particularly $scCO_2$. This topic is subject of recent research, however only few quantitative studies have been published so far. Karacan (2003) performed a detailed x-ray computed tomography study on a bituminous coal sample and found that CO_2 sorption and swelling is heterogeneous within a coal sample and depends on the different lithotypes. Laxminarayana et al. (2004), Zutshi and Harpalani (2004), Reucroft and Sethuraman (1987) and Reucroft

and Patel (1986) found a volumetric increase due to coal swelling of 0.26-4.2 % at pressures varying from 0.1 to 15 MPa. Reucroft and Sethuraman (1987) found that swelling increases with increasing pressure and decreases with increasing coal rank. For the various coals the determination of swelling factors is difficult and time-consuming but crucial for the assessment of absolute CO_2-sorption isotherms. So far, the determination of absolute sorption isotherms does not consider this effect and, therefore, still bears additional and significant uncertainties in the total sorption capacity.

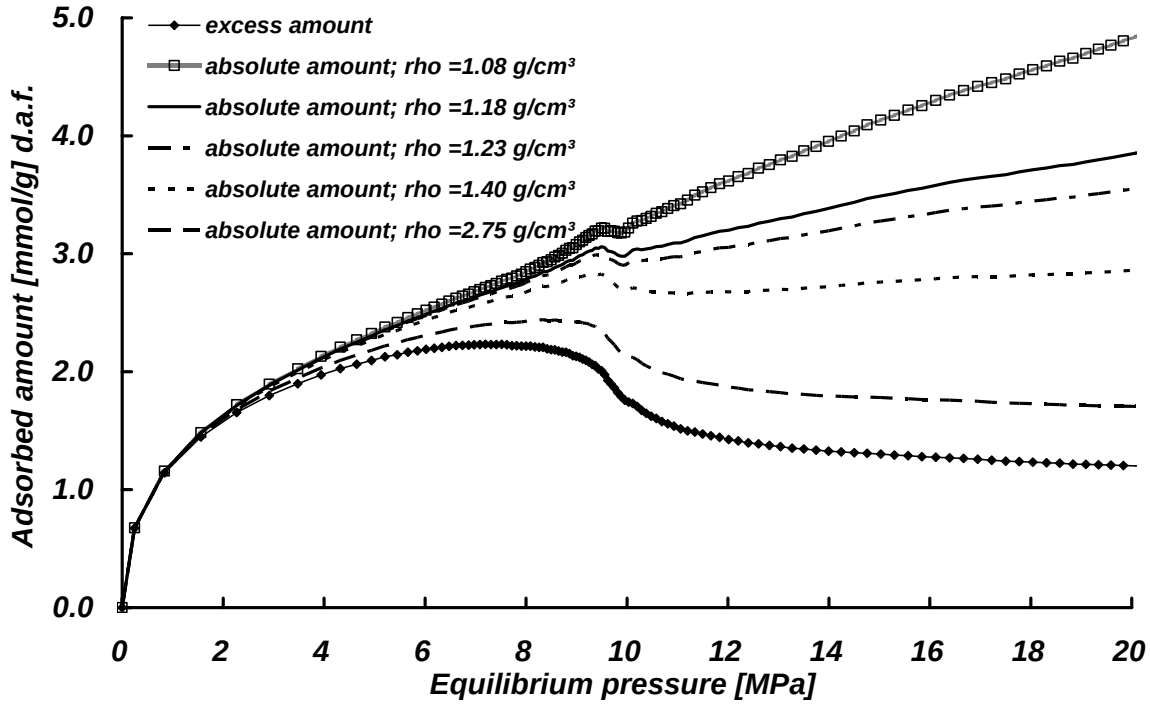

Figure 5.4: Calculation of absolute sorption for Silesia sample taking into account various sorbed CO_2 densities.

Further, CO_2 is able to dissolve (absorb) in the coal polymer structure as described by Larsen (2004). This effect might have additional impacts on the estimation of absolute sorption capacities; for example, Mahajan (1991) states that compared to CO_2, He is not able to dissolve into the coal polymer structure, resulting in an underestimation of the void volume accessible to CO_2.

Hol et al. (2005) and Kolak and Burruss (2006) observed chemical changes of coals with $scCO_2$. The latter found for coal samples of various rank that alkane

concentrations are mobilized, while the highest amounts were measured for lignites, the lowest for anthracites.

Another uncertainty is associated with He-pycnometry measurements to determine the solid/free gas volume. Here, He is considered to be a non-sorbing gas which, in fact, has been shown to be incorrect at low temperatures and high pressures (Malbrunot et al. 1997).

A fourth uncertainty may be introduced due to the change in the coal volume at higher pressures activated by compression or shrinkage (Ozdemir et al. 2003). This observation may have an opposing effect: the coal gets compressed at high pressures, hence decreasing the solid volume. At the same time, pore entrances may be closed due to this compression, consequently prohibiting gas molecules from entering these pores, resulting in an increase in the solid volume. However, these opposing effects are difficult to quantify and can only be incorporated in a general volume factor.

In summary, these different effects bear important uncertainty factors in the determination of total sorption isotherms and, at the present state of research, it is difficult to separate them from each other. In the further course of this study, only one factor will be determined accounting for all volumetric effects associated with CO_2 sorption on natural coals.

5.6.2 Void volume correction procedure

Following the procedure of Mavor et al. (1990), the amount of sorbed gas (n^{sorb}) is defined as the difference between the total amount of gas n^{tot} present in the system and the amount of gas (n^{gas}) occupied by the void volume (V_{void}). The amount n^{gas} is calculated from the molar concentration (c^{gas}) in the free gas phase obtained from the equation of state. Hence we obtain:

$$n^{sorb} = n^{tot} - n^{gas} := n^{tot} - c^{gas} V_{void} . \qquad Eq.\ 5.7$$

The value for V_{void} has to be found over the entire pressure range such that sorption data points can be represented by a non decreasing function of pressure, e.g. by the Langmuir function (*Eq. 5.3*). Three unknown parameters, n_L and P_L

describing the Langmuir isotherm, and a void volume value V_{void} have to be determined. In this interpretation, a single value of V_{void} (*Eq.5.5)* was chosen to keep the problem uniquely defined. The three parameters are not determined at once but with the use of a stepwise procedure as follows:

1. Determination of n^{sorb} (*Eq. 5.7*) with the initial void volume determined by He-pycnometry (filled diamonds in *Figure 5.5*).
2. Determination of the theoretical Langmuir sorption amount n_L^{sorb} using n_L and P_L parameters. This is done for the pressure range where the initial excess isotherm is monotonically increasing (up to ~7.5 MPa), shown as a black line in *Figure 5.6*.
3. Extrapolation of the Langmuir isotherm towards the end pressure of the individual experiment.
4. Calculation of the sum of squared differences with a target function *T* (*Eq.5.6*). The target function,

$$T = \sum_i (n_i^{sorb} - n_{Li}^{sorb})^2 \qquad \textit{Eq. 5.8}$$

   is minimized with respect to the three parameters e.g. the void volume V_{void} and the Langmuir parameters n_L and P_L.
5. The void volume is changed to find an optimal value of T (*Eq. 5.7*).
6. The Langmuir parameters are changed to find an optimal value of T *(Eq. 5.3).*
7. Step 4 & 5 are repeated until no further minimisation for T can be obtained (see *Figure 5.5*).

For the implementation of this optimisation procedure, the Excel solver function was utilised, which, in our case, used the Newton-Raphson scheme with a central difference.

This resulting isotherm is called the total sorption isotherm (filled triangles in *Figure 5.5*). It is seen that by this procedure excess sorption values are forced to follow the monotonically increasing Langmuir isotherm.

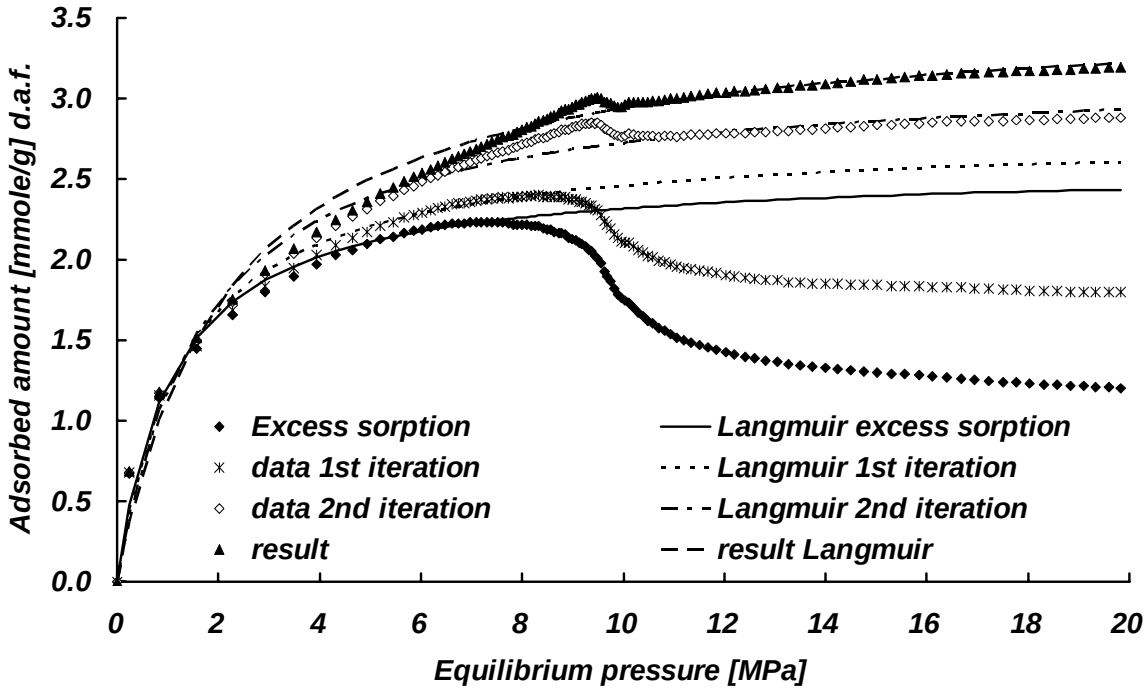

Figure 5.5: Sorption isotherms of Silesia coal sample. Documented are the experimental data points (symbols) and their corresponding Langmuir isotherms (lines). In the first iteration step, the void volume was decreased by 2.1% (stars), in the second by 5.2% (open diamonds) and for the final result by 5.7% (filled triangles).

In addition to using the Langmuir formulation, the iterative scheme based on the D-A model (*Eq. 4*) was applied to Silesia coal. The heterogeneity factor n is obtained by a least squares fit and its optimal value was found to be 1.65, i.e. well within the range for micro-porous adsorbents. The empirical Dubinin equation (Dubinin 1975) for the pseudo saturated vapor pressure P_S yielded a value of 8.09 MPa. This means, that the sorption isotherm is not defined above this pressure value (*Figure 5.6*). However, the P_S-value saturation vapor pressure can be chosen along with the experimental end pressure, the heterogeneity factor n, and βE to fit the experimental data over the whole pressure range. Results are shown in Figure 5.5. The maximum sorbed amount at 20 MPa is with 3.32 mmol/g, somewhat higher than predicted by the Langmuir model (3.20 mmol/g).

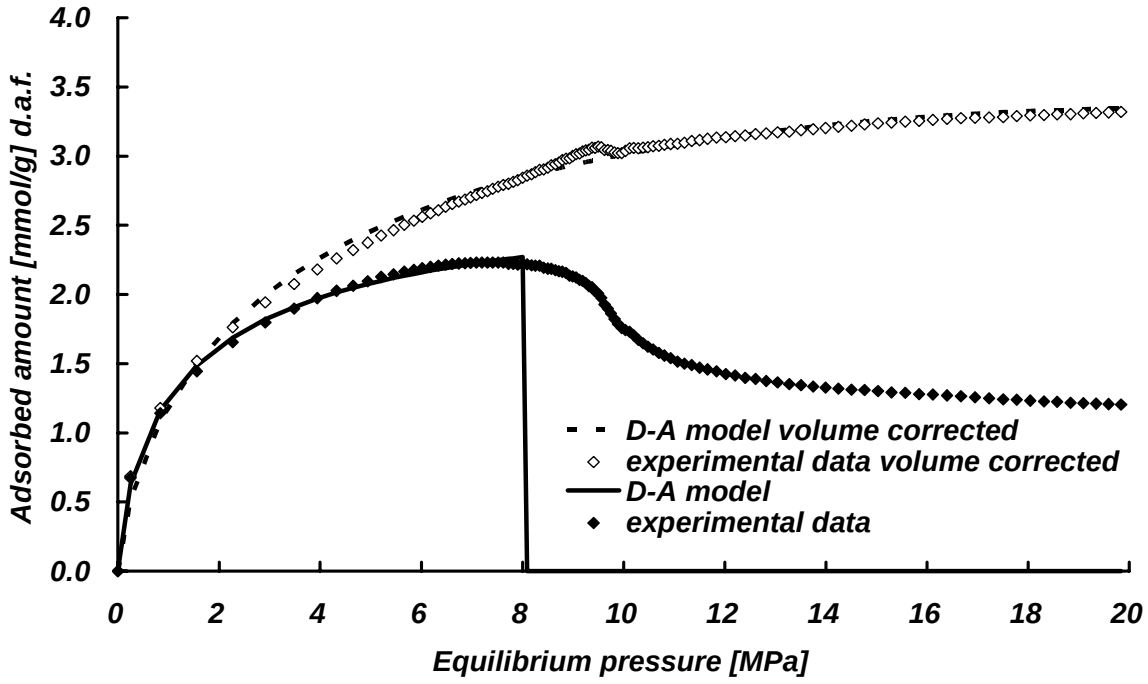

Figure 5.6: Silesia dry sorption isotherm and corresponding D-A model isotherm for the original and volume corrected data. The D-A model is not defined beyond the pseudo saturation vapor pressure. The volume corrected isotherm assumes a pseudo saturation vapor pressure of 20 MPa.

5.6.3 Void volume correction results

The iterative scheme for the Langmuir model was applied to all measured excess sorption isotherms (*Figure 5.7 and Figure 5.8*).

Trends observed for the excess sorption are also valid for the total sorption isotherms: Coals containing water adsorb less than dry coals and show an increasing sorption capacity with increasing rank. Langmuir volumes for total sorption capacities are 17 to 45 % higher than the corresponding excess sorption capacities. The shape of the isotherms changes significantly and can be separated in three domains. All isotherms show a monotonically increasing sorption capacity from zero to ~8-9 MPa. From ~9-11 MPa the isotherms show an increase followed by a decrease in sorption capacity. Beyond 11 MPa, no general trend is

recognizable. Isotherms exhibiting a high sorption capacity (above 1.5 mmol) show a moderate

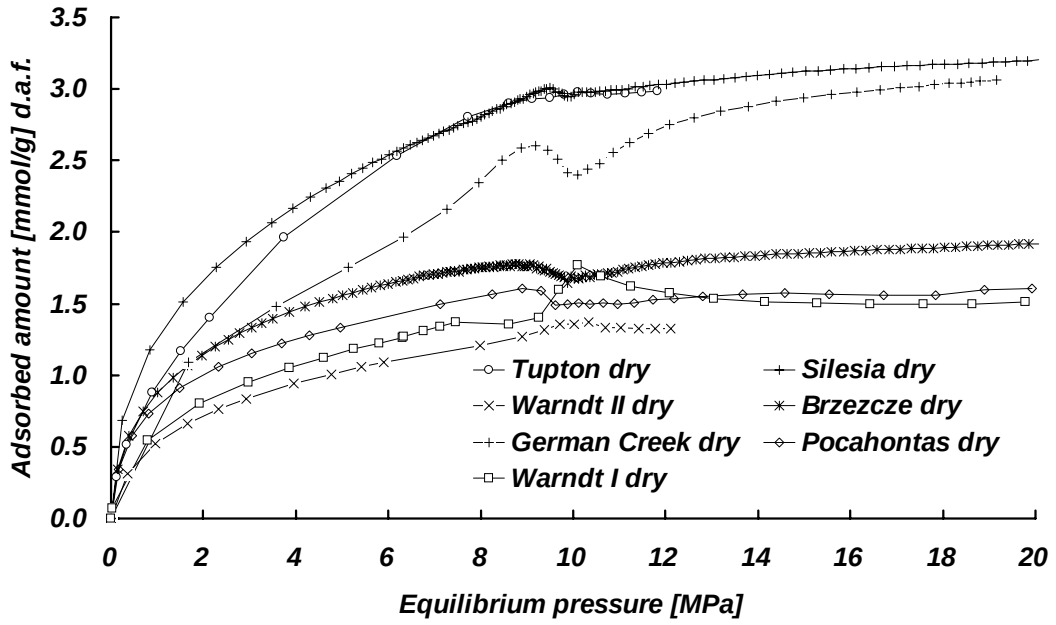

Figure 5.7: Results of the void volume fitting for different dry coal samples.

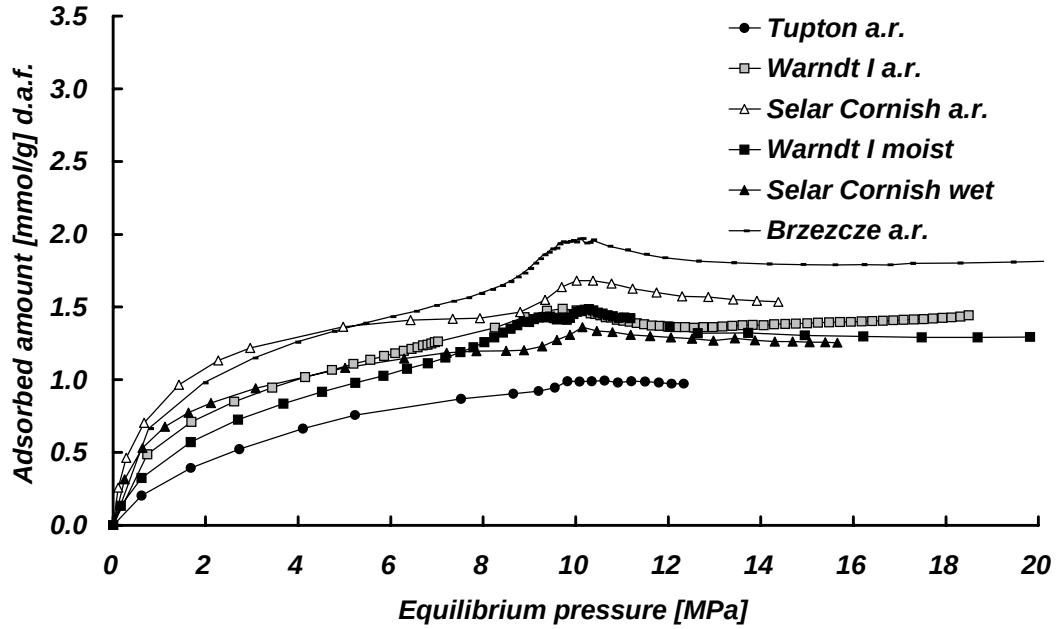

Figure 5.8: Results of the void volume fitting for different coal samples containing water.

rise in sorption capacity with pressure. With the exception of Warndt 1 ("as received"), isotherms measured on coals containing water decrease slightly. However, the steep decrease of excess sorption isotherms beyond ~9 MPa shown in *Figure 5.3* has vanished. For isotherms with end pressure values of 20 MPa this decrease cannot be observed.

The comparison of the excess sorption and total sorption isotherms yields an overall increase in total sorption capacity for all samples after the volume correction was applied (Table 3). For the dry samples, the Langmuir volume increased between 20 and 44 % with the exception of the German Creek sample (increase of ~83 %). For the samples containing water, this increase in Langmuir volume is smaller, ranging from 30 to 44 %.

Table 5.3 Sample weight and Langmuir parameters of the excess and total sorption isotherms. The cell volumes are given in Chapter 5.4.2

		Excess Sorption isotherms			Total Sorption isotherms		
Sample	weight [g] d.a.f.	P_L [MPa]	m_L [mmol/g]	Initial volume V_{void} (cm^3)	P_L [MPa]	m_L [mmol/g]	Reduced volume V_{void} (cm^3)
Tupton dry	10.871	1.70	2.65	9.723	2.61	3.69	8.448
Tupton ar	12.306	2.34	0.91	8.266	3.77	1.31	7.787
Silesia dry	3.684	1.09	2.57	5.926	2.13	3.56	5.527
Warndt II dry	12.187	1.20	1.13	7.791	2.42	1.62	7.364
Warndt I dry	3.931	0.48	1.20	6.281	1.64	1.69	5.987
Warndt I a.r.	6.249	1.31	1.04	5.884	2.24	1.63	5.626
Warndt I moist	4.202	1.53	1.06	6.996	2.46	1.49	5.736
Brzezcze dry	3.141	0.92	1.68	6.237	1.50	2.03	6.069
Brzezcze a.r.	3.676	1.33	1.63	5.489	1.88	2.09	5.339
German Creek dry	3.188	2.31	2.19	7.028	5.78	4.01	6.657
Pocahontas dry	3.097	0.52	1.21	6.696	1.08	1.68	6.417
Selar Cornish a.r.	12.761	0.62	1.41	8.310	0.96	1.70	7.824
Selar Cornish wet	10.207	0.65	1.064	9.781	1.08	1.384	9.311

In order to quantify the volumetric effects, the increase of the volume of the condensed phases (coal & sorbed phase) was calculated from the reduction of the

void volume (the difference between the initial volume and the reduced volume in *Table 5.3*) and plotted versus rank for the different measurements (*Figure 5.9*). Generally, there seems to be a difference between the measurements on dry coals and coals containing water. No specific trend can be observed for the coals containing water while for the dry coals the increase in coal volume decreases at low rank and increases again at higher rank with a minimum at ~1.1 to 1.3 % VR_r. In particular, the low rank coals show a large increase in volume (~11-13 %). Coals containing water show no rank dependency. The volume increase for all samples varies between 4 and 8 %. The Tupton coal sample shows a ~9 % difference in volume increase between the dry and "as received" (13.5 % H_2O) samples. For the highest rank Selar Cornish "as received" (0.7 % H_2O) and wet (23 % H_2O) samples, such large difference has not been observed. Here the difference is only ~0.2 %.

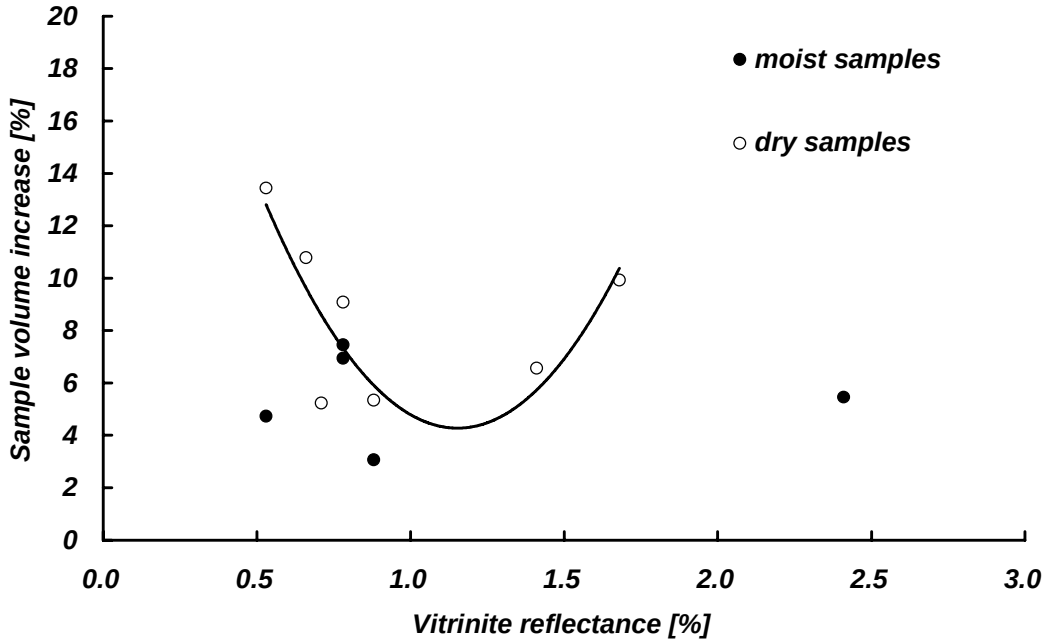

Figure 5.9: Results of the calculated coal volume increase for dry and water-containing samples. The trend line indicates a fit for the coal samples in the dry state.

5.7 Discussion

5.7.1 Excess and total sorption isotherms

Two different volumetric sorption devices have been used for this study, designed in a similar way but with different volumetric dimensions. No sample has been measured in both set-ups to compare the quantitative results. The reason for this is that all coal samples were collected and measured for different projects. However, the two different Warndt coals originate from the same colliery and are very similar in coal properties (difference in vitrinite reflectance is 0.06 % VRr). Both isotherms show a similar shape and similar excess sorption (1.20 and 1.13 mmol/g) and total sorption values (1.63 and 1.69 mmol/g) for the dry samples, respectively (*Table 5.3*). This justifies the comparison of quantitative results obtained with each set-up.

The coal samples used in this study originate from various coal basins. Coals from different coal basins are difficult to compare since the coal basin evolution (e.g. degree of metamorphism) and the organic precursors are different (Prinz 2004, Ceglarska-Stefańska and Zarębska, 2005). This leads to variations in the structure and composition of the coals of the same rank and therefore to variations in the adsorption capacity.

The comparison of the excess sorption shows no trend in sorption capacity with coal rank. Even if coal rank dependence can be observed for coals originating from the same coal basin, this trend cannot be observed for coals from different coal basins as explained above.

Only Tupton, Warndt I and Brzeszcze coals have been measured in the dry state as well as with a certain moisture content. A comparison yields a higher sorption capacity for the dry samples. This observation is common knowledge and has already been published in literature (e.g. Krooss et al. 2002; Clarkson and Bustin 2000; Levy et al. 1997). Nishino (2001) found that water competes with carbon dioxide for adsorption sites and therefore reduces the sorption capacity for CO_2.

5.7.2 Non-linearity effects in the near critical region

An unusual feature of some excess sorption isotherms is expressed in the 8 to 10 MPa region (*Figure 5.2 and Figure 5.3*) where in some instances the isotherm shows an increase followed by a decrease in sorption capacity.

This may be attributed to one or a combination of the following reasons. First, a possible inadequacy of the EOS in the near critical region may lead to inaccurate density estimates. Sun et al. (2005) compared precise PVT experiments with the CO_2 density values calculated from the Span and Wagner EOS (Span and Wagner, 1996) and found that specifically near the critical region density data may vary up to 0.1 %. It is unlikely that this has a strong effect on the shape of the isotherm in the near critical region. Secondly, as described in a study by Cahn (1977) and reviewed by De Gennes (1985) a first order wetting transition takes place somewhat below the critical point. This means that the adsorbed phase near the surface shows a sudden increase in density at the so called wetting temperature $T_W < T_C$. Possibly, such effects can also occur when the pressure approaches the critical region. This idea is supported by Humayun & Tomasko (2000), who found the same phenomena when measuring CO_2 sorption on activated carbons up to 20 MPa at various temperatures (30.5-45°C). The explanation they give is that the calculated density in this region, based on the assumption of a constant adsorbed phase volume, is greater than the liquid phase density of the CO_2.

Bae & Bhatia (2006) ascribe this effect to the inflection point of the CO_2 density plotted against the pressure in the vicinity of the critical density at a given temperature. They suggest that an inflection point may also appear in the value of the excess amount sorbed, under the assumption that the density of the adsorbed phase increases less than the density of the bulk gas phase.

Thirdly, the non monotonic behavior observed can also be an artifact of the conversion of P, T, and volumes to CO_2 density. The accuracy of the temperature control was 0.1-0.2°C. Similar inaccuracies in the temperature control have been recorded for high pressure CO_2 sorption experiments by Fitzgerald et al. (2005) and Krooss et al. (2002). This inaccuracy may introduce an error in the estimation of CO_2 density of up to 1.2 % for the experimental temperature used and, hence, may change the shape of the isotherm visibly near the critical CO_2 density.

Finally, state of the art sorption models do not consider a transition from a gaseous state to a supercritical high density state. The Langmuir model only considers the interaction between the sorbed molecule and the matrix whereas models based on the theory of micro-pore-filling explicitly consider an interaction between the adsorbate and the adsorbent in the sub-critical region (Aranovich & Donohue, 1997). In this study, the data was fitted with two different sorption models. The S-shaped part of the experimental sorption isotherm remains localized near the critical point. Therefore it is concluded that the anomalous behavior in the critical region is responsible for the observed deviations.

5.7.3 Volumetric effects

It is well known that volumetric effects occur during sorption measurements. These volumetric effects successively increase the sample volume and, hence reduce the void volume during the experiment. This effect becomes visible when the volume increase can no longer be compensated by gas uptake in the coal porous structure. This leads to the "apparent" decreasing sorption behavior above ~8-10 MPa.

As mentioned earlier, several volumetric effects need to be accounted for which are, however difficult to distinguish. Therefore, a single-value volume correction has been applied to the whole excess sorption measurement in this study. This approach results in monotonically increasing total sorption isotherms for experiments attaining high final pressure values (20 MPa).

However, after fitting experiments with lower end pressures a slight decrease is still visible. This may be related to the fact that complete gas saturation has not been reached for these samples. Therefore, it is assumed that correcting for an increase in coal volume is difficult to perform for samples measured up to low or medium pressures where no maximum gas saturation has been achieved.

Ozdemir et al. (2003) provide a model to account for the increase in coal volume in volumetric sorption measurements, measured on Argonne Premium Coal Samples at 22°C and pressures up to 3.5 MPa. The correction includes the swelling or shrinkage of the solid phase, the uncertainties associated with He-pycnometry and a certain volume change due to the dissolution of the sorbing gas.

Ozdemir et al. (2003) applied this correction to absolute sorption isotherms where the density of the sorbed phase has already been accounted for. Values for this density, as discussed in the literature (*Table 5.2*), vary tremendously (*Figure 5.4)*. For this reason it is more appropriate to use only one factor to account for all volumetric effects, including the density of the sorbed phase. Additionally, a good fit of the $scCO_2$ excess sorption isotherms can only be achieved by determining very high pressure sorption isotherms (above ~10 MPa). Here the pressure range where coal has reached or is close to reach maximum surface coverage has been accounted for.

Assuming that volumetric effects are small at low pressures total sorption capacities calculated are overestimated in this pressure range. This is because the same factor for the volumetric increase has been applied over the whole experimental pressure range in this study. However, the increase in total sorption is less than 5% at 1 MPa and less than 10% at 3 MPa compared to the excess sorption, indicating that the inaccuracy is rather small. At very high pressures (>15 MPa) this effect decreases because it can be assumed that the coal sample is achieving saturation and the volume increase successively diminishes.

The comparison of the excess sorption and total sorption isotherms yields an overall increase in sorption capacity for all samples (Table 3). Furthermore, no trend in sorption capacity with coal rank was observed for the samples investigated, before and after the volume correction.

5.7.4 Rank dependent volumetric effects

Results of the volume correction for dry coals and coals containing water are plotted in *Figure 5.9*. For dry coals the increase in volume decreases with rank increase in the low rank range (<1.1 % VRr). Similar results have been reported by Reucroft and Sethuraman (1987), who reported a decrease in coal swelling from lignite to high volatile bituminous rank. In this study, the increase in coal volume decreases (from 13 to 5 %) and exhibits a minimum around 1.1-1.3 % VRr. After passing this minimum, the coal volume increases again (up to 10 %) for the coal samples investigated in this study. The minimum between these two trend lines coincides with the minimum in the micropore volume of dry coals with rank as

reported by Prinz and Littke (2005). In different studies it is assumed that sorption mainly takes place in the microporous system of coals (e.g. Clarkson and Bustin; 1999, Crosdale et al. 1998). If the micropore volume correlates with the sorption capacity it seems to be reasonable to expect that volumetric effects are partly dependent on this relationship.

Coals containing water do not show any specific trend for the volume increase with rank. The volume increase varies between 4 and 8 %, independent of rank and moisture content. However, the full rank range has not been covered by our measurements. Especially above 1 % VRr, there is a lack of representative experimental data. The reason for the effect of water is, so far, not well understood. A further investigation of the influence of coal rank on the volume increase of coals containing water is required.

5.8 Conclusions

- Sorption measurements with scCO2 on various coals have augmented the available data set in the literature.
- The data, partly measured at TU Delft and RWTH Aachen, show similar trends.
- The interpretation of the data requires a high-resolution equation of state (EOS). The Span-Wagner EOS (Span and Wagner, 1996) appears to be adequate for our purposes.
- Both, the Langmuir and D-A model have been used to estimate several volumetric effects related to CO2 sorption on coal. With this volume correction the measured data show monotonous behavior except around the critical region.
- Small oscillations in the isotherms around the critical region are attributed to the variation in the adsorbed phase density near the critical point.
- The Langmuir mass for the total sorption isotherms is generally 20 - 44% higher than for the excess sorption isotherms.

- For dry coals, the volume correction factor shows agreement with micropore volume changes as a function of rank as reported by Prinz and Littke (2005).
- For wet coals, volume correction factors are generally smaller; however, no trend can be discerned in the few points measured.
- The procedure described in this paper leads to a more accurate estimate of the sorption capacity of carbon dioxide in coals. However, a fundamental model that describes sorption behavior in the supercritical region is still missing.
- In addition, the procedure quantifies rank dependent swelling effects during high pressure sorption in coal.

5.9 Acknowledgements

The research reported in this chapter was carried out as a part of the RECOPOL (NNE5-2001-00122) and ICBM (ENK6-CT-00095) projects of the European Commission. Furthermore, parts of this study have been conducted in the scope of the GEOTECHNOLOGIEN R&D-Programme funded by the German Ministry of Education and Research (BMBF) and the German Research Foundation (DFG) (publication no. GEOTECH-208, Grant-Nr. 03G0614A). The financial support is gratefully acknowledged.

5.10 References

Alexeev, A.D., Vsilenkoand, T.A., Ulyonova, E.V., 1999. Closed porosity in fossil coals. Fuel 78, 635-638.

Aranovich, G., Donohue, M., 1997. Predictions of multilayer adsorption using Lattice Theory. Journal of Colloid and Interface Science 197, 101-108.

Arri, L.E., Yee, D., Morgan, W.D., & Jeansonne, M.W., 1992. Modelling coalbed methane production with binary gas sorption. SPE 24363, Society of Petroleum Engineers Rocky Mountain Regional Meeting, Casper, Wyoming.

Bae, J.S., Bhatia, K., 2006. High-pressure adsorption of methane and carbon dioxide on coal. Energy & Fuels, 20, 2599 -2607.

Busch, A., Gensterblum, Y., Krooss B.M., 2003. Methane and CO_2 sorption and desorption measurements on dry Argonne Premium Coals: Pure components and mixtures. International Journal of Coal Geology 55, 205-224.

Busch, A., Gensterblum, Y., Krooss, B.M., Littke, R., 2004. Methane and Carbon Dioxide Adsorption/Diffusion Experiments on Coal: An Upscaling- and Modeling Approach. International Journal of Coal Geology 60, 151-168.

Busch A., Gensterblum Y., Krooss B.M., Siemons N., 2006. Investigation of high-pressure selective adsorption/desorption behaviour of CO2 and CH4 on coals: An experimental study. International Journal of Coal Geology 66, 53-68.

Cahn, J.W., 1977. Critical point wetting. Journal of Chemical Physics 66, 3667-3672.

Ceglarska-Stefańska, G., Zarębska, K., 2005. Sorption of carbon dioxide-methane mixtures. International Journal of Coal Geology 62, 211-222.

Clarkson, C.R, Bustin, R.M., Levy, J.H., 1997. Application of the mono/multilayer and adsorption potential theories to coal methane adsorption isotherms at elevated temperature and pressure. Carbon 35, 1689-1705.

Clarkson, C.R., Bustin, R.M., 1999. The effect of pore structure and gas pressure upon the transport properties of coal: a laboratory and modeling study. 1. Isotherms and pore volume distributions. Fuel 78, 1333-1344.

Clarkson, C.R., Bustin, R.M., 2000. Binary gas adsorption/ desorption isotherms: Effect of moisture and coal composition upon carbon dioxide selectivity over methane, International Journal of Coal Geology 42, 241-271.

Crosdale, P.J., Beamish, B.B., Valix, M., 1998. Coalbed methane sorption related to coal composition. International Journal of Coal Geology 35, 147-158.

De Gennes P.G., 1985. Wetting: statics and dynamics. Reviews of Modern Physics 57, 827-863.

Dubinin, M.M., 1975. Physical adsorption of gases and vapors in micropores. Progress in Surface and Membrane Science, Vol. 9, Academic Press, New York, 1-70.

Dubinin, M.M., Astakhov, V.A., 1971. Description of adsorption equilibria of vapors on zeolites over wide ranges of temperature and pressure. Advances in Chemistry Series 102, 69-85.

Fitzgerald, J.E., Pan, Z., Sudibandriyo, M., Robinson, Jr., R.L., Gasem, K.A.M., Reeves, S., 2005. Adsorption of methane, nitrogen, carbon dioxide and their mixtures on wet Tiffany coal. Fuel 84, 2351-2363.

Goodman, A.L., Busch, A., Duffy, G., Fitzgerald, J.E., Gasem, K.A.M., Gensterblum, Y., Krooss, B.M., Levy, J., Ozdemir, E., Pan, Z., Robinson, Jr., R.L., Schroeder, K., Sudibandriyo, M., White, C., 2004. Inter-laboratory reproducibility of CO2 adsorption isotherms measured for the Argonne premium coal samples. Energy and Fuels 18, 1175-1182.

Hall, F.E., Chunhe, Z., Gasem, K.A.M., Robinson, R.L., Yee, D., 1994 Adsorption of pure methane, nitrogen and carbon dioxide and their binary mixtures on wet Fruitland Coal, SPE 29194, Society of Petroleum Engineers, Eastern Regional Conference and Exhibition.

Herbst, A., Beutekamp, S., Harting, P., Staudt, R., 2002. Reinstoff- und Gemischadsorption an porösen Feststoffen bis 50 MPa. Chemie Ingenieur Technik 74, 1405-1409.

Hol, S., van Bergen, F., Peach, C.J., Spiers, C.J., 2005. Swelling behavious of coal due to CO2 and effects of stress. Proceedings 6th European Coal Conference, Belgrade, Serbia and Montenegro.

Humayun, R., Tomasko, D.L., 2000. High-resolution adsorption isotherms of supercritical carbon dioxide on activated carbon. AICHE Journal 10, 2065-2075.
Karacan, C.Ö., 2003. Herogeneous sorption and swelling in a confined and stressed coal during CO2 injection. Energy and Fuels 17, 1595-1608.

Kolak, J.J., Burruss, R.C., 2006. Geochemical investigation of the potential for mobilizing non-methane hydrocarbons during carbon dioxide storage in deep coal beds. Energy and Fuels 20, 566-574.

Krooss, B.M., Van Bergen, F., Gensterblum, Y., Siemons, N., Pagnier, H.J.M., David, P., 2002. High pressure methane and carbon dioxide adsorption isotherms on dry and moisture-equilibrated Pennsylvanian Coals, International Journal of Coal Geology 51, 69-92.

Kühn M., Asmus S., Azzam R., Back M., Busch A., Class H., Clauser C., Dengel A., Dose T., Ewers J., Helmig R., Jaeger K., Kempka T., Krooß B.M., Littke R., Peiffer S., Schlüter R., Stanjek H., Strobel J., Vosbeck K., Waschbüsch M., 2005. CO2Trap - development and evaluation of innovative strategies for mineral and physical trapping of CO2 in geological formations and of long-term cap rock integrity. In: Stroink, L. (ed). GEOTECHNOLOGIEN Science Report: Investigation, utilization and protection of the underground, 144 p.

Larsen, J.W., 2004. The effects of dissolved CO2 on coal structure and properties. International Journal of Coal Geology 57, 63-70.

Laximinarayana, C., Cui, X., Bustin, M.R., 2004. Implications of volumetric swelling/shrinkage of coal in sequestration of acid gases. Paper 0435. Proceedings International Coalbed Methane Symposium, Tuscaloosa, Alabama.

Levy, J.H., Day, S.J., Killingley, J.S., 1997. Methane capacities of Bowen Basin coals related to coal properties. Fuel 74, 1–7.

Mahajan, O.P., 1991. CO2 Surface Area of coals: The 25 year paradox. Carbon 29, 735-742.

Malbrunot, P., Vidal, D., Vermesse, J., 1997. Adsorbent helium density measurement and its effect on adsorption isotherms at high pressure. Langmuir 13, 539-544.

Mavor, M.J.; Owen, L.B. & Pratt, T.J., 1990. Measurement and evaluation of coal sorption isotherm data. SPE 20728, 157-170.

Mavor, M.J., Hartman, C., Pratt, T.J., 2004. Uncertainty in sorption isotherm measurements. Proceedings International Coalbed Methane Symposium, Tuscaloosa, Alabama.

Mazumder, S., van Hemert, P., Busch, A., Wolf, K-H.A.A., Tejera-Cuesta, P., 2006. Flue gas and pure CO2 sorption properties of coal: A comparative study. International Journal of Coal Geology, in press.

Michels, G., Wouters, H., 1941. In Landolt-Börnstein (1971): Zahlenwerte und Funktionen aus Physik, Chemie, Astromomie Geophysik und Technik. 6th. edition Vol. 2 part 1, p14 Springer.(in German).
Nodzenski, A., 1998. Sorption and desorption of gases (CH4, CO2) on hard coal and activated carbon at elevated pressures, Fuel, 77, 1243-1246.

Nishino, J., 2001. Adsorption of water vapor and carbon dioxide at carboxylic functional groups on the surface of coal. Fuel 80, 757– 764.

Ozdemir, E., Morsi, B.I., Schroeder, K., 2003. Importance of volume effects to adsorption isotherms of carbon dioxide on coals. Langmuir 19, 9764-9773.

Ozdemir, E., Morsi, B.I., Schroeder, K., 2004. CO2 adsorption capacity of Argonne Premium Coals. Fuel 83, 1085-1094.

Pagnier, H.J.M., Van Bergen, F., and Van der Meer, L.G.H., 2003. Field experiment of ECBM in the Silesian Coal Basin of Poland (RECOPOL). Proceedings International Coalbed Methane Symposium, Tuscaloosa, Alabama.

Piessens K., Dusar M., 2002. Feasibility of CO2 sequestration in coal mines. Report Geological Survey of Belgium, Geological Storage of CO2 from Fossil Fuel Combustion (GESTCO), 50 p.

Prinz, D., Littke, R., 2005. Development of the micro- and ultra-microporous structure of coals with rank as deduced from the accessibility to water. Fuel 84, 1645-1652.

Prinz, D., 2004. Die Porenstruktur von Kohlen. Dissertation RWTH Aachen University, 184 pp (in German).

Reucroft, P.J., Patel, H., 1986. Gas-induced swelling in coal. Fuel 65, 816-820.

Reucroft, P.J., Sethuraman, A.R., 1987. Effect of Pressure on carbon dioxide induced coal swelling. Energy and Fuels 1, 72-75.

Siemons, N., Bruining, H., Castelijns, H., Wolf, K.-H., 2006. Pressure dependence of the contact angle in a CO2-H2O-coal system. Journal of Colloid and Interface Science, in press.

Sircar S., (1999). Gibbsian surface excess for gas adsorption - revisited. Ind. Eng. Chem. Res. 38, 3670-3682.

Span, R. and Wagner, W., 1996. A new equation of state for carbon dioxide covering the fluid region from the triple-point temperature to 1100 K at pressures up to 800 MPa. Journal of Physical and Chemical Reference Data 25, 1509-1596.
Stevenson, M.D., Pinczewski, W.V., Somers, M.L. & Bagio, S.E., 1991. Adsorption/desorption of multi-component gas mixtures at in-seam conditions, SPE 23026, Society of Petroleum Engineers, Asia Pacific Conference, Perth, Australia.

Sudibandriyo, M., Pan, Z., Fitzgerald, J.E., Robinson, Jr., R.L. & Gasem, K.A.M., 2003. Adsorption of methane, nitrogen, carbon dioxide, and their binary mixtures on dry activated carbon at 318.2 K and pressures up to 13.6 MPa. Langmuir 19, 5323-5331.

Van der Waals, J.H. & Platteeuw, J.C., 1959. Clathrate solutions. Adv. In Chem. Phys 2, 1-57.

Wolf, K.H.A.A., Siemons, N., Ephraim, R., 2002. Laboratory research as a backing to CO2-sequestration improved coalbed methane production. Proceedings JCOAL International Workshop: Present status and outlook of CO2 sequestration in coal systems. September 5-6, Tokyo, Japan, 1-11.

Yee, D., Seidle, J.P., Hanson, W.B., 1993. Gas sorption on coal and measurements of gas content, AAPG Studies in Geology 38, 203-218.

Zhu, T., McGrail, B.P., Kulkarni, A.S., White, M.D., Phale, H., Ogbe, D., 2005. Development of a thermodynamic model and reservoir simulator for the CH4, CO2, and CH4-CO2 gas hydrate system. SPE Western Regional Meeting, Irvine, USA. 30 march -1april SPE 93976.

Zutshi, H., Harpalani, S., 2004. Matrix swelling with CO2 injection in a CBM reservoir and its impact on permeability of coal. Paper 0425. Proceedings International Coalbed Methane Symposium, Tuscaloosa, Alabama.

Conclusions

In this thesis three aspects of CO_2 coal interaction are investigated. The first investigation concerns the wetting behavior of the CO_2-water-coal system. It is shown that the wettability is pressure and coal-rank-dependent and in all cases the samples are CO_2-wet at high pressures. The second investigation concerns diffusion in coal particles. The study shows that it is possible to distinguish between fast and slow sorption. It is shown that fast sorption dominates at low pressures, where as slow sorption dominates at high pressures. Finally the third investigation concerns the sorption process in coal. It is shown that volumetric effects cause a decrease in sorption capacity with increasing pressure. It is possible to use a single correction factor to obtain a Langmuir like sorption isotherm, from which the total sorption on coal can be quantified. The volume correction factor can be interpreted as a rank dependent swelling coefficient.

All these aspects contribute to a fundamental understanding of the CO_2-coal interaction and can be used for optimal design of field applications. Detailed conclusions for each of the studies are repeated below for convenience.

Wetting behavior

- Reproducible contact angles were measured in two water-CO_2-coal systems for pressures ranging between atmospheric and 144 bar.

- When the bubble is released from the tip of the injection capillary, the apparent contact angles are below 90°, indicating the influence of the tip on the bubble shape.
- From the behavior of the contact angle of the bubble after its detachment from the tip it is concluded that the observed contact angle is a good representation of the equilibrium contact angle.
- At atmospheric pressure the semi-anthracite remains water-wet with contact angles θ of 85°. Above 2.6 bar the contact angle increases with pressure i.e. $\theta = (111° \pm 10.5°) + (0.17 \pm 0.14)$ P bar with 95% confidence limits. This shows that Selar Cornish behaves CO_2-wet at pressures above 2.6 bar.
- Sample Warndt Luisenthal changes its wetting behavior towards CO_2 wetting at much higher pressures. At high pressures the contact angle θ increases with pressure i.e. $\theta = (87.7° \pm 10.7°) + (0.34 \pm 0.11)$ P [bar].
- For Selar Cornish It is unlikely that the different behavior of the atmospheric experiment with the higher pressure experiments starting at 2.6 bar is due to a difference in interaction energy between the coal surface and the gas molecules. It is more plausible that this behavior is related to the difference in stability of the water film between the coal and the CO_2.
- At atmospheric pressure the captured CO_2 bubble dissolves in the water in a time span of several hours. At higher pressures (>2.6 bar) dissolution takes place in several tens of minutes. This may suggest that the same mechanism accounts for the stability of the water film (low contact angles) and the slow dissolution rate of the bubble at atmospheric pressure.
- Water film stability may also be the reason for the water-wet behavior of sample Warndt Luisenthal for pressures below 90 bar.
- We conclude that for the Selar Cornish sample the water-CO_2 -coal system is CO_2-wet at all pressures, becoming slightly more CO_2 -wet at higher pressures.
- For the relevant pressures during CO_2 storage semi-anthracitic coal behaves CO_2-wet.

- For CO_2 storage in the hvBb coal the injection pressure has to overcome a pressure threshold of 90 bar to carbon dioxide wet the surface.

Interpretation of CO_2 diffusion behavior

- The pressure history of each individual step in a sorption experiment can be measured with a volumetric set-up.
- The pressure history can be split in a fast and a slow diffusion process and by that expressed in two exponentially declining functions using the Levenberg-Marquardt algorithm (LMA).
- The fast process shows characteristic times of 0.01 – 0.2 hrs, however, the first data points are influenced by adiabatic temperature effects.
- The slow process has characteristic times of 0.8 - 2 hours, i.e., ten times longer than the fast process.
- The amount sorbed by the fast process is generally much smaller than the amount sorbed by the slow process, except at pressures below 0.5 MPa. Between 6-8 MPa, the amount sorbed in the fast process advances towards zero.
- The amount sorbed by the slow process increases with pressure and becomes the only identifiable sorption mechanism at high pressures.
- The dry and moist samples show the same qualitative behavior, except that the moist samples sorb less than the dry samples. Moreover, the pressure at which the contribution of the fast process becomes zero is ~ 7MPa for the moist samples and ~ 8MPa for the dry samples.
- For pressures relevant in field applications (P > 8MPa) only the slow process contributes to the sorption capacity of coal.

Measurement and interpretation of CO_2 sorption

- Sorption measurements with $scCO_2$ on various coals have augmented the available data set in the literature.
- The data, partly measured at TU Delft and RWTH Aachen, show similar trends.
- The interpretation of the data requires a high-resolution equation of state (EOS). The Span-Wagner EOS (Span and Wagner, 1996) appears to be adequate for our purposes.
- Both, the Langmuir and D-A model have been used to estimate several volumetric effects related to CO_2 sorption on coal. With this volume correction the measured data show monotonous behavior except around the critical region.
- Small oscillations in the isotherms around the critical region are attributed to the variation in the adsorbed phase density near the critical point.
- The Langmuir mass for the total sorption isotherms is generally 20 - 44% higher than for the excess sorption isotherms.
- For dry coals, the volume correction factor shows agreement with micropore volume changes as a function of rank as reported by Prinz and Littke (2005).
- For wet coals, volume correction factors are generally smaller; however, no trend can be discerned in the few points measured.
- The procedure described in this paper leads to a more accurate estimate of the sorption capacity of carbon dioxide in coals. However, a fundamental model that describes sorption behavior in the supercritical region is still missing.
- In addition, the procedure quantifies rank dependent swelling effects during high pressure sorption in coal.

Summary

Fossil fuel will be the main contributor to cover the worldwide demand of energy for the next decades. The main challenge of using fossil fuel appears to be rather the problem of greenhouse gas emissions, which are considered to be the main contributor to the current global heating. Carbon dioxide enhanced coal bed methane (ECBM) produces natural gas for energy generation with ideally no effective greenhouse gas emissions. The key parameter for application of ECBM is the amount of CO_2 that can be stored in the target seams and the rate with which the adsorption occurs.

Transport in the cleat system can be slow when the smaller cleats are filled with water; however it will be much faster if they are filled in CO_2. Therefore the contact angles are measured in the CO_2-water-coal system. This is described in Chapter 3. It is shown the two coals studied become CO_2-wet at high pressures. Secondly, we need to know how much CO_2 can be stored in the matrix blocks. The literature contains a large data set of CO_2 sorption on coal; however, data covering the range of field application are scarce. Experimentally, sorption capacities are obtained using the volumetric method, in which a mass of CO_2 in a reference cell is expanded into a vessel containing the coal sample. These experiments put severe demands on the set up itself (wide pressure range and leakage problems) and on the interpretation of the data in terms of sorption. The interpretation is complex, in particular at near critical conditions due to the sensitivity of the EOS, swelling effects of the sample and slow rate of diffusion into the coal.

In this thesis these aspects are addressed in Chapter 4 and Chapter 5. In Chapter 4, it is shown that it is possible to distinguish between slow and fast diffusion process. However, both are slower than Knudsen diffusion. The amount sorbed during the fast diffusion process will be referred to as fast sorption. Analogously the slow sorption is defined. The fast sorption dominates at low pressures, but at higher pressures the contribution due to fast sorption becomes zero and the sorption becomes dominated by the slow sorption process. From this it is concluded that the sorption process alters the structure of the coal.

Chapter 5 deals with the interpretation of sorption experiments. Volumetric cause the excess sorption to decrease at high pressures. A single volumetric correction factor allows describing the sorption as a Langmuir type isotherm. This quantifies the total sorption capacity. The values are up to 40% higher than the excess sorption. The volume correction factor can be interpreted in terms of the rank dependent coal swelling.

All these aspects contribute to a fundamental understanding of the CO_2-coal interaction and can be used for optimal design of field applications. The abstracts of Chapter 3 to 5 are included below.

Wetting behavior

Carbon dioxide (CO_2) injection into coal layers serves the dual purpose to enhance coal bed methane production (ECBM) and to store CO_2. The efficiency of this process is expected to be much higher if water is the non-wetting phase in the coal-water-gas system. Therefore, carbon dioxide contact angles in two coal-water-CO_2 systems have been measured. The captive bubble technique was used within a pressure range from atmospheric pressure and 140 bar at a constant temperature of 45° C.

Two sets of measurements have been performed, one on a polished semi-anthracite, the second set on a polished high volatile bituminous B (hvbB) coal sample. For the anthracite the following observations have been made. At atmospheric pressure, the contact angle of a CO_2 droplet increases with time, but stays below 90°. At higher pressures (>3 bar) the contact angle increases beyond

90°. This shows that the semi-anthracite coal sample behaves CO_2-wet at system pressures above 3 bar.

CO_2 contact angles on the bituminous coal sample show a different behavior. In the pressures range from atmospheric to 85 bar, CO_2 contact angles are independent of pressure and exhibit values of around 85°. At pressures beyond 100 bar, the coal surface becomes CO_2 wet. The bituminous coal sample is water wet up to much higher pressures than the anthracite. This behavior is related to the difference in stability of the water film between the coal surface and the CO_2. The hydrophobicity of coal increases with rank due to a loss of functional groups which are responsible for hydrogen bonds between coal molecules and water. For the relevant pressures during CO_2 storage, the anthracitic coal behaves CO_2-wet, whereas in bituminous coal the injection pressure has to exceed a pressure of 100 bar in order to wet the coal surface.

It can be concluded that the efficiency of carbon dioxide injection and retention in coal strongly depends on surface properties of the prevailing coal.

Interpretation of CO_2 diffusion behavior

The CO_2 storage in unminable coal seams has the advantage that it can sequestrate CO_2 emissions from industrial processes and can be used to enhance coalbed methane recovery (CO_2-ECBM). For this purpose, the storage capacity of coal is an important economical parameter. While the amount of CO_2 sorption data on various natural coals has increased in recent years, only few measurements have been performed to estimate the rate of CO_2 sorption under reservoir conditions. Gas transport processes are crucial for the understanding of the phenomena associated with CO_2 injection and storage and enhanced coalbed methane (ECBM) production.

A volumetric experimental set-up has been used to determine the rate of sorption of carbon dioxide in coal particles at various pressures and grain sizes. The pressure history during each pressure step was measured. The measurements are interpreted in terms of temperature relaxation and transport/sorption processes within the coal. The characteristic times of sorption increase with increasing

pressure. No clear dependence of the characteristic time with respect to the particle size was found. At low pressures (below 1 MPa) fast gas diffusion is the prevailing mechanism for sorption, whereas at higher pressures, the slow diffusion process controls the gas uptake by the coal.

Measurement and interpretation of CO_2 sorption

While the amount of CO_2 sorption data on various natural coals has increased in recent years, only few measurements have been reported under the experimental condition of supercritical CO_2 ($scCO_2$) at very high pressure (>5 MPa). The estimation of realistic CO_2 sorption capacities for different coals is crucial for the understanding of the processes associated with CO_2 storage and enhanced coalbed methane (ECBM) production.

In this study CO_2 sorption experiments up to 20 MPa at 45°C have been performed on dry and water-containing coals from various coal basins. The coal samples cover a broad spectrum in rank, ranging from 0.52 to 2.41 % vitrinite reflectance (V_{Rr}). As shown in various studies on activated carbon, $scCO_2$ surface excess sorption isotherms do not increase continuously with pressure up to complete surface coverage of the sample. This is mainly caused by the static interpretation of excess sorption isotherms, not taking into consideration changes in the sample volume such as the volume of the sorbed phase, coal swelling, etc. This leads to difficulties in the interpretation of the experimental data in terms of adsorption isotherms, as they require models for all volumetric effects.

In this context, this study provides an approach to account for the volumetric effects and, hence for the estimation of total sorption capacities. For the fitting procedure, one generalized correction factor for the volume increase was calculated for each coal sample and applied to the whole experimental pressure range.

Generally, it was observed that coals containing water show a smaller volume increase than their corresponding dry samples and no specific trend with coal rank was observed. Contrary, a trend for the dry samples was observed: The sample volume increase follows a U-shaped trend, i.e., decreasing from 0.5 to 1.1% V_{Rr} and increasing again from 1.1 to 1.7% V_{Rr}.

Samenvatting

Fossiele brandstoffen zullen in de komende decennia voor het grootste deel de wereldwijde vraag naar energie dekken. Het grootste probleem bij het gebruik van fossiele brandstof is de emissie van broeikasgassen, die wordt beschouwd als een hoofdreden voor de huidige globale klimaatverandering.
ECBM (Enhanced Coal Bed Methane) produceert aardgas voor energieopwekking met in het ideale geval neutrale broeikasgasemissies. De meest belangrijkste parameter voor het toepassen van ECBM is de hoeveelheid CO_2 die zo snel mogelijk door sorptie kan worden opgeslagen in steenkoollagen.
Tijdens CO_2 injectie in het scheursysteem van een koollaag is gas transport traag als de kleinere scheurtjes met water gevuld zijn en zal sneller gaan als deze met CO_2 zijn gevuld. Om dit voorkeursgedrag te bepalen worden de contacthoeken gemeten in een steenkool – CO_2 – water systeem. Dit wordt beschreven in Hoofdstuk 3. Er is aangetoond dat twee bestudeerde kolensoorten bij hoge druk CO_2-adhesief worden, waardoor de transportsnelheid bij hoge druk toeneemt.
Daarnaast is het belangrijk te weten wat de CO_2 opslagcapaciteit van de matrixblokken is. De literatuur bevat een grote hoeveelheid experimentele data van CO_2 sorptie op steenkool, echter relevante gegevens voor toepassing onder in-situ condities in koollagen zijn schaars.
De volumetrische methode wordt gebruikt om experimenteel sorptie capaciteiten te meten, waarin een hoeveelheid CO_2 in een referentiecel geëxpandeerd wordt naar een monstercel die steenkool bevat. Voor deze experimenten zijn er strenge eisen met betrekking tot het experimentele systeem (de nauwkeurigheid van de

drukmeting, temperatuur, de mogelijkheid van lekkage) en op de interpretatie van de metingen met betrekking tot sorptiegedrag. De interpretatie is vooral complex bij drukken rond het kritische punt als gevolg van de gevoeligheid die van de EOS (Equation of State), en door zwelling van steenkool tijdens een experiment. In dit proefschrift worden deze aspecten in Hoofdstuk 4 en Hoofdstuk 5 behandeld. In Hoofdstuk 4 wordt aangetoond dat het mogelijk is tussen een langzaam en een snel verspreidingsproces te onderscheiden, met een langzame (tauB) en een snelle (tauA) karakteristieke tijd. Beide processen zijn langzamer dan verspreiding door een Knudsen-type diffusie. De hoeveelheid gas dat tijdens het snelle verspreidingsproces zal worden geabsorbeerd, wordt als snelle sorptie beschreven. Analoog wordt de langzame sorptie beschouwt. De snelle sorptie overheerst bij lage druk, maar bij hogere druk is de bijdrage van snelle sorptie nul en wordt deze door het langzame sorptie proces overheerst. Uit deze resultaten wordt geconcludeerd dat het sorptieproces de structuur van de steenkool verandert.
Hoofdstuk 5 behandelt de interpretatie van sorptie-experimenten. Volumetrische metingen veroorzaken "excess"-sorptie die bij hoge druk vermindert. Excess sorptie beschouwt niet het volume van de geadsorbeerde fase en andere volumetrische effecten.
Een enkele volumetrische correctiefactor is in staat om deze sorptie als Langmuir type isotherm te beschrijven. Daardoor kan de "totale" sorptiecapaciteit worden kwantificeert. Deze waarden zijn tot 40% hoger dan de excess sorptie. De volumecorrectie-factor kan in termen van inkolingsgraad-afhankelijke zwelling worden geïnterpreteerd. Al deze aspecten dragen bij tot een fundamenteel inzicht in de CO_2-steenkool interactie en kunnen voor reservoir optimalisatie toepassingen worden benut (Hoofdstuk 3, 4 en 5).

Bevochtiginggedrag

CO_2 injectie in steenkoollagen dient twee doelen: productie van het methaan verbeteren (ECBM) en CO_2 opslag. De efficiëntie van dit proces kan veel hoger zijn als het water de niet bevochtende component in het steenkool-water-gas

systeem is. Daarom zijn de contacthoeken van het kooldioxide in twee steenkool-water-CO_2 systemen gemeten.

De "captured bubble" techniek is gebruikt van atmosferische druk tot 140 bar, bij een constante temperatuur van 45°C. De twee reeksen metingen zijn uitgevoer, op en gepolijste semi-antracieten en gepolijste bitumineuze steenkoolmonsters. Voor het semi-antraciet monster zijn de volgende observaties gemaakt: bij atmosferische druk wordt de contacthoek van een druppeltje van CO_2 groter met tijd, maar blijft beneden de 90°. Bij een hogere vloeistofdruk stijgt de contacthoek boven 90°. Dit toont aan dat de semi-antraciet zich CO_2-nat gedraagt bij een systeemdruk boven 3 bar.

De contacthoeken van CO_2 op een bitumineus monster tonen variatie in gedrag. Bij drukken van atmosferisch tot 85 bar zijn de contacthoeken van CO_2 onafhankelijk van de druk en geven waarden van rond 85° weer. Bij drukken boven 100 bar wordt het steenkooloppervlakte CO_2-nat. De bitumineuze kool is tot veel hogere druk water-nat dan antraciet. Dit gedrag wordt veroorzaakt door het verschil in stabiliteit van de waterfilm tussen het steenkooloppervlakte en de CO_2. Hydrofoob gedrag van steenkool neemt toe met de inkolingsgraad en is toe te schrijven aan een verlies van functionele groepen die verantwoordelijk zijn voor waterstofbindingen tussen steenkoolmoleculen en water.

Voor de relevante in-situ druk condities bij CO_2 opslag gedraagt de anthracitische steenkool zich CO_2-nat, terwijl voor bitumineuze kolen de injectiedruk 100 bar moet overschrijden voor hetzelfde effect. Men kan concluderen dat de efficiëntie van CO_2-injectie en opname in steenkool sterk afhankelijk zijn van de oppervlakte-eigenschappen van het soort steenkool (rang).

Interpretatie van CO_2 diffusiegedrag

De opslag van CO_2 in diepe steenkoollagen heeft als voordeel dat de emissies van CO_2 uit industriële processen kunnen worden gebruikt om de winning van methaan te verbeteren (CO_2-ECBM). Met dit in gedachte is de opslagcapaciteit van steenkool een belangrijke economische parameter. Terwijl de hoeveelheid aan CO_2-sorptiegegevens van natuurlijke steenkolen is toegenomen in de jaren zijn er slechts

weinig metingen uitgevoerd om de sorptie van CO_2 onder reservoiromstandigheden te bepalen. Het begrip van transportprocessen van gas in kool is essentieel voor de injectie en opslag van CO_2 met een verbeterde productie van het steenkool gas methaan. Een volumetrische experimentele opstelling is ontworpen en gebruikt om de hoeveelheid sorptie van CO_2 in steenkooldeeltjes van verschillende grote en bij verschillende gasdrukken te bepalen. De drukgeschiedenis van elke drukstap is gemeten. De metingen worden geïnterpreteerd in termen van temperatuurrelaxatie en sorptiegedrag in de steenkoolkorrels. De kenmerkende sorptietijden stijgen met toenemende druk. Er is geen duidelijke afhankelijkheid van de tijd met betrekking tot de deeltjesgrootte gevonden. Bij lage drukken (onder 1 MPa) is snelle gasverspreiding het dominante mechanisme voor sorptie, terwijl bij hogere druk een langzaam verspreidingsproces in de steenkool overheerst (Hoofdstuk 4).

Meting en interpretatie van CO_2 sorptie

De schatting van realistische sorptiecapaciteiten van CO_2 voor verschillende koolsoorten is essentieel voor het begrip van de processen die gerelateerd zijn aan de opslag van CO_2 en productie van methaan uit steenkoollagen (ECBM). In dit proefschrift worden experimentele studies van CO_2 sorptie tot 20 MPa bij 45°C op droge en waterhoudende steenkolen van diverse steenkoolbassins gepresenteerd. De inkolingsgraad varieert van 0.52 tot 2.41% vitrinietreflectie (VRr). Zoals aangetoond in diverse studies met geactiveerde koolstof, stijgen CO_2 excess sorptie isothermen niet continu met druk tot volledige oppervlaktedekking is bereikt. Dit wordt hoofdzakelijk veroorzaakt door de statische interpretatie van excess sorptie-isothermen, aannemende dat er geen verandering plaatsvindt in het volume of wel het volume van de geabsorbeerde fase, steenkool zwelling wordt negeert. Dit leidt tot onnauwkeurigheden in de interpretatie van de experimentele resultaten, in termen van sorptie-isothermen, aangezien er geen model voor alle volumetrische verschijnsel existeert. Daarom geeft deze studie een benadering om voor volumetrische efffecten een schatting van totale sorptie-capaciteiten te geven. Een

algemene correctiefactor wordt geïntroduceerd voor de volumeverandering van elk steenkoolmonster dat wordt toegepast op het gehele drukgebied.

Over het algemeen kan geconcludeerd worden dat steenkolen die water bevatten een kleinere volumevergroting laten zien dan overeenkomstige droge kolen. Er is geen specifieke trend met steenkoolrang voor natte monsters waargenomen. Echter is een tendens voor de droge steekproeven waargenomen: De verhoging van het koolvolume volgt een U-vormige tendens die, van 0.5 tot 1.1% VRr een vermindering in zwelling, en een verhoging van 1.1 tot 1.7% VRr toont.

Research Output

2007

Review articles

Nikolai Siemons and Andreas Busch, 2007. Measurement and interpretation of supercritical CO_2 sorption on various coals. International Journal of Coal Geology, 69, 229-241.

Nikolai Siemons Karl-Heinz A.A. Wolf and Johannes Bruining, 2007. Interpretation of CO_2 diffusion behaviour in coals. International Journal of Coal Geology, xx, xxx-xxx. In press.

2006

Review articles

Nikolai Siemons, Johannes Bruining, Hein Castelijns and Karl-Heinz A.A. Wolf, 2006. Pressure dependence of the contact angle in a CO2–H2O–coal system. Journal of Colloid and Interface Science 297, 755-761.

Andreas Busch, Yves Gensterblum, Bernhard M. Krooss and Nikolai Siemons (2006). Investigation of high-pressure selective adsorption/desorption behaviour of CO2 and CH4 on coals: An experimental study. International Journal of Coal Geology 66, 53-68.

Conference proceedings

Nikolai Siemons, Johannes Bruining and Karl-Heinz A.A. Wolf, 2006. Pressure dependence of the contact angle in a CO2–H2O–coal system. International coalbed methane symposium, Alabama May 22-26.

Oral presentations

Nikolai Siemons, Johannes Bruining, Hein Castelijns and Karl-Heinz Wolf, 2006. Pressure dependence of the contact angle in a CO2–H2O–coal system. International coalbed methane symposium, Alabama May 2006.

Reports

Raoul van Lier, Nikolai Siemons and Karl-Heinz A..A. Wolf, 2006. Shell gamechanger final report. Confidential.

2005

Oral presentations

Nikolai Siemons (2005). Carbon dioxide sequestration in coal. CATO-Symposium, 1 July, Delft, Netherlands.

Nikolai Siemons (2005). Carbon Dioxide sorption in coal. ECBM workshop, 5 December, Delft, Netherlands.

2004

Review articles

Nikolai Siemons Johannes Bruining Bernhard M.Krooss 2004.Upscaled diffusion in coal particles. Geologica Belgica (Geol. Belg.) 7, 129-135.

Karl-Heinz A.A. Wolf, Nikolai Siemons, Johannes Bruining, 2004. Multiphase flow experiments in order to understand the behavior of (partly) saturated coals as a gas reservoir: Examples 2004. Geologica Belgica (Geol. Belg.) 7, 115-121.

Karl-Heinz A. A. Wolf, Dan Bossie Codreanu, Rudy Ephrahim, Nikolai Siemons 2004. Analysing cleat angles in coal seams using image analysis techniques on artificial drilling cuttings and prepared coal blocks. Geologica Belgica (Geol. Belg.) Vol. 7, 105-113.

Oral presentations

Nikolai Siemons 2004. Assessing the Kinetics and Capacity of Gas Adsorption in Coals by a Combined Adsorption/ Diffusion Method. Annual Geotechnology Research Meeting 27 January, Delft Netherlands.

2003

Conference proceedings

Siemons, N.; Krooss, B. M.; Bruining, H.: Assessing the Kinetics and Capacity of Gas Adsorption in Coals by a Combined Adsorption/ Diffusion Method. SPE 84340 SPE Annual Conference and Exhibition October 2003 Denver, USA.

A. Busch, Y. Gensterblum, N. Siemons, B.M. Krooss,F. van Bergen, H.J.M Pagnier, P. David (2003) Investigation of preferential sorption behavior of CO2 and CH4 on coals by high pressure adsorption/desorption experiments with gas

mixtures. XV International Congress on Carboniferous and Permian Stratigraphy (XV ICCP), Utrecht August 2003.

Oral presentations

Siemons, N.; Krooss, B. M.; Bruining, H.: Assessing the Kinetics and Capacity of Gas Adsorption in Coals by a Combined Adsorption/ Diffusion Method. Oral presentation at the SPE Annual Conference and Exhibition, October 2003 Denver, USA.

Siemons, N., Wolf K.-H., & Bruining H.: Scaled Flooding Experiments for Combined CO2 Sequestration and CH4 Production from Carboniferous Coal, Oral presentation, XV International Congress on Carboniferous and Permian Stratigraphy (XV ICCP),Utrecht August 2003.

Reports

Wolf, K.H.A.A., Bruining, J. Siemons, N. and Mazumder, S., 2003. Development of advanced reservoir characterization and simulation tools for improved coal bed methane recovery. EU Contr. nr. ENK6-2000-00095, proj. nr. NNE5-1999-20174. Delft, The Netherlands: Delft University of Technology, 35 pp.

2002

Review article

B.M. Krooss, F. van Bergen, Y. Gensterblum, N. Siemons, H.J.M. Pagnier, P. David (2002): High-pressure methane and carbon dioxide adsorption on dry and moisture-equilibrated Pennsylvanian coals. Int. J. Coal Geology, 51, 69-92.

Conference proceedings

Nikolai Siemons, Johannes Bruining, Berhard M.Krooss, 2002.Upscaled diffusion in coal particles. Conference proceedings 5th European Coal Conference, September 17-19, Mons-Frameries, Belgium.

Karl-Heinz A.A. Wolf, Nikolai Siemons, Johannes Bruining, 2004. Multiphase flow experiments in order to understand the behavior of (partly) saturated coals as a gas reservoir: Examples 2004. Conference proceedings 5th European Coal Conference, September 17-19, Mons-Frameries, Belgium.

Karl-Heinz A. A. Wolf, Dan Bossie Codreanu, Rudy Ephrahim, Nikolai Siemons 2004. Analysing cleat angles in coal seams using image analysis techniques on artificial drilling cuttings and prepared coal blocks. Conference proceedings 5th European Coal Conference, September 17-19, Mons-Frameries, Belgium.

Nikolai Siemons and Johannes Bruining, 2002. Upscaled diffusion in coal particles. Poster presentation at Gordon Research Conference, Flow & Transport in Permeable Media, Proctor Academy, Andover, NH, August 4--9, 2002.

Oral presentations

Nikolai Siemons, Johannes Bruining, Berhard M.Krooss, 2002.Upscaled diffusion in coal particles.Upscaled diffusion in coals. 5th European Coal Conference, September 17-19, Mons-Frameries, Belgium.

2001

Reports

Durucan, S., K.H.A.A. Wolf, D. Bossie-Codreanu, N. Siemons, J. Bruining, H.J. Kaltwang, D. Creedy, T. Espie, J.Q. Shi, X.D. Jing,E. Syahrial; Development of advanced reservoir characterization and simulation tools for improved coalbed

methane recovery. rapport 1-10-2000 - 30-9-2001. Confidential report to European Community. Dec. 2001. Contr. Nr. ENK6-2000-00095. Project. No. ICBM - NNE5-1999-20174. 76 p.

Durucan, S., K.H.A.A. Wolf, D. Bossie-Codreanu, N. Siemons, J. Bruining, H.J. Kaltwang, D. Creedy, T. Espie, J.Q. Shi, X.D. Jing,E. Syahrial; Development of advanced reservoir characterization and simulation tools for improved coalbed methane recovery. Confidential report to European Community. May 2001. Contr. Nr. ENK6-2000-00095. Project. No. ICBM -NNE5-1999-20174. 14 p..

Acknowledgements

Last but not least, it is time to acknowledge everyone who contributed in any way to the results presented in the preceeding pages. Writing a book requires support at all levels; initiating the research project, producing results, staying on track, and, of course, the writing.

I express gratitude to my promoter Cor van Kruijsdijk who gave me the opportunity to begin working in his department and who made this research possible. I would like to thank the committee and the anonymous reviewers for helping me improve this text considerably.

I would like to thank my supervisors, Hans Bruining and Karl-Heinz Wolf for giving me freedom, confidence, motivation and scientific support. You were there whenever I needed you. Your diverse knowledge, interest in my research and your curiosity in general motivated me and kept me going through the final years. Hans, thank you very much for the time you spent on our countless evening sessions. It was a luxury for a PhD-student and I greatly appreciate it.

I have spent five pleasant years in the Dietz laboratory; many people have come and gone. I shared great moments with many and some not so great moments with few. Without Leo Vogt and Henk van Asten would it have been impossible to perform the experiments, the basis for this thesis. I like to thank the Dietz-laboratory staff Karel Heller, Jan Etienne, Andre Hoving and Ellen Meijvogel for the support, the work atmosphere and the chats. My dear office

mates; Ainhoa, Koen, Willem-Jan and Bouko, it was a wonderful time sharing this little space with you. The coffee breaks and daily lunch gatherings with you all played an important role in relieving the pressure, alleviating problems and gaining a better insight into the Dutch way of life.

I would also like to thank my friends in Delft who took care of my social life and helped me to integrate and feel at home. Thank you very much, Eva, Roald, Lena, Sandra, Alex, Koen, Astrid, Julia, Luuk and Nico. My time in the Netherlands is over; I hope to see you all in Norway, some of you have already made it to Bergen. Åse, I thank you for the wonderful last year. It has not always been easy. The spatial distance between us has now decreased considerably and will soon be zero.

A vital part of the research has of course been the financial support. This research was performed under the framework of the following research programs:

1: The European EEC-FP5 program (ICBM)

2: Shell Game-changer cold injection project

3: CO_2-capture, Transport and storage (CATO), the Senter-BSIK program of the Dutch Government.

The financial support is gratefully acknowledged.

About the author

Nikolai Siemons was born in Essen, Germany, on 30.04.1973, between the coking plant "Zollverein", the coalmine "Emil Emscher" and approximately 1000 m above high-quality bituminous coal. Two years later, his family moved southwest and settled in Aachen, in the Limburg (NL) – Liege (B) – Aachen (BRD) coal region. He attended secondary school at the Inda-Gymnasium in Kornelimünster and received his "Abitur" (university entry degree) in 1992.

After serving the alternative national service at the School for Multiple-handicapped Children in Aachen, he joined the Faculty of Applied Geosciences at the Rheinisch-Westfälische Technische Hochschule (RWTH) Aachen in 1993. During his studies in applied geology, he specialized in geology and geochemistry of petroleum and coal. He graduated in May 2001 and joined the Dietz laboratory, Faculty of Civil Engineering and Geotechnology (CITG) at TU Delft one month later. Here, he investigated the fundamental aspects of CO_2 sequestration in coal. The scientific work, carried out in various national and international projects, was the basis for this thesis. In 2005, he took part in a coal-research project with Shell. In March 2007, he joined Norsk Hydro (now StatoilHydro) in Bergen, Norway, working as a reservoir engineer and is, for the time being, not related to coal, scientifically or locally, any more.